View metadata, citation and similar papers at core.ac.uk

brought to you by CORE

provided by Edinburgh Research Archive

Highly Degenerate Diffusions for Sampling Molecular Systems

Emad Noorizadeh

Doctor of Philosophy
University of Edinburgh
2009

To my parents

Acknowledgments

I am heartily thankful to my supervisor, Ben Leimkuhler, for his generous support, his invaluable assistance, his constant encouragements, for many interesting discussions and involving me in his research projects, inviting and supporting me to go to workshops and conferences, for his brilliant feedback on this thesis. I am exceedingly fortunate to be his student and I am excited about future collaboration with him.

Special thanks also to Florian Theil and Oliver Penrose, for research collaboration and many interesting research discussions, I learned much from them. I would also like to thank my office mates, especially Patricia Ritter for reading my thesis and her encouragement.

This project was supported by funds from UK Engineering and Physical Sciences Research Council and Maxwell Institute.

Declaration

I declare that this thesis was composed by myself and that the work contained therein is my own, except where explicitly stated otherwise in the text.

Chapter 4 is based on a joint paper [Leimkuhler B. and Noorizadeh E. and Theil F., J. Stat. Phys. 135, 261-277 (2009)]. In this collaboration, I contributed to the theoretical analysis (especially work on geometric ergodicity) and performed all numerical experiments. The idea of proof for hypoellipticity of the quadratic potential was due to Florian Theil, while the method studied was proposed by Ben Leimkuhler.

The work presented in Chapter 5 is entirely due to the present author but the idea of studying the ratio of the rate of convergence to the growth of the perturbations was suggested by Oliver Penrose; it is part of a planned joint paper involving Oliver Penrose and Ben Leimkuhler.

Chapter 6 is based on a joint paper [Leimkuhler B., Legoll F. and Noorizadeh E., J. Chem. Phys., 128, 074105 (2008)]. The author contributed to all aspects and was solely responsible for the numerical analysis presented there.

(*Emad Noorizadeh*)

Abstract

This work is concerned with sampling and computation of rare events in molecular systems. In particular, we present new methods for sampling the canonical ensemble corresponding to the Boltzmann-Gibbs probability measure. We combine an equation for controlling the kinetic energy of the system with a random noise to derive a highly degenerate diffusion (i.e. a diffusion equation where diffusion happens only along one or few degrees of freedom of the system). Next the concept of hypoellipticity is used to show that the corresponding Fokker-Planck equation of the highly degenerate diffusion is well-posed, hence we prove that the solution of the highly degenerate diffusion is ergodic with respect to the Boltzmann-Gibbs measure. We find that the new method is more efficient for computation of dynamical averages such as autocorrelation functions than the commonly used Langevin dynamics, especially in systems with many degrees of freedom. Finally we study the computation of free energy using an adaptive method which is based on the adaptive biasing force technique.

Contents

Chapter 1

Introduction

Molecular simulation is an effective tool for finding a more accurate description of material and chemical systems or biological systems. Indeed, understanding the microscopic behaviour of matter using experiment in a laboratory is a daunting task (because of the need for small scales both in time and space). Hence molecular simulation is used to complement the experiment when the latter is difficult or impossible to perform. With increasing computer power the molecular simulations are becoming more accurate and reliable, as a result many industries such as drug design and material design use molecular simulation as one of their main tools in combination with experiment. Moreover the decrease of cost in high performance computing and the development of better algorithms indicate that the role of molecular simulation will increase rapidly.

Molecular modeling begins with the eigenvalue problem of the *autonomous Schrödinger equation*

$$H\Psi = E\Psi,$$

where E is the smallest eigenvalue of the Hamiltonian operator H, which is defined by wellknown fundamental constants of nature and Coulomb interactions of all nuclei and electrons. The state of the system is described by the unknown corresponding eigenvector Ψ which is a complex value wave function, depending on the coordinates of all nuclei and electrons and on the spins of all electrons in the system. The existence of Ψ is guaranteed by results of spectral theory.

The main issue with this modelling is its computational complexity, which is due to the high dimensionality of the space where Ψ is defined, see [1]. For instance simulation of a single water molecule requires solving a partial differential equation in

39-dimensional space [1]. Therefore it becomes necessary to use some coarse-grained approximation. An old approximation is *Ehrenfest dynamics* which approximates the nuclear dynamics by classical paths, and hence introduces a *nonautonomous Schrödinger equation* for electrons. Another coarse-grained method is *Born-Oppenheimer* which approximates the electronic wave function by the electronic ground state for the current nuclei positions, see [2] and references there. A widely used coarse-grained approximation is *molecular dynamics* (MD) which simulates a system of n particles with fixed volume and temperature

Here we are concerned with classical molecular dynamics where the nucleus and its electronic cloud are considered as one particle. Hence we consider a system of n particles interacting through an empirically defined potential energy. Mathematically the system of n particles is described by a Hamiltonian function $H(q,p) : \mathcal{M} \times \mathbb{R}^n \to \mathbb{R}$ which is defined as

$$H(q,p) = \frac{p^T M^{-1} p}{2} + V(q), \tag{1.1}$$

where $q = (q_1, \cdots, q_n)^T \in \mathcal{M} \subseteq \mathbb{R}^n$ is the position vector, $p = (p_1, \cdots, p_n)^T \in \mathbb{R}^n$ is the momentum vector, and $V : \mathcal{M} \to \mathbb{R}$ is the potential energy function which governs interaction between particles.

We denote the phase space by $\mathbb{X} = \mathcal{M} \times \mathbb{R}^n$, and the state of the system at a given time t is defined by $(t; q, p)$ which represents a point in phase space. The phase space $\mathbb{X}$ has a natural symplectic structure which is given by the following nondegenerate differential 2-form

$$\omega^2 = \mathrm{d}p \wedge \mathrm{d}q = \mathrm{d}p_1 \wedge \mathrm{d}q_1 + \cdots + \mathrm{d}p_n \wedge \mathrm{d}q_n.$$

The equations of motion are given by

$$\begin{pmatrix} \mathrm{d}q/\,\mathrm{d}t \\ \mathrm{d}p/\,\mathrm{d}t \end{pmatrix} = \mathbb{J}\nabla H = \begin{pmatrix} \nabla_p H \\ -\nabla_q H \end{pmatrix}, \tag{1.2}$$

where

$$\mathbb{J} = \begin{pmatrix} 0_n & I_n \\ -I_n & 0_n \end{pmatrix}$$

is the matrix of a map that takes differential of H to the phase space, I_n and 0_n denote identity and zero matrix of size $n \times n$. $\mathbb{J}\nabla H$ is called Hamiltonian vector field. The

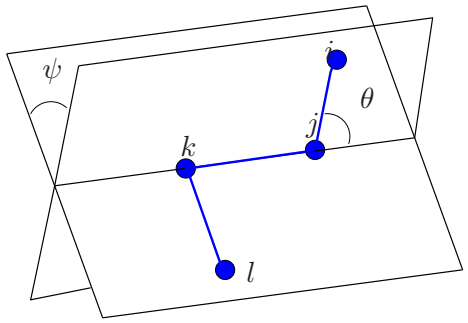

Figure 1.1: Bonds, bend angle and dihedral angel for a simple chain molecule.

flow of the Hamiltonian vector field is the collection of maps $\varphi_t : \mathbb{X} \to \mathbb{X}$ satisfying

$$\frac{\mathrm{d}}{\mathrm{d}t}\varphi_t(z) = \mathbb{J}\nabla H(\varphi_t(z)) \tag{1.3}$$

for each $z = (q^T, p^T)^T \in \mathbb{X}$ and $t \in [0, \infty)$ (i.e., $z(t; z_0) = \varphi_t(z_0)$). The flow map φ_t preserves the symplectic structure of the phase space:

$$\varphi_t^* \omega^2 = \omega^2.$$

An immediate consequence of this is Liouville's theorem which says that the Hamiltonian flow preserves volume. An important feature of Hamiltonian dynamics is the conservation of the energy:

$$H(\varphi_t(z)) = H(z).$$

Indeed, using the chain rule and symplectic structure we have

$$\begin{aligned}\frac{\mathrm{d}}{\mathrm{d}t}H(\varphi_t(z)) =& \nabla H(\varphi_t(z)) \cdot \frac{\mathrm{d}\varphi_t(z)}{\mathrm{d}t} = \omega^2(\mathbb{J}\nabla H(\varphi_t(z)), \frac{\mathrm{d}\varphi_t(z)}{\mathrm{d}t}) \\ =& \omega^2(\mathbb{J}\nabla H(\varphi_t(z)), \mathbb{J}\nabla H(\varphi_t(z))) = 0.\end{aligned}$$

For more detail on Hamiltonian dynamics see [3, 4, 5, 6].

1.1 Molecular Interactions

In molecular dynamics the potential function $V(q)$ consists of two main types of interactions, namely *non-bonded* and *bonded* interactions:

$$V(q) = V_{nb}(q) + V_b(q).$$

1.1.1 Non-Bonded Interactions

This part of the potential describes the effect of atoms on each other and usually is decomposed as follows:

$$V_{nb}(q) = \sum_i U(q_i) + \sum_i \sum_{j>i} U(q_i, q_j) + \sum_i \sum_{j>i} U_C(q_1, q_j),$$

where $U(q_i)$ represents an external potential field, for instance the effect of a container wall on the atoms, this term is usually neglected in simulation with *periodic boundary* conditions which is explained bellow. The term $U(q_i, q_j)$ represents Van der Waals interaction between a pair of atoms and is usually modelled by a Lennard-Jones potential:

$$U_{LJ}(r_{ij}) = 4\epsilon \left[\left(\frac{\sigma}{r_{ij}} \right)^{12} - \left(\frac{\sigma}{r_{ij}} \right)^{6} \right], \quad r_{ij} = \|q_j - q_i\| = \sqrt{(q_j - q_i) \cdot (q_j - q_i)}.$$

The parameters are σ, the diameter and ϵ, the well depth. This potential is very short-ranged and is typically used with a smooth cutoff around 3σ. The long-ranged Coulomb potential $U_C(q_i, q_j) \propto 1/r_{ij}$ represents electrostatic interaction between pairs of atoms.

1.1.2 Bonded Interactions

For a simple molecular chain the bonding potential is of the form

$$V_b(q) = \sum_{\text{bonds}} U_r(q_i, q_j) + \sum_{\text{bend angles}} U_\theta(q_i, q_j, q_k) + \sum_{\text{dihedral angles}} U_\psi(q_i, q_j, q_k, q_l).$$

The bond stretch interaction is described by $U_r(q_i, q_j) \propto (r_{ij} - r_{eq})^2$ where r_{eq} is the equilibrium separation between the atoms i and j. The bond angle interaction is described by $U_\theta(q_i, q_j, q_k) \propto (\theta_{ijk} - \theta_{eq})^2$, where θ_{eq} is the equilibrium angle and θ_{ijk} is the angel between successive atoms indexed by i, j and k:

$$\cos\theta_{ijk} = \frac{(q_j - q_i)}{\|q_j - q_i\|} \cdot \frac{(q_k - q_j)}{\|q_k - q_j\|}.$$

$U_\psi(q_i, q_j, q_k, q_l) = U_\psi(\psi_{ijkl})$ describes dihedral or torsion angle interaction between four atoms, indexed by i, j, k and l, which are linked by neighbouring bonds:

$$\cos\psi_{ijkl} = -\frac{(q_j - q_i) \times (q_k - q_j)}{\|(q_j - q_i) \times (q_k - q_j)\|} \cdot \frac{(q_k - q_j) \times (q_l - q_k)}{\|(q_k - q_j) \times (q_l - q_k)\|}.$$

See Figure 1.1 for illustration of bend and dihedral angles. For more detailed information on potentials see [7, 8, 9].

1.1.3 Periodic Boundary Conditions

We are constrained by the number of particles that can be simulated by computer. For such a small system the choice of the boundary conditions will affect its thermodynamics properties. In fact for a system of n particles the fraction of particles that are at the surface is proportional to $n^{-1/3}$ [8]. Hence we use periodic boundary conditions to avoid the surface effect. In periodic boundary conditions our n particles system is surrounded by its images. In this way a particle interacts with other particles in the system and their periodic images. The position space for a system with periodic boundary conditions is $\mathcal{M} = \mathbb{T}^n$ (a n dimensional torus).

1.2 Numerical Integration

In molecular dynamics we are concerned with numerical approximation of the flow map φ_t of the differential equation (1.3):

$$\frac{\mathrm{d}}{\mathrm{d}t}\varphi_t(z) = \mathbb{J}\nabla H(\varphi_t(z)),$$

where H is a smooth function and the potential function has a short repulsive term which stops particles getting too close.

A one-step numerical integrator of order $d \geq 1$ is a discrete map $\Phi_{\Delta t}$, such that

$$z^{k+1} = \Phi_{\Delta t}(z^k) \quad \text{and} \quad \Phi_{\Delta t}(z) - \varphi_{\Delta t}(z) = \mathcal{O}(\Delta t^{d+1}),$$

where $z^k = z(k\Delta t)$. One way to derive a one-step method is to integrate (1.3)

$$\varphi_{t+\Delta t}(z) - \varphi_t(z) = \int_0^{\Delta t} \mathbb{J}\nabla H(\varphi_{t+s}(z))\,\mathrm{d}s,$$

and replace the integral on the right hand side with a suitable quadrature approximation. For example using

$$\int_0^{\Delta t} \mathbb{J}\nabla H(\varphi_{t+s}(z))\,\mathrm{d}s = \Delta t\mathbb{J}\nabla H(\varphi_t(z)) + \mathcal{O}(\Delta t^2),$$

gives Euler's method.

In Molecular dynamics long time stability of the numerical method is much more important than having very accurate trajectories. It is known that preserving the symplectic structure, such as conservation of energy in numerical integration, implies long time stability [10, 11]. A class of integrators that preserve symplectic structure are called symplectic or geometric integrators. A map Φ is called symplectic if its Jacobian $D\Phi$ satisfies

$$D\Phi^T \mathbb{J}^{-1} D\Phi = \mathbb{J}^{-1}.$$

The Hamiltonian dynamics is time reversible, hence in many molecular simulations for statistical and sampling reasons it is important to preserve the time reversibility of the dynamics. A map Φ is called time reversible with respect to involution $\hat{z} = Sz$, where $\hat{z} = (q^T, -p^T)^T$, if it satisfies

$$S\Phi(Sz) = \Phi^{-1}(z).$$

The fundamental result of [12, 13, 14, 15] is that for any symplectic method Φ of order $d \geq 1$ there exist a modified Hamiltonian $\tilde{H}$ of the form

$$\tilde{H} = H + \mathcal{O}(\Delta t^d),$$

and a modified differential equation

$$\frac{\mathrm{d}}{\mathrm{d}t}\tilde{\varphi}_t(z) = \mathbb{J}\nabla\tilde{H}(\tilde{\varphi}_t(z)).$$

The symplectic map Φ follows the solution of the the modified differential equation very closely, moreover it is possible to find constants c_1 and c_2 such that

$$\|\Phi_{\Delta t}(z) - \tilde{\varphi}_t(z)\| \leq c_1 e^{-c_2/\Delta t}.$$

Since

$$\tilde{H} - H = \mathcal{O}(\Delta t^d),$$

the energy is conserved up to the order of the method over exponentially long time interval. For a detailed discussion of symplectic methods see [10, 5, 16, 17].

1.2.1 The Störmer-Verlet Method

Consider a systems of second order differential equations

$$M\frac{\mathrm{d}^2 q}{\mathrm{d}t^2} = -\nabla_q H(q,p) = F(q), \tag{1.4}$$

where M is a positive definite mass matrix, and $F(q)$ is the force vector. A simple discretization of (1.4) is

$$M\left(q^{k+1} - 2q^k + q^{k-1}\right) = \Delta t^2 F(q^k), \tag{1.5}$$

which is known as the leapfrog method. The leapfrog method determines an interpolating parabola between q^{k-1}, q^k and q^{k+1} such that the middle point q^k satisfies (1.4).

For the systems of first order differential equations

$$\begin{aligned}\frac{\mathrm{d}q}{\mathrm{d}t} =& M^{-1}p,\\ \frac{\mathrm{d}p}{\mathrm{d}t} =& -\nabla_q V(q),\end{aligned}$$

the leapfrog method (1.5) can be interpreted as a one-step method $\Phi_{\Delta t} : (q^k, p^k) \to (q^{k+1}, p^{k+1})$, given by

$$p^{k+1/2} = p^k - \frac{\Delta t}{2}\nabla_q V(q^k), \tag{1.6}$$

$$q^{k+1} = q^k + \Delta t M^{-1} p^{k+1/2}, \tag{1.7}$$

$$p^{k+1} = p^{k+1/2} - \frac{\Delta t}{2}\nabla_q V(q^{k+1}). \tag{1.8}$$

The discretization (1.6)-(1.8) is known as Störmer-Verlet method, it was used first by C. Störmer in 1907 and was proposed for molecular dynamics integration by L. Verlet in 1967 [18]. The Störmer-Verlet method is symplectic and time reversible.

1.2.2 A Simple Example: Double Well Potential

Here to illustrate the concept of numerical integration we consider a simple one dimensional model with double well potential which was used in [10]. The Hamiltonian is

$$H(q,p) = \frac{p^2}{2} + V(q), \text{ where } V(q) = \tfrac{1}{2}(q^2-1)^2.$$

Let $z = (q,p)^T$ and $F(z) = (p, -V'(q))^T$, then we can write the Hamiltonian equations as

$$\dot{z} = F(z). \tag{1.9}$$

Let $\varphi_t(z)$ be the exact solution of (1.9), the numerical solution $\Phi_{\Delta t}$ using Störmer-Verlet (1.6)-(1.8) takes the form of

$$\Phi_{\Delta t}(q,p) = \begin{pmatrix} q + \Delta t p - \frac{\Delta t^2}{2} V'(q) \\ p - \frac{\Delta t}{2} V'(q) - \frac{\Delta t}{2} V'(q + \Delta t p - \frac{\Delta t^2}{2} V'(q)) \end{pmatrix}.$$

The Taylor expansion of $\Phi_{\Delta t}$ assumes the form of

$$\Phi_{\Delta t}(z) = z + \Delta t F(z) + \Delta t^2 D_2(z) + \Delta t^3 D_3(z) + \cdots, \tag{1.10}$$

where

$$D_2(q,p) = \frac{1}{2} \begin{pmatrix} -V'(q) \\ -V''(q)p \end{pmatrix}, \quad D_3(q,p) = \frac{1}{4} \begin{pmatrix} 0 \\ -V''(q)V'(q) - V'''(q)p^2 \end{pmatrix}.$$

Now assume that there is a modified differential equation

$$\dot{z} = F(z) + \Delta t F_2(z) + \Delta t^2 F_3(z) + \cdots$$

with exact flow $\tilde{\varphi}_t(z)$. The Taylor expansion of $\tilde{\varphi}_t(z)$ gives

$$\begin{aligned} \tilde{\varphi}_t(z) =& z + \Delta t \frac{\mathrm{d}}{\mathrm{d}t}\tilde{\varphi}_t(z) + \frac{\Delta t^2}{2}\frac{\mathrm{d}^2}{\mathrm{d}t^2}\tilde{\varphi}_t(z) + \frac{\Delta t^3}{3!}\frac{\mathrm{d}^2}{\mathrm{d}t^2}\tilde{\varphi}_t(z) + \cdots \\ =& z + \Delta t \left(F(z) + \Delta t F_2(z) + \Delta t^2 F_3(z) + \cdots\right) \\ &+ \frac{\Delta t^2}{2}\left(F'(z) + \Delta t F_2'(z) + \Delta t^2 F_3'(z) + \cdots\right)\left(F(z) + \Delta t F_2(z) + \Delta t^2 F_3(z) + \cdots\right) \\ &+ \frac{\Delta t^3}{3!}\left(F'(z) + \Delta t F_2'(z) + \Delta t^2 F_3'(z) + \cdots\right)\left(F'(z) + \Delta t F_2'(z) + \Delta t^2 F_3'(z) + \cdots\right) \\ &\left(F(z) + \Delta t F_2(z) + \Delta t^2 F_3(z) + \cdots\right) + \frac{\Delta t^3}{3!}\left(F''(z) + \Delta t F_2''(z) + \Delta t^2 F_3''(z) + \cdots\right) \\ &\left(F(z) + \Delta t F_2(z) + \Delta t^2 F_3(z) + \cdots\right)\left(F(z) + \Delta t F_2(z) + \Delta t^2 F_3(z) + \cdots\right) + \cdots \end{aligned} \tag{1.11}$$

We obtain F_2 and F_3 by comparing like powers of Δt in (1.11) and (1.10)

$$
\begin{aligned}
F_2(z) =& D_2(z) - \frac{1}{2}F'(z)F(z), \\
F_3(z) =& D_3(z) - \frac{1}{3!}\left[F''(z)F(z)F(z) + F'(z)F'(z)F(z)\right] - \frac{1}{2}\left[F'(z)F_2(z) + F_2'(z)F(z)\right],
\end{aligned}
$$

which gives

$$
F_2(q,p) = 0, \quad F_3(q,p) = \frac{1}{12}\begin{pmatrix} 2V''(q)p \\ V''(q)V'(q) - V'''(q)p^2 \end{pmatrix}.
$$

Thus the truncated modified equation is

$$
\dot{z} = F(z) + \Delta t^2 F_3(z),
$$

which comes from the following modified Hamiltonian

$$
\tilde{H}(q,p) = H(q,p) + \Delta t^2 \left[\frac{1}{12}V''(q)p^2 + \frac{1}{24}V'(q)^2\right].
$$

Thus the Störmer-Verlet method preserves the energy with an error term of order $\mathcal{O}(\Delta t^2)$. In Figure 1.2 we compare conservation of energy for the symplectic Störmer-Verlet method and Euler method. We see that for Euler method energy grows even with very small step size.

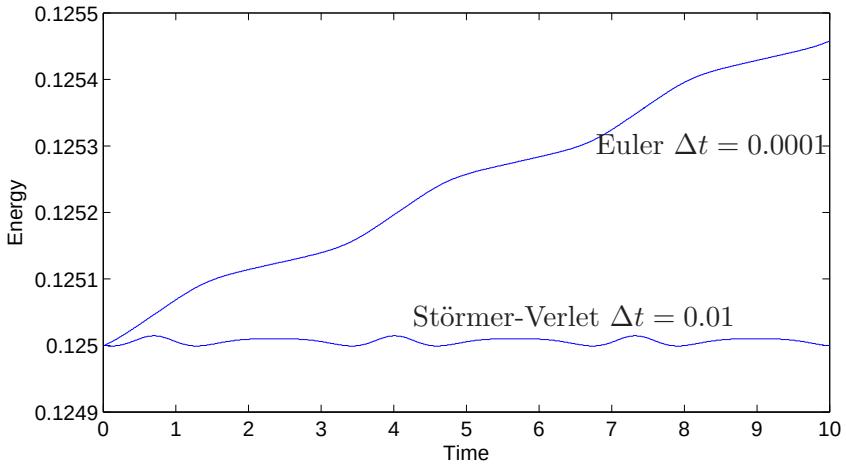

Figure 1.2: Conservation of energy for the numerical solutions of (1.9) using Störmer-Verlet and Euler methods.

1.3 Statistical Ensembles

A subset $U \subseteq \mathbb{X}$ is *invariant* if $z_0 = (q(0), p(0)) \in U$ implies $\varphi_t(z_0) \in U$ for all $t > 0$. The invariant sets of phase space play essential role in statistical physics and molecular dynamics. The main aim of molecular dynamics is to compute the averages of macroscopic observables (functions of phase space variables) in the right statistical ensemble for the experiment. For an observable $O = O(q, p)$, its average is given by

$$\rho_\infty(O) = \langle O, f_\infty \rangle = \int_{\mathcal{M}\times\mathbb{R}^n} O(q,p)\, \mathrm{d}\rho_\infty(q,p), \tag{1.12}$$

where ρ_∞ is a probability measure associated to a statistical ensemble and f_∞ is the density of ρ_∞.

Two important statistical ensembles that we are mainly concerned with are the *microcanonical ensemble* and the *canonical ensemble*. The microcanonical ensemble describes an isolated system, whereas the canonical ensemble describes a system in contact with *heat bath*.

1.3.1 The Microcanonical Ensemble

This is the fundamental statistical ensemble which describes an isolated system. This ensemble is generated by Hamiltonian dynamics:

$$\frac{\mathrm{d}q}{\mathrm{d}t} = \nabla_p H(q,p) = M^{-1}p, \tag{1.13}$$

$$\frac{\mathrm{d}p}{\mathrm{d}t} = -\nabla_q H(q,p) = -\nabla_q V(q). \tag{1.14}$$

Liouville's theorem states that the measure of measurable (in the sense of Lebesgue) set of points is invariant along the motion of (1.13)-(1.14). In addition, for an isolated system total energy which is given by the Hamiltonian function (1.1) is constant along (1.13)-(1.14). Therefore for any $E \geq 0$ the energy surface defined by $H(q, p) = E$ and denoted by Σ_E is an invariant subset of phase space $\mathbb{X}$. Thus, every subset S of Σ_E remains in Σ_E during any interval of time, but the measure of S would not necessarily remain invariant.

In order to obtain statistics from the dynamics on the surface Σ_E, we need to define a probability measure ρ_E such that $\rho_E(S)$ remains invariant. Let $O(q, p) \in \mathcal{D}(\mathbb{X})$ ($\mathcal{D}(\mathbb{X})$ denotes space of test functions on $\mathbb{X}$), then, the microcanonical probability measure

(microcanonical distribution) $\rho_E : \mathcal{D}(\mathbb{X}) \to \mathbb{R}$ is given by

$$\rho_E(O) = \frac{1}{Z(\Sigma_E)} \int_{\mathbb{X}} O(q,p)\, \delta(H(q,p) - E)\ \mathrm{d}q\, \mathrm{d}p = \frac{1}{Z(\Sigma_E)} \int_{\Sigma_E} O(q,p) \frac{\mathrm{d}\Sigma_E}{||\nabla H||}, \quad (1.15)$$

where δ is Dirac's delta function, $\mathrm{d}\Sigma_E$ is the volume element of the surface Σ_E, $Z(\Sigma_E)$ defined by

$$Z(\Sigma_E) = \int_{\mathbb{X}} \delta(H(q,p) - E)\ \mathrm{d}q\, \mathrm{d}p = \int_{\Sigma_E} \frac{\mathrm{d}\Sigma_E}{||\nabla H||}$$

is a normalization constant and

$$||\nabla H|| = (\nabla H \cdot \nabla H)^{\frac{1}{2}} = \left(\sum_{i=1}^{N} \left[\left(\frac{\partial H}{\partial q_i} \right)^2 + \left(\frac{\partial H}{\partial p_i} \right)^2 \right] \right)^{\frac{1}{2}}.$$

1.3.2 Canonical Ensemble

This is one of the most important and widely used ensembles. It describes a system in contact with a heat bath (*a thermostat*), that is, a system with fixed number of particles, with fixed volume and temperature. Its corresponding probability measure $\rho_\beta : \mathcal{D}(\mathbb{X}) \to \mathbb{R}$ is called Boltzmann-Gibbs measure (Boltzmann-Gibbs distribution) and is defined by

$$\rho_\beta(O) = \int_{\mathbb{X}} O(q,p)\, f_\beta(q,p)\ \mathrm{d}q\, \mathrm{d}p, \quad (1.16)$$

where

$$f_\beta(q,p) = \frac{1}{Z} \exp(-\beta H(q,p)) \quad (1.17)$$

is its probability density, $\beta = \frac{1}{k_B T}$ (K_B denotes Boltzmann constant and T denotes the temperature), and $Z = \int_{\mathbb{X}} f_\beta(q,p)\ \mathrm{d}q\, \mathrm{d}p$ is a normalization constant which is also called Gibbs partition function in statistical physics.

To generate the canonical ensemble, we need to modify or to perturb Hamiltonian dynamics (1.3), so that the new process which is defined in $U \subseteq \mathbb{X}$ would have a probability measure $\rho(q,p,t)$ such that $\rho(\chi_U) = 1$ and $\rho(\chi_{U^c}) = 0$ (where

$$\begin{cases} \chi_U(z) & = 1, \quad z = (q^T, p^T)^T \in U, \\ & = 0, \quad x \notin U, \end{cases}$$

is the characteristic function), and $\rho(q,p,t)$ would converges in time to ρ_β. Thus, after some time which is known as the equilibration time, the measure $\rho(q,p,t)$ tends to be

very close to $\rho_\beta(q,p)$.

One way to generate the canonical ensemble is to replace the Hamiltonian dynamics by an appropriate stochastic differential equation (SDE). We demonstrate this in the spirit of [19, 20, 21], similar to the exposition of [22]. Consider a heavy particle with position q and momentum p interacting with a heat bath which is a system of infinitely many light particles. The state $\phi = (\varphi, \pi)$ of the system of light particles takes values in some appropriate Hilbert space $\mathcal{H}$ with an inner product defined by

$$\langle \phi, \phi \rangle_{\mathcal{H}} = \int \left[\pi(x)^2 + \|\nabla \varphi(x)\|^2 \right] \mathrm{d}x,$$

φ is the configuration variable and can be interpreted as a measure of the displacement from equilibrium of a homogeneous elastic medium, and π is its conjugate momentum. Hence the Hamiltonian function of the heat bath takes the form of

$$H_B(\phi) = \frac{1}{2}\|\phi\|_{\mathcal{H}}^2,$$

and its equation of motion is given by

$$\frac{\mathrm{d}}{\mathrm{d}t}\phi = \begin{pmatrix} \partial\varphi/\partial t \\ \partial\pi/\partial t \end{pmatrix} = \begin{pmatrix} \delta H_B/\delta\pi \\ -\delta H_B/\delta\varphi \end{pmatrix} = \mathcal{L}\begin{pmatrix} \varphi \\ \pi \end{pmatrix} = \mathcal{L}\phi,$$

where $\delta F/\delta g$ denotes the functional derivative of the functional F, and $\mathcal{L} : \mathcal{H} \to \mathcal{H}$ is a linear operator defined by

$$\mathcal{L} = \begin{pmatrix} 0 & 1 \\ \Delta & 0 \end{pmatrix},$$

where $\Delta = \nabla \cdot \nabla$ is the Laplace operator.

Let us assume that $q(0) = 0$ and introduce $\alpha = (\alpha(x), 0)^T \in \mathcal{H}$. We also assume that the heavy particle and the heat bath are linked through a quadratic potential of the form $\frac{1}{2}\|\phi - \alpha q\|_{\mathcal{H}}^2$, so that the total Hamiltonian of the combined system is

$$H(q,p,\phi) = \frac{p^2}{2m} + V(q) + \frac{1}{2}\|\phi - \alpha q\|_{\mathcal{H}}^2.$$

The equations of motion are

$$\frac{\mathrm{d}q}{\mathrm{d}t} = m^{-1}p, \tag{1.18}$$

$$\frac{\mathrm{d}p}{\mathrm{d}t} = -\nabla V(q) + \langle \phi - \alpha q, \alpha \rangle_{\mathcal{H}}, \tag{1.19}$$

$$\frac{\mathrm{d}\phi}{\mathrm{d}t} = \mathcal{L}(\phi - \alpha q). \tag{1.20}$$

Solving equation (1.20) yields

$$\phi(t) = e^{\mathcal{L}t}\phi(0) - \int_0^t \mathcal{L}e^{\mathcal{L}(t-s)}\alpha q(s)\ \mathrm{d}s.$$

Integrating by part and using the fact that $q(0) = 0$, we have

$$\phi(t) = e^{\mathcal{L}t}\phi(0) + \alpha q(t) - \frac{1}{m}\int_0^t e^{\mathcal{L}(t-s)}\alpha p(s)\ \mathrm{d}s.$$

Substituting ϕ in (1.19) gives

$$\frac{\mathrm{d}p}{\mathrm{d}t} = -\nabla V(q) + \langle e^{\mathcal{L}t}\phi(0), \alpha \rangle_{\mathcal{H}} - \frac{1}{m}\int_0^t \langle e^{\mathcal{L}(t-s)}\alpha, \alpha \rangle_{\mathcal{H}}\, p(s)\ \mathrm{d}s.$$

We assume that the energy of isolated heat bath is conserved, that is,

$$\frac{\mathrm{d}}{\mathrm{d}t}H_B(\phi) = \langle \mathcal{L}\phi, \phi \rangle_{\mathcal{H}} + \langle \phi, \mathcal{L}\phi \rangle_{\mathcal{H}} = \langle \phi, (\mathcal{L} + \mathcal{L}^*)\phi \rangle_{\mathcal{H}} = 0,$$

thus $\mathcal{L}^* = -\mathcal{L}$ and we have

$$\frac{\mathrm{d}p}{\mathrm{d}t} = -\nabla V(q) + \langle \phi(0), e^{-\mathcal{L}t}\alpha \rangle_{\mathcal{H}} - \int_0^t \langle e^{\mathcal{L}(t-s)}\alpha, \alpha \rangle_{\mathcal{H}}\, p(s)\ \mathrm{d}s. \tag{1.21}$$

Now we assume that the heat bath is in thermal equilibrium at inverse temperature β, this means that the probability distribution of the initial condition $\phi(0)$ is Gaussian with density given by

$$\rho(\phi) = \frac{1}{Z}\exp\left(-\frac{\beta}{2}\|\phi\|_{\mathcal{H}}^2\right),$$

where Z is the normalization constant.

Next we introduce a Gaussian process $X(t) = \langle \phi(0), e^{-\mathcal{L}t}\alpha \rangle_{\mathcal{H}}$ with covariance given

by

$$\begin{aligned}\mathbf{E}[X(s)X(t)] =&\mathbf{E}\left[\langle\phi(0), e^{-\mathcal{L}s}\alpha\rangle_{\mathcal{H}} \cdot \langle\phi(0), e^{-\mathcal{L}t}\alpha\rangle_{\mathcal{H}}\right] \\ =&\int\left(\int \nabla\varphi\cdot\nabla(e^{-\mathcal{L}s}\alpha)\,\mathrm{d}x\right)\cdot\left(\int\nabla\varphi\cdot\nabla(e^{-\mathcal{L}t}\alpha)\,\mathrm{d}x\right)\rho(x)\,\mathrm{d}x \\ =&\frac{1}{\beta}\langle e^{-\mathcal{L}s}\alpha, e^{-\mathcal{L}t}\alpha\rangle_{\mathcal{H}} = \frac{1}{\beta}\langle e^{\mathcal{L}(t-s)}\alpha,\alpha\rangle_{\mathcal{H}}.\end{aligned}$$

Thus, we have

$$\langle e^{\mathcal{L}(t-s)}\alpha,\alpha\rangle_{\mathcal{H}} = \beta\mathbf{E}[X(s)X(t)].$$

Here the fact that the covariance of X also appears in the memory kernel of the friction term can be seen as a consequence of the *fluctuation-dissipation* theorem.

If we further assume that the field generated by heat bath is strongly localised in spacial direction, then it is reasonable to approximate

$$\langle e^{\mathcal{L}(t-s)}\alpha,\alpha\rangle_{\mathcal{H}} \sim 2m\gamma\delta(t-s),$$

where $\delta(\cdot)$ is the Dirac delta function and γ is a constant. Finally we model the deterministic equation (1.18)-(1.20) by the following stochastic differential equations:

$$\begin{aligned}\frac{\mathrm{d}q}{\mathrm{d}t} =&m^{-1}p, \\ \frac{\mathrm{d}p}{\mathrm{d}t} =&-\nabla V(q) - \gamma p(t) + X(t),\end{aligned}$$

where $X(t)$ is a Gaussian process with mean zero and covariance

$$\mathbf{E}[X(t)X(s)] = \frac{2m\gamma}{\beta}\delta(t-s).$$

If we introduce a rescaled process

$$X(t) = \sqrt{\frac{2m\gamma}{\beta}}\bar{X}(t),$$

then the above system can be written as

$$\begin{aligned}\frac{\mathrm{d}q}{\mathrm{d}t} =&m^{-1}p, \\ \frac{\mathrm{d}p}{\mathrm{d}t} =&-\nabla V(q) - \gamma p(t) + \sqrt{\frac{2m\gamma}{\beta}}\bar{X}(t),\end{aligned}$$

where $\bar{X}(t)$ is a Gaussian process with mean zero and covariance $\mathbf{E}[\bar{X}(t)\bar{X}(s)] = \delta(t-s)$, which is known as white noise. The Itô interpretation of the above is

$$\begin{aligned}\frac{\mathrm{d}q}{\mathrm{d}t} =& m^{-1}p,\\ p =& p(0) - \int_0^t \nabla V(q(s))\,\mathrm{d}s - \int_0^t \gamma p(s)\,\mathrm{d}s + \int_0^t \sqrt{\frac{2m\gamma}{\beta}}\,\mathrm{d}W(s),\end{aligned}$$

or in differential form

$$\frac{\mathrm{d}q}{\mathrm{d}t} = m^{-1}p, \tag{1.22}$$

$$\mathrm{d}p = -\nabla V(q)\,\mathrm{d}t - \gamma p(t)\,\mathrm{d}t + \sqrt{\frac{2m\gamma}{\beta}}\,\mathrm{d}W, \tag{1.23}$$

where $W(t)$ is the Wiener process. Therefore, we have replaced the white noise $\bar{X}(t)$ by $\dot{W}(t)$ to obtain (1.22)-(1.23). The above system is a degenerate diffusion known as Langevin dynamics.

In the next chapter we describe methods that are used in molecular simulation to sample the canonical ensemble.

Chapter 2

Sampling Techniques

In this chapter we briefly review sampling methods in molecular simulation. The techniques can be categorised into three categories, stochastic methods such as Markov chain, stochastic dynamics which rely on stochastic perturbation of Hamiltonian dynamics, and dynamical methods which employ dynamical perturbation of Hamiltonian dynamics by using auxiliary control variables.

2.1 Preliminaries

Let $x(t, \omega; x_0)$, $t \in [0, \infty)$ be a homogeneous Markov process starting at x_0, defined on a probability space $(\mathbb{X}, \mathcal{B}(\mathbb{X}), P)$ and assuming values in phase space $\mathbb{X}$. We denote the transition probability of this process by

$$P(t, x_0, A) := \Pr(x(t, \omega; x_0) \in A), \quad t \in [0, \infty),\ x_0 \in \mathbb{X},\ A \in \mathcal{B}(\mathbb{X}),$$

where Pr denotes the probability associated with the Wiener process and $\mathcal{B}(\mathbb{X})$ denotes the Borel σ-algebra on $\mathbb{X}$. The process $x(t, \omega; x_0)$ induces a probability measure ρ on $\mathbb{X}$, defined by

$$\rho(A) = P(t, x_0, x^{-1}(A)),$$

where $x^{-1}(A) := \{\omega \in \mathbb{X} \mid x(t, \omega; x_0) \in A\}$, ρ is called the distribution of x.

For any measurable function $g : \mathbb{X} \to \mathbb{R}$, the value

$$\mathbf{E}[g(x(t))] := \int_{\mathbb{X}} g(x(t))\ \mathrm{d}P(t, x_0, \omega) = \int_{\mathbb{X}} g(x)\, \mathrm{d}\rho(x)$$

is called the expectation of g with respect to P.

Definition 1 (Ergodicity)**.** *The process $x(t,\omega;x_0)$ is ergodic on $\mathbb{X}$, if there exist a unique invariant probability measure ρ_∞ such that for any measurable function g with finite integral $\int_{\mathbb{X}} g(x)\,\mathrm{d}\rho_\infty(x) < \infty$*

$$\lim_{t\to\infty} |\mathbf{E}[g(x(t))] - \rho_\infty(g)| = 0.$$

We use the concept of geometric ergodicity [23, 24, 25, 26, 27] to strength the ergodic property of $x(t,\omega;x_0)$ and obtain information on the rate at which it converges to its limiting measure ρ_∞.

Definition 2 (Geometric Ergodicity)**.** *The process $x(t,\omega;x_0)$ is geometrically ergodic on $\mathbb{X}$, if there exist a unique invariant probability measure ρ_∞, positive constants C, λ and positive function $\mathcal{V}:\mathbb{X}\to[1,\infty)$ such that for any measurable function $g:\mathbb{X}\to\mathbb{R}$ with finite integral $\int_{\mathbb{X}} g(x)\,\mathrm{d}\rho_\infty(x) < \infty$ and with $|g(x)| \le \mathcal{V}(x)$*

$$|\mathbf{E}^{x_0}[g(x(t))] - \rho_\infty(g)| \le C\mathcal{V}(x_0)e^{-\lambda t}.$$

2.2 Stochastic Methods

2.2.1 Monte Carlo Method

Monte Carlo method is a statistical method of approximating expectations. It was first used by Ulam, Von Neumann and Metropolis to study the diffusion of neutrons in fissionable material. Let $x(t) \in \mathcal{M} \subseteq \mathbb{R}^n$ be a stochastic process and $f(x) > 0$ its transition probability density. Then the expectation (the average) of $g:\mathcal{M}\to\mathbb{R}$ is

$$\mathbf{E}[g(x)] = \int_{\mathcal{M}} g(x)f(x)\,\mathrm{d}x.$$

The Monte Carlo method is based on the following approximation

$$\mathbf{E}[g(x)] \simeq \frac{1}{n}\sum_{i=1}^{n} g(\bar{x}_i),$$

where $\bar{x}$ is a discrete process which approximates x (e.g., numerical solution of x). Let

$$S_n(g) = \frac{1}{n}\sum_{i=1}^{n} g(\bar{x}_i),$$

denote the Monte Carlo estimator of $\mathbf{E}[g(x)]$, then by the strong law of large numbers

$$\lim_{n\to\infty} P(|S_n(g) - \mathbf{E}[g(x)]| \geq \epsilon) = 0,$$

that is, $S_n(g)$ converges to $\mathbf{E}[g(x)]$ with probability 1. We also note that $S_n(g)$ is unbiased:

$$\mathbf{E}[S_n(g)] = \mathbf{E}\left[\frac{1}{n}\sum_{i=1}^{n} g(\bar{x}_i)\right] = \frac{1}{n}\sum_{i=1}^{n}\mathbf{E}[g(\bar{x}_i)] = \mathbf{E}[g(x)].$$

Moreover, if the variance

$$\mathrm{Var}(g(x)) = \mathbf{E}\left[(g(x) - \mathbf{E}[g(x)])^2\right]$$

exists, then by central limit theorem (CLT),

$$\sqrt{n}(S_n(g) - \mathbf{E}[g]) \to \mathcal{N}(0, \sigma^2) \quad \text{as } n \to \infty,$$

where $\sigma = \sqrt{\mathrm{Var}(g(x))}$ and $\mathcal{N}(0, \sigma^2)$ denotes Gaussian random variables with mean 0 and variance σ^2.

A simple application of the Monte Carlo method is the calculation of an integral. Let $g(x)$ be a continuous function and consider its integral $\int_a^b g(x)\,\mathrm{d}x$. Let X be a random variable uniformly distributed between a and b with probability density $f(X) = \frac{1}{(b-a)}$. Then we have

$$\int_a^b g(x)\,\mathrm{d}x = (b-a)\int_a^b g(x)\frac{1}{(b-a)}\,\mathrm{d}x = (b-a)\int_a^b g(x)f(x)\,\mathrm{d}x = (b-a)\mathbf{E}[g(X)].$$

Thus using the Monte Carlo we obtain the following approximation

$$\int_a^b g(x)\,\mathrm{d}x \simeq \frac{(b-a)}{n}\sum_{i=1}^{n} g(X_i).$$

Note that numerical quadrature techniques such as Simpson's Rule are efficient for low dimensional integral such as the above example, but such methods become useless for large dimensional integral such as computing averages for molecular systems. For a system of n atoms in three dimensional space, if we take m quadrature points in each direction, then the number of evaluations of the integrand is of order of m^{3n}. Moreover, in most systems the potential function that governs the interaction between atoms is a rapidly varying function and therefore quadrature techniques would require a fine mesh.

Therefore probabilistic interpretations of integral are the only sensible approaches for calculating large dimensional integral.

2.2.2 Importance Sampling

Importance Sampling is a type of Mote Carlo method which allows function evaluations to be concentrated in the regions that make the major contribution to the value of the expectation. Consider

$$\mathbf{E}[g(x)] = \int_{\mathcal{M}} g(x)f(x)\,\mathrm{d}x.$$

The idea is to choose random variables with probability density $\bar{f}(x)$, having the same support as $f(x)$. Next reformulate the above expectation as a weighted average:

$$\mathbf{E}[g(x)] = \int_{\mathcal{M}} g(x)f(x)\,\mathrm{d}x = \int_{\mathcal{M}} \left(g(x)\frac{f(x)}{\bar{f}(x)}\right)\bar{f}(x)\,\mathrm{d}x.$$

Then

$$S_N(g) = \frac{1}{n}\sum_{i=1}^{n} g(x_i)\frac{f(x_i)}{\bar{f}(x_i)}$$

is an unbiased estimator of $\mathbf{E}[g(x)]$. We call ρ the *target* density and $\bar{f}$ the *proposal* or the *sampling* density. For importance sampling to work the variation of the *important weights*:

$$\omega(x_i) = \frac{f(x_i)}{\bar{f}(x_i)}, \quad i = 1, \dots n,$$

should not be too large. For more detail on importance Sampling see the book by Robert and Casella [28], also see [7, 8].

2.2.3 Markov Chain Monte Carlo

The Metropolis-Hastings algorithm [29, 30] is a Markov chain Monte Carlo (MCMC) technique which provides an efficient way to sample from complicated probability distributions by using a Markov chain. Suppose we are given a density, for instance the Boltzmann-Gibbs density f_β which was defined in (1.17). We want to estimate the expectation of $g : \mathbb{X} = \mathcal{M} \subseteq \mathbb{R}^n \times \mathbb{R}^n \to \mathbb{R}$ with respect to f_β:

$$\mathbf{E}[g(x)] = \int_{\mathbb{X}} g(x)f_\beta(x)\,\mathrm{d}x,$$

where $x = (q, p) \in \mathbb{X}$ and $\mathrm{d}x = \mathrm{d}q\,\mathrm{d}p$. We would like to use the Monte Carlo method to get the following estimate

$$\mathbf{E}[g(x)] \simeq \frac{1}{n}\sum_{i=1}^{n} g(x_i).$$

However it is assumed to be very difficult to sample from f_β. The MCMC overcomes the sampling issue by constructing a Markov chain X_t on $\mathbb{X}$ which has transition probability

$$P(x, y) = \Pr(X_{t+1} = y | X_t = x)$$

and invariant measure with density f_β:

$$\int_{\mathbb{X}} f_\beta(x) P(x, y)\,\mathrm{d}q = f_\beta(y).$$

We also define the t-step transition probability by

$$P_t(x, y) = \begin{cases} P(x, y) & t = 1 \\ \sum_{z\in\mathbb{X}} P(x, z) P_{t-1}(z, y) & t > 1 \end{cases}$$

Therefore, for large t we expect that the distribution of X_t converges to ρ_β, so we can choose $x_1 = X_t$, and repeat the process n times to obtain a set of n independent samples and then use the Monte Carlo method to estimate the expectations. However, in practice, often rather than repeating the process n times an entire tail of Markov chain $\{X_t, \ldots, X_{t+n}\}$ is used to estimate the expectation. In that way the samples are not independent, but can be much cheaper computationally. We next describe an example of such a method.

The Metropolis-Hastings algorithm. The aim is to construct a Markov chain on $\mathbb{X}$ with transition density P that it is *reversible*, *irreducible* and *aperiodic* with ρ_β as its invariant probability measure.

- *Reversible*: $f_\beta(x)P(x, \tilde{x}) = f_\beta(\tilde{x})P(\tilde{x}, x)$ for all $x, \tilde{x} \in \mathbb{X}$;
- *Irreducible*: for all $x, \tilde{x} \in \mathbb{X}$ there exist a time t (possibly depends on x and $\tilde{x}$) such that $P_t(x, \tilde{x}) > 0$;
- *Aperiodic*: for all $\tilde{x} \in \mathbb{X}$, $\gcd\{t : P_t(\tilde{x}, \tilde{x}) > 0\} = 1$, (gcd means greatest common

divisor).

Let $P(x, y)$ be the *proposal* probability density for y, and assume that we know how to draw y from $P(x, y)$. In general

$$f_\beta(x)P(x, y) \neq f_\beta(y)P(y, x),$$

for example, if $f_\beta(x)P(x, y) > f_\beta(y)P(y, x)$, then the process moves from x to y frequently and from y to x rarely. To correct for this bias we introduce the *acceptance rate* function

$$\alpha(x, y) = \min\left\{1, \frac{f_\beta(y)P(y, x)}{f_\beta(x)P(x, y)}\right\},$$

such that

$$f_\beta(x)\alpha(x, y)P(x, y) = f_\beta(y)\alpha(y, x)P(y, x),$$

then we will have a reversible process with invariant f_β.

The Algorithm. In summary, the Metropolis-Hastings algorithm proceeds as follow: start from some initial configuration x_0, then, for $j \geq 1$ move from x_j to x_{j+1} by

1. Generate y_{j+1} from $P(x_j, y_{j+1})$.
2. Draw a random variable u from $\mathcal{U}[0, 1]$ (uniformly distributed in $[0, 1]$).
3. Compute
$$\alpha(x_j, y_{j+1}) = \min\left\{1, \frac{f_\beta(y_{j+1})P(y_{j+1}, x_j)}{f_\beta(x_j)P(x_j, y_{j+1})}\right\}.$$
4. If $u < \alpha(x_j, y_{j+1})$, then $x_{j+1} = y_{j+1}$. Otherwise $x_{j+1} = x_j$.

The Metropolis-Hastings algorithm depends on the choice of the proposal density, and a different choice of $P(x, .)$ leads to a different algorithm. Some of the popular choices of $P(x, .)$ are:

- **Symmetric**. Here $P(x, y) = P(y, x)$, hence the acceptance rate simplifies to
$$\alpha(x, y) = \min\left\{1, \frac{f_\beta(y)}{f_\beta(x)}\right\}.$$
- **Random walk**. Here $P(x, y) = P(y-x)$, for instance $y = x+\epsilon$, where ϵ is chosen from a normal distribution $N(0, \sigma^2)$ or a uniform distribution $\mathcal{U}[x-1, x+1]$. Note

that the acceptance rate depends on the choice of $\sigma^2 = \mathbf{E}[\epsilon^2]$. A small σ^2 will lead us to accept most draws, but not move very much, hence we will have difficulty covering the whole support of f_β. On the other hand, a large σ^2 increases the chance that a draw comes from the area where f_β is small, hence we will reject many draws. In either case the samples become highly correlated and we would need more draws to get a good estimate.

- **Independence sampler**. Here $P(x, y) = P(y)$, that is $P(\cdot)$ does not depend on x.

- **Metropolis-Adjusted Langevin**. Consider the Langevin diffusion process

$$\mathrm{d}X_t = \frac{1}{2}\nabla \ln\left(f_\beta(X_t)\right)\,\mathrm{d}t + \,\mathrm{d}W_t, \tag{2.1}$$

where W_t is a standard Brownian motion. It can be shown that the density of the stationary distribution of X_t is f_β. Furthermore

$$\|P_t(x,.) - f_\beta(.)\|_{L^1} \to 0 \text{ as } t \to \infty \quad \forall x \in \mathbb{X},$$

(see Chapter 3, for similar convergence result). The Metropolis Adjusted Langevin method [25] generates the proposal by a suitable discretization of (2.1). For example, starting at x we generate y according to

$$y = x + \frac{\Delta t}{2}\nabla \ln\left(f_\beta(x)\right)\,\mathrm{d}t + \sqrt{\Delta t}W_n,$$

where Δt is the step size and $W_n \sim N(0, 1)$.

For mathematical analysis of MCMC methods see the book by Meyn and Tweedie [23] and [31, 32, 33, 34].

2.3 Stochastic Molecular Dynamics

We have encountered several stochastic methods for sampling the canonical distribution. In this section, we will show how these methods may sometimes be combined to improve the efficiency of the sampling.

2.3.1 Hybrid Monte Carlo Method

When simulating a large system using the Monte Carlo technique, moves are made locally, that is, only some of the positions are allowed to change at each step. On the other hand in molecular dynamics (MD) all positions move according to the dynamics that have Boltzmann-Gibbs as its invariant measure. However, MD's estimation of the averages of functions of phase space is dependent on the step size in the integration method and if the dynamics are Hamiltonian or isokinetic, then the sampling is not ergodic with respect to the Boltzmann-Gibbs distribution.

The hybrid Monte Carlo (HMC) method [35] combines the advantages of MD and Monte Carlo methods. Let $\Phi_{\Delta t} : \mathbb{X} \to \mathbb{X}$, be a numerical flow map of some discretization of the equations of motion. For some initial position q and initial momenta p drawn from Maxwellian distribution, HMC integrates the equations of motion on the time interval $[0, m\Delta t = \tau]$ with initial data $x = (q, p)$ to obtain a new proposal

$$\tilde{x} = (\tilde{q}, \tilde{p}) := \Phi_{m\Delta t}(x) := \Phi_{\Delta t} \circ \cdots \circ \Phi_{\Delta t}(x)$$

for the Metropolis algorithm. The rate of the acceptance of $\tilde{x}$ is

$$\alpha(\tilde{x}) = \min\left\{1, e^{-\beta \delta H}\right\},$$

where $\delta H = H(\Phi_{m\Delta t}(x)) - H(x)$, i.e., the numerical error in energy conservation. The Boltzmann-Gibbs measure is invariant, if the Markov process generated by HMC is *reversible* (or satisfies *detailed balance*)

$$f_\beta(x) P(\tilde{x}|x) = f_\beta(\tilde{x}) P(x|\tilde{x}),$$

where $P(.,.)$ is the transition probability of HMC. In this way the computation of averages is independent of the step size and it does not suffer from numerical instabilities due to large step size. Thus, generally we can use a larger step size in HMC integration in comparison to standard molecular dynamics.

The Algorithm. The HMC algorithm proceeds as follow: start from some initial configuration q_0 and sampling time $\tau = m\Delta t$, then for $j \geq 0$ move from q_j to q_{j+1} by

1. Generate momenta p_j from Maxwellian distribution, and set $x = (q_j, p_j)$.

2. Compute the initial energy $H(x)$.

3. Integrate Hamilton equations of motion on the time interval $[0, \tau]$, i.e., use initial data x to obtain $\tilde{x} = (\tilde{q}, \tilde{p}) := \Phi_{m\Delta t}(x)$.

4. Compute the energy $H(\tilde{x})$, and generate a random number u uniformly distributed in $[0, 1]$.

5. Compute the acceptance rate

$$\alpha = \min\left\{1, e^{-\beta\delta H}\right\},$$

where $\delta H = H(\tilde{x}) - H(x)$. Then $q_{j+1} = \tilde{q}$, if $u < \alpha$. Otherwise $q_{j+1} = q_j$.

The ergodicity and convergence of HMC was proved in [36]. The HMC described here is known as the standard HMC, there are several enhanced versions. The acceptance can be improved by using a symplectic integrator and a modified Hamiltonian instead of the original Hamiltonian, the bias introduced is corrected by re-weighting, see [37, 38, 39, 40, 41].

2.3.2 Anderson Thermostat

One of the earliest and commonly used method to sample the canonical ensemble in molecular dynamics is the Anderson thermostat [42]. The idea is to represent the collision between the heat bath and the system by selecting all or some particles at each step Δt and replacing their momentum with probability $\gamma\Delta t$ by a momentum drawn from a Maxwellian distribution with density:

$$f_M = \frac{1}{Z_M} \exp\left(-\frac{\beta}{2}\|p\|^2\right).$$

The strength of the coupling to the heat bath is determined by the frequency of stochastic collisions, γ . If successive collisions are uncorrelated, then the distribution of time intervals between two successive stochastic collisions, $P(t;\gamma)$, is of the Poisson form

$$P(t;\gamma) = \gamma e^{-\gamma t},$$

where $P(t;\gamma)dt$ is the probability that the next collision will take place in the interval $[t, t + dt]$.

Here we describe a variant of the Anderson thermostat. Consider the flow map $\varphi_t(x)$ defined by

$$\frac{\mathrm{d}}{\mathrm{d}t}\varphi_t(x) = \mathbb{J}\nabla H(\varphi_t(x)),$$

where $x = (q, p) \in \mathbb{X}$ and $\mathbb{J}\nabla H$ is Hamiltonian vector field which was defined in (1.2). We let $\Phi_{\Delta t}(x)$ to be a numerical approximation of φ_t, for example the Störmer-Verlet approximation of the Hamiltonian flow map. For an integer $i \in [0, \cdots, n]$ we define the Anderson substitution map $S(i) : \mathbb{X} \to \mathbb{X}$ as:

$$S(i; x) := (q, p_1, \cdots, p_{i-1}, z, p_{i+1}, \cdots, p_n),$$

where z is the solution of

$$\mathrm{d}z = \frac{1}{2}\nabla \ln(f_M(z))\,\mathrm{d}t + \mathrm{d}W.$$

Let $\{Y_n\}$ be random variables such that

$$\Pr(Y_n = i) = \frac{1}{n} \text{ for any } i \in [0, \cdots, n],$$

and $\{U_n\}$ random variables uniformly distributed in $[0, 1]$. Starting form initial state x_0, the Anderson thermostat proceeds as follow:

$$x(\Delta t) = \begin{cases} S(Y_n) \circ \Phi_{\Delta t}(x_0) & \text{if } U_n < \gamma \Delta t \\ \Phi_{\Delta t}(x_0) & \text{otherwise.} \end{cases}$$

It was proved in [43] that the Anderson thermostat is uniformly ergodic, also an improved rate of convergence for one-dimensional case and n-dimensional free-steaming particles (constant potential) was proved in [44].

A similar method which is a combination of the Anderson thermostat and the dissipative particle dynamics (DPD) [45] is called Lowe-Anderson thermostat [46]. The Lowe-Anderson thermostat is Galilean invariant thermostat that conserves momentum, it also satisfies detailed balance. It was shown in [47] that the Lowe-Anderson thermostat perturbs the system to a less extent than the Anderson thermostat, hence it is better for computation of the dynamical averages such as diffusion constant. A generalised form for the Lowe-Anderson thermostat with momentum conservation which allowed for larger step size was proposed by Peters in [48] and by Pastewka et al in

[49].

2.3.3 Langevin Dynamics

A popular way to model a system in contact with a heat bath is to introduce a stochastic perturbation of dynamics which ignores the details of motion in heat bath itself [20, 19, 21, 50, 51]. This is the basis of the Langevin dynamics which we derived in the previous chapter. The Langevin dynamics replaces the Hamiltonian dynamics by the following stochastic differential equations.

$$\mathrm{d}q = M^{-1}p \ \mathrm{d}t, \tag{2.2}$$

$$\mathrm{d}p = -\nabla_q V(q) \ \mathrm{d}t - \gamma(q)p \ \mathrm{d}t + \sigma(q) \, \mathrm{d}W, \tag{2.3}$$

where $\gamma : \mathbb{R}^n \to \mathbb{R}^{n\times n}$ is the dissipation matrix, $\sigma : \mathbb{R}^n \to \mathbb{R}^{n\times n}$ is the diffusion matrix and we assume the fluctuation-dissipation relation $\sigma\sigma^T = \frac{2}{\beta}\gamma M$, which implies that the density of Boltzmann-Gibbs measure (1.17) is invariant under the evolution of (2.2)-(2.3). The above equations are also known as Klein-Kramers-Chandrasekhar equation, it was first studied by Krameres [52] for diffusion of chemical reactions.

The Langevin dynamics is a degenerate diffusion equation, since ellipticity only appears in the momenta direction, nonetheless it can be shown using hypoellipticity results [53, 54, 55] that the regularity in momenta effectively implies regularity in all directions, and ergodicity can be seen as a consequence of regularity. We will study the ergodicity and convergence rate of Langevin dynamics in Chapter 3.

2.4 Deterministic Methods

Another intriguing approach to generate the canonical ensemble is to augment the original system using one or several auxiliary variables ξ (or ξ_1, $\xi_2, \cdots$). These auxiliary variables are coupled to the original system and their dynamics is governed by some control equations on the kinetic energy, in such a way that the evolution of the extended system has an invariant measure which is proportional to the Boltzmann-Gibbs measure. We term these methods *deterministic thermostats*.

Here we briefly describe some of the most commonly used deterministic thermostats. In Chapter 6 we introduce a new dynamics for controlling temperature in non-equilibrium molecular dynamics simulations.

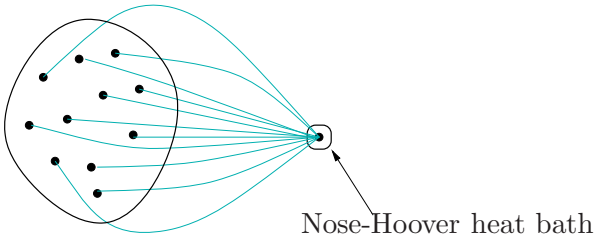

Figure 2.1: One variable ξ represents the heat bath and interacts with all degrees of freedom of the system.

2.4.1 Nosé-Hoover

One commonly used scheme which generates a canonical ensemble is Nosé-Hoover dynamics (NHD) [56, 57, 58]. NHD augments the physical system with one additional variable ξ which represents the interaction with an artificial heat bath and is coupled to all the degrees of freedom of the physical system. The dynamics of ξ is governed by a control function which regulates the kinetic energy of the system, (See Figure 2.1).

NHD replaces Hamiltonian dynamics with the following extended dynamical system:

$$\frac{\mathrm{d}q}{\mathrm{d}t} = M^{-1}p, \tag{2.4}$$

$$\frac{\mathrm{d}p}{\mathrm{d}t} = -\nabla_q V(q) - \xi p, \tag{2.5}$$

$$\frac{\mathrm{d}\xi}{\mathrm{d}t} = \frac{1}{\mu}\left(p^T M^{-1}p - \frac{n}{\beta}\right), \tag{2.6}$$

where μ is a constant which influences the coupling of the artificial heat bath to the system. It can be checked that the augmented Boltzmann-Gibbs density:

$$f_{NH}(q,p,\xi) = \frac{1}{Z_{NH}} \exp\left(-\beta\left(H(q,p) + \frac{\mu}{2}\xi^2\right)\right), \tag{2.7}$$

where

$$Z_{NH} = \int_{\mathbb{X}\times\mathbb{R}} \exp\left(-\beta\left(H(q,p) + \frac{\mu}{2}\xi^2\right)\right) \mathrm{d}q\,\mathrm{d}p\,\mathrm{d}\xi$$

is invariant under the evolution of (2.4)-(2.6), i.e.,

$$\frac{\partial f_{NH}}{\partial t} = \mathcal{L}_{NH} f_{NH} = \mathcal{L}_H f_{NH} - \nabla_p \cdot (\xi p f_{NH}) + \frac{\partial}{\partial \xi}\left[\frac{1}{\mu}\left(p^T M^{-1}p - \frac{1}{\beta}\right) f_{NH}\right] = 0,$$

where

$$\mathcal{L}_H f_{NH} = \nabla_q \cdot (\nabla_p H f_{NH}) - \nabla_p \cdot (\nabla_q H f_{NH}) = \{f_{NH}, H\}$$

is the Liouville operator applied to f_{NH}. Nosé-Hoover thermostat has been used suc-

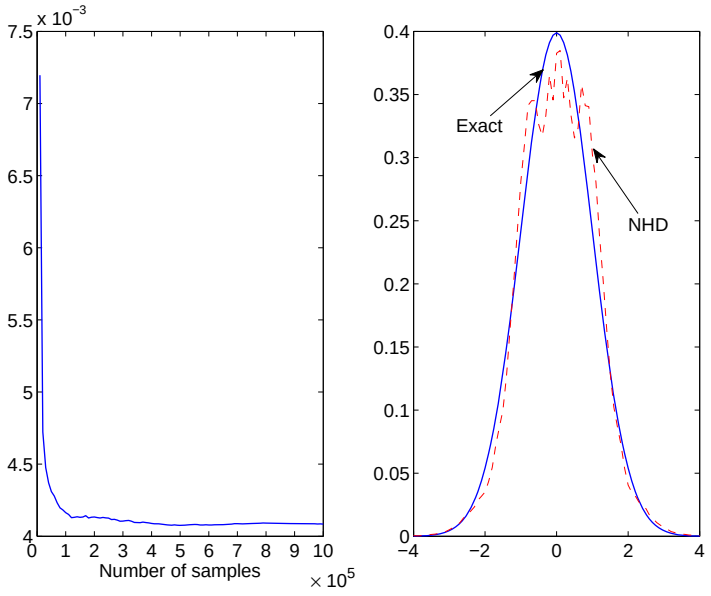

Figure 2.2: Nonergodicity of Nosé-Hoover for harmonic oscillator; the error in distribution remains unchanged in time.

cessfully in many MD simulations, its success is due to its control of kinetic energy and the fact that its perturbation to the dynamics is often seen to be less invasive than stochastic thermostats such as Langevin [59]. On the other hand, the evolution of Nosé-Hoover thermostat is not ergodic, see [60, 61, 58, 62, 63]. For example for harmonic oscillator with Hamiltonian:

$$H(q,p) = \frac{p^2}{2} + \frac{q^2}{2}$$

there are invariant islands in phase space (i.e., there exist $c, C > 0$ such that $c \leq q^2(t) + p^2(t) \leq C$ for all t) and no matter what initial condition we choose the distribution does not converge to Boltzmann-Gibbs distribution on a computationally accessible time scale, see Figure 2.2. For more details and generalisation of Nosé-Hoover for constant pressure simulation see [64, 65, 66, 67, 68].

2.4.2 Nosé-Hoover Chains

An alternative approach to NHD which can improve the the sampling is the Nosé-Hoover chain method (NHC) [62]. NHC is an extension of NHD which connects the system to a chain of artificial heat baths described by variables ξ_i, $i = 1, \ldots, m$ (not one ξ as in the case for NHD). ξ_1 interacts directly with the physical variables, ξ_2 is

connected to ξ_1, ξ_3 is connected to ξ_2 and so on, see Figure 2.3. In this way NHC adds more mixing and the evolution becomes close to ergodic. The equations of motion for NHC are:

$$\frac{\mathrm{d}q}{\mathrm{d}t} = M^{-1}p, \tag{2.8}$$

$$\frac{\mathrm{d}p}{\mathrm{d}t} = -\nabla_q V(q) - \xi_1 p, \tag{2.9}$$

$$\frac{\mathrm{d}\xi_1}{\mathrm{d}t} = \frac{1}{\mu_1}\left(p^T M^{-1}p - \frac{n}{\beta}\right) - \xi_2\xi_1, \tag{2.10}$$

$$\frac{\mathrm{d}\xi_k}{\mathrm{d}t} = \frac{1}{\mu_k}\left(\mu_{k-1}\xi_{k-1}^2 - \frac{1}{\beta}\right) - \xi_{k+1}\xi_k, \qquad k = 2, 3, \ldots, m-1 \tag{2.11}$$

$$\frac{\mathrm{d}\xi_m}{\mathrm{d}t} = \frac{1}{\mu_m}\left(\mu_{m-1}\xi_{m-1}^2 - \frac{1}{\beta}\right), \tag{2.12}$$

where m is the length of the chain and $\mu_i,\ i = 1, \cdots, m$ are coupling parameters associated to ξ_i. NHC preserves again an augmented version of Boltzmann-Gibbs measure with density:

$$f_{NHC}(q, p, \xi_1, \cdots, \xi_m) = \frac{1}{Z_{NHC}} \exp\left(-\beta\left[H(q,p) + \sum_{k=1}^{m}\frac{\mu_k}{2}\xi_k^2\right]\right), \tag{2.13}$$

where

$$Z_{NHC} = \int_{\mathbb{X}\times\mathbb{R}^m} \exp\left(-\beta\left[H(q,p) + \sum_{k=1}^{m}\frac{\mu_k}{2}\xi_k^2\right]\right) \mathrm{d}q\,\mathrm{d}p\,\mathrm{d}\xi_1\cdots\mathrm{d}\xi_m$$

is invariant under evolution of (2.8)-(2.12), more precisely

$$\frac{\partial f_{NHC}}{\partial t} = \mathcal{L}_{NHC} f_{NHC} = 0,$$

where

$$\mathcal{L}_{NHC} f_{NHC} = \mathcal{L}_H f_{NHC} - \nabla_p \cdot (\xi_1 p f_{NHC}) + \frac{\partial}{\partial \xi_1}\left[\left(\frac{1}{\mu_1}\left(p^T M^{-1}p - \frac{n}{\beta}\right) - \xi_2\xi_1\right) f_{NHC}\right]$$
$$+\sum_{k=2}^{m-1}\frac{\partial}{\partial \xi_k}\left[\left(\frac{1}{\mu_k}\left(\mu_{k-1}\xi_{k-1}^2 - \frac{1}{\beta}\right) - \xi_{k+1}\xi_k\right) f_{NHC}\right] + \frac{\partial}{\partial \xi_m}\left[\frac{1}{\mu_m}\left(\mu_{m-1}\xi_{m-1}^2 - \frac{1}{\beta}\right) f_{NHC}\right].$$

It is worth noting that the values of $\mu_i,\ i = 1, \cdots, m$ influence the sampling and they should be chosen such that the sampling is optimal. It was proposed in [62] that for a system with dominant frequency of ω one should choose $\mu_1 = n/\beta\omega^2$ and

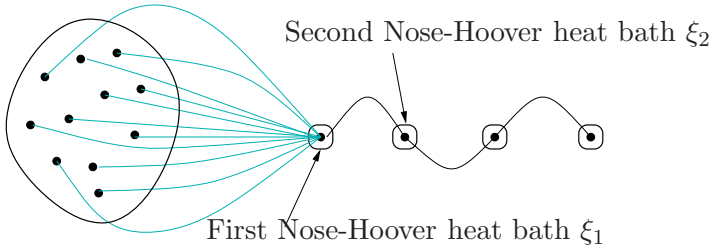

Figure 2.3: Each thermostat is connected to the previous one to form a chains of thermostats.

$\mu_k = 1/\beta\omega^2$, hence, the extended system maintains an average frequency of ω.

A nice review of numerical methods for equations of motion of NHC is given in [69], and explicit methods based on splitting technique are given in [70]. Our results have been obtained with method proposed in [69].

2.4.3 Nosé-Poincaré

Nosé-Hoover and Nosé-Hoover Chains are not Hamiltonian (their equations of motion cannot be derived from a Hamiltonian). The advantage of Hamiltonian system is that we can use symplectic integrator for which the energy is approximately preserved by the numerical flow [13, 5]. An alternative Hamiltonian-based formulation to NHD is the Nosé-Poincaré method (NP) [71].

NP is based on the following Hamiltonian:

$$H_{NP}(q,p,\xi,\eta) = \xi\left[\frac{p^T M^{-1} p}{2\xi^2} + V(q) + \frac{\eta^2}{2\mu} + \frac{n}{\beta}\ln\xi - H_0\right], \tag{2.14}$$

where ξ is the additional variable that represents the interaction with the heat bath and η is its conjugate momentum. For initial conditions $q(0) = q_0$, $p(0) = p_0$, $\xi(0) = \xi_0$, $\eta(0) = \eta_0$, H_0 is given by

$$H_0 = \frac{p_0^T M^{-1} p_0}{2\xi_0^2} + V(q_0) + \frac{\eta_0^2}{2\mu} + \frac{n}{\beta}\ln\xi_0,$$

hence $H_{NP} = 0$ for any given initial conditions. The equations of motion are:

$$\frac{\mathrm{d}q}{\mathrm{d}t} = \nabla_p H_{NP} = \frac{M^{-1}p}{\xi}, \tag{2.15}$$

$$\frac{\mathrm{d}p}{\mathrm{d}t} = -\nabla_q H_{NP} = -\xi \nabla_q V(q), \tag{2.16}$$

$$\frac{\mathrm{d}\xi}{\mathrm{d}t} = \frac{\partial H_{NP}}{\partial \eta} = \xi \frac{\eta}{\mu}, \tag{2.17}$$

$$\frac{\mathrm{d}\eta}{\mathrm{d}t} = -\frac{\partial H_{NP}}{\mathrm{d}\xi} = \frac{p^T M^{-1} p}{2\xi^2} - \frac{n}{\beta} - \Delta H, \tag{2.18}$$

where

$$\Delta H = \frac{p^T M^{-1} p}{2\xi^2} + V(q) + \frac{\eta^2}{2\mu} + \frac{n}{\beta} \ln \xi - H_0.$$

Note that by construction ΔH is zero for initial conditions and remains zero or close to zero, hence in (2.18), ΔH is considered as a small random force with mean zero.

As in the original Nosé dynamics [56, 57] the idea of NP is to compute canonical averages of functions of phase space by averaging along constant energy trajectories of the extended system. Let us introduce a change of variables

$$(q, p, \xi, \eta) \to (q, \tilde{p}, \xi, \eta), \text{ with } \tilde{p} = \frac{p}{\xi}$$

which is well defined since $\xi > 0$. Consider an observable $O(q, \tilde{p})$, its Nosé-Poincaré average is the microcanonical average of the extended system:

$$\rho_{NP}(O(q,\tilde{p})) = \frac{\int_{\mathbb{X}} \int_{\mathbb{R}} \int_{\mathbb{R}} O(q,\tilde{p}) \delta\left(H_{NP}(q,\tilde{p},\xi,\eta)\right) \xi^n \,\mathrm{d}q \,\mathrm{d}\tilde{p} \,\mathrm{d}\xi \,\mathrm{d}\eta}{\int_{\mathbb{X}} \int_{\mathbb{R}} \int_{\mathbb{R}} \delta\left(H_{NP}(q,\tilde{p},\xi,\eta)\right) \xi^n \,\mathrm{d}q \,\mathrm{d}\tilde{p} \,\mathrm{d}\xi \,\mathrm{d}\eta},$$

where ξ^n is the Jacobian for the above change of variables. For $f(x)$ and a smooth function $g(x)$, with $g(x_0) = 0$ we have the following relation for Dirac delta function

$$\int f(x) \delta(g(x)) \,\mathrm{d}x = \frac{f(x_0)}{|g'(x_0)|}.$$

Since $H_{NP}(q, \tilde{p}, \xi_0, \eta) = 0$ for

$$\xi_0 = \exp\left(-\frac{\beta}{n}\left[\frac{\tilde{p}^T M^{-1} \tilde{p}}{2} + V(q) + \frac{\eta^2}{2\mu} - H_0\right]\right),$$

applying the above relation we get

$$\rho_{_{NP}}(O(q,\tilde{p})) = \frac{e^{\beta H_0}\int_{\mathbb{X}} O(q,\tilde{p})\int_{\mathbb{R}} \exp\left(-\beta\left[\frac{\tilde{p}^T M^{-1}\tilde{p}}{2}+V(q)\right]\right) e^{-\frac{\beta}{2\mu}\eta^2}\,\mathrm{d}q\,\mathrm{d}\tilde{p}\,\mathrm{d}\eta}{e^{\beta H_0}\int_{\mathbb{X}}\int_{\mathbb{R}} \exp\left(-\beta\left[\frac{\tilde{p}^T M^{-1}\tilde{p}}{2}+V(q)\right]\right) e^{-\frac{\beta}{2\mu}\eta^2}\,\mathrm{d}q\,\mathrm{d}\tilde{p}\,\mathrm{d}\eta}.$$

Integration with respect to η:

$$\int_{\mathbb{R}} e^{-\frac{\beta}{2\mu}\eta^2}\,\mathrm{d}\eta = \sqrt{\frac{2\mu\pi}{\beta}},$$

yields

$$\begin{aligned}\rho_{_{NP}}(O(q,\tilde{p})) =& \frac{e^{\beta H_0}\sqrt{\frac{2\mu\pi}{\beta}}\int_{\mathbb{X}} O(q,\tilde{p})\exp\left(-\beta\left[\frac{\tilde{p}^T M^{-1}\tilde{p}}{2}+V(q)\right]\right)\,\mathrm{d}q\,\mathrm{d}\tilde{p}}{e^{\beta H_0}\sqrt{\frac{2\mu\pi}{\beta}}\int_{\mathbb{X}}\exp\left(-\beta\left[\frac{\tilde{p}^T M^{-1}\tilde{p}}{2}+V(q)\right]\right)\,\mathrm{d}q\,\mathrm{d}\tilde{p}}\\ =& \frac{\int_{\mathbb{X}} O(q,\tilde{p})\exp\left(-\beta H(q,\tilde{p})\right)\,\mathrm{d}q\,\mathrm{d}\tilde{p}}{\int_{\mathbb{X}}\exp\left(-\beta H(q,\tilde{p})\right)\,\mathrm{d}q\,\mathrm{d}\tilde{p}}\\ =& \rho_\beta(O(q,\tilde{p}))\end{aligned}$$

where $H(q,\tilde{p}) = \frac{\tilde{p}^T M^{-1}\tilde{p}}{2} + V(q)$. This concludes that, given the assumption that the dynamics of $H_{_{NP}}$ is ergodic, then the canonical average in $(q,\tilde{p})$ can be obtained by time average along trajectories of $H_{_{NP}}$.

Symplectic and time-reversible integrator for NP can be derived using generalised leapfrog method [10, 11, 72] or splitting techniques [10, 13]. We use an integrator based on generalised leapfrog which was proposed in [71].

2.4.4 Recursive Multiple Thermostats

A Hamiltonian-based formulation that can add more thermostats variables to the system is Recursive Multiple Thermostats (RMT) which was proposed in [73]. RMT with m thermostats variables is based on the following Hamiltonian

$$\begin{aligned}H_{_{RMT}}(q,p,\xi_1,\cdots,\xi_m,\eta_1,\cdots,\eta_m) = \xi_1\cdots\xi_m\Big(&\frac{p^T M^{-1}p}{2\xi_1^2\cdots\xi_m^2} + V(q) + \sum_{i=1}^{m-1}\frac{\eta_i^2}{2\mu_i\xi_{i+1}^2\cdots\xi_m^2}\\ &+ \frac{\eta_m^2}{2\mu_m} + \frac{n+1}{\beta}\ln\xi_1 + \sum_{i=2}^{m}\left(\frac{n+i-1}{\beta}\ln\xi_i + f_i(\xi_i)\right) - H_0\Big),\end{aligned} \tag{2.19}$$

where, again as was the case for NP, H_0 is chosen such that $H_{_{RMT}} = 0$, $\mu_i,\ i = 1,\cdots,m$ are coupling parameters associated to ξ_i and $f_i(\xi_i)$ is an auxiliary function that is

included to make the integral with respect to ξ_i finite:

$$\int_0^\infty e^{-\beta f_i(x)}\,\mathrm{d}x < \infty.$$

For an observable $O(q,\tilde{p})$, where $\tilde{p} = \frac{p}{\xi_1 \cdots \xi_m}$, similarly to NP one can show that micro-canonical average yields canonical average for $(q,\tilde{p})$:

$$\rho_\beta(O(q,\tilde{p})) = \frac{\int_{\mathbb{X}}\int_{\mathbb{R}^m}\int_{\mathbb{R}^m} O(q,\tilde{p})\delta\left(H_{RMT}(q,\tilde{p},\xi,\eta)\right)\xi^n\,\mathrm{d}q\,\mathrm{d}\tilde{p}\,\mathrm{d}\xi\,\mathrm{d}\eta}{\int_{\mathbb{X}}\int_{\mathbb{R}^m}\int_{\mathbb{R}^m} \delta\left(H_{RMT}(q,\tilde{p},\xi,\eta)\right)\xi^n\,\mathrm{d}q\,\mathrm{d}\tilde{p}\,\mathrm{d}\xi\,\mathrm{d}\eta}.$$

It was observed in [73, 74] that at least for some potentials the results of sampling can be less dependent on the choice of parameters μ_i than the Nosé-Hoover chains method. The generalised leapfrog method [10, 11, 72] or splitting techniques [10, 13] can be used to derive symplectic and time-reversible integrator for RMT. A such numerical integrator is proposed in [74, 75].

2.5 Numerical Integrators for Langevin Dynamics

The sampling performance of Langevin dynamics is dependent on the integration method that we use to solve equations (2.2)-(2.3). We want the numerical integration to preserve the Boltzmann-Gibbs measure (1.17). A general technique for designing integrator is based on extending the Hamiltonian schemes to Langevin dynamics. Examples are quasi-symplectic integrators [76, 77, 78]. Another approach is to extend the idea of splitting of operator that is used in deterministic flows to Langevin dynamics [10, 79, 80, 81]. The general result of error analysis holds for integrator of Langevin dynamics when the forces are globally Lipschitz.

Consider a simplified version of Langevin dynamics:

$$\mathrm{d}q = M^{-1}p\,\mathrm{d}t, \tag{2.20}$$

$$\mathrm{d}p = -\nabla_q V(q)\,\mathrm{d}t - \gamma p\,\mathrm{d}t + \sigma\,\mathrm{d}W, \tag{2.21}$$

where $\gamma > 0$ is constant, $M = mI_n$ and $\sigma^2 = \frac{2}{\beta}\gamma m$. Integrating Langevin's equations

we obtain

$$\begin{aligned} q(t+\Delta t) =& q(t) + \int_t^{t+\Delta t} M^{-1} p(s)\,\mathrm{d}s, \\ p(t+\Delta t) =& p(t) - \int_t^{t+\Delta t} \nabla_q V(q(s))\ \mathrm{d}s - \gamma \int_t^{t+\Delta t} p(s)\,\mathrm{d}s + \sigma \int_t^{t+\Delta t} \mathrm{d}W(s), \end{aligned}$$

where $\int_t^{t+\Delta t} \mathrm{d}W(s)$ are Gaussian with mean zero and variance

$$\mathbf{E}\left[\left(\int_t^{t+\Delta t} \mathrm{d}W(s)\right)^2\right] = \Delta t.$$

Hence $\int_t^{t+\Delta t} \mathrm{d}W(s)$ in distribution is equal to $\sqrt{\Delta t}\eta$, where η is n-dimensional normal random variable (i.e., $\eta_i \sim \mathcal{N}(0,1)$). Using the approximations:

$$\int_t^{t+\Delta t} p(s)\,\mathrm{d}s = \Delta t p(t) + \mathcal{O}(\Delta t^2) \text{ and } \int_t^{t+\Delta t} \nabla_q V(q(s))\ \mathrm{d}s = \Delta t \nabla_q V(q(t)) + \mathcal{O}(\Delta t^2)$$

in (2.20)-(2.21) and neglecting terms of order $\Delta t^{3/2}$ or higher yields

$$q^{k+1} = q^k + \Delta t M^{-1} p^k, \tag{2.22}$$

$$p^{k+1} = p^k - \Delta t \nabla_q V(q^k) - \Delta t \gamma p^k + \sigma\sqrt{\Delta t}\eta^k, \tag{2.23}$$

where $\{\eta^k\}$ are n-dimensional normal random variables. The above method is known as Euler-Maruyama [82, 83]. We denote numerical approximation of $(q(k\Delta t), p(k\Delta t))$ by (q^k, p^k). For globally Lipschitz force, the resulting Markov chain (2.22)-(2.23) is ergodic and for small Δt its invariant measure is close to ρ_β [84].

Integrators Based on Splitting

One way to design an integrator for Langevin dynamics (2.2)-(2.3) is to split it into a Hamiltonian:

$$\mathrm{d}q = M^{-1} p\ \mathrm{d}t, \tag{2.24}$$

$$\mathrm{d}p = -\nabla_q V(q)\ \mathrm{d}t, \tag{2.25}$$

and a stochastic part:

$$\mathrm{d}q = 0, \tag{2.26}$$

$$\mathrm{d}p = -\gamma p \, \mathrm{d}t + \sigma \, \mathrm{d}W. \tag{2.27}$$

The stochastic equation (Ornstein-Uhlenbeck process)

$$\mathrm{d}p = -\gamma p \, \mathrm{d}t + \sigma \, \mathrm{d}W$$

can be solve exactly:

$$\begin{aligned} p(t) =& e^{-\gamma t} p(0) + \sigma \int_0^t e^{\gamma(s-t)} \, \mathrm{d}W(s) \\ =& e^{-\gamma t} p(0) + B(t). \end{aligned}$$

The $B(t) = \sigma \int_0^t e^{\gamma(s-t)} \, \mathrm{d}W(s)$ are Gaussian with mean zero and variance

$$\mathbf{E}[B(t)B(t)] = \sigma^2 \mathbf{E}\left[\left(\sigma \int_0^t e^{\gamma(s-t)} \, \mathrm{d}W(s) \right)^2 \right].$$

Using Itô isometry we obtain

$$\mathbf{E}[B(t)B(t)] = \sigma^2 \mathbf{E}\left[\int_0^t e^{2\gamma(s-t)} \, \mathrm{d}s \right] = \sigma^2 \left(\frac{1 - e^{-2\gamma t}}{2\gamma} \right) = \frac{m(1 - e^{-2\gamma t})}{\beta}.$$

Hence, for $x = (q, p) \in \mathbb{X}$ we can introduce $\Theta_{\Delta t} : \mathbb{X} \to \mathbb{X}$ as a discrete solution of the stochastic part by

$$\Theta_{\Delta t}(x) := (q, e^{-\gamma \Delta t} p + \sqrt{\frac{m(1 - e^{-2\gamma \Delta t})}{\beta}} \eta),$$

where η is n-dimensional normal random variable with mean zero and variance 1. Let $\Phi_{\Delta t}$ be the Störmer-Verlet solution of the Hamiltonian part, the composite method is

$$(q^{k+1}, p^{k+1}) := \Phi_{\Delta t} \circ \Theta_{\Delta t}(q^k, p^k)$$

defined by

$$\begin{aligned} p^{k+1/2} :=& e^{-\gamma\Delta t}p^k - \frac{\Delta t}{2}\nabla_q V(q^k) + \sqrt{\frac{m(1-e^{-2\gamma\Delta t})}{\beta}}\eta^k, \\ q^{k+1} =& q^k + \Delta t M^{-1}p^{k+1/2}, \\ p^{k+1} =& p^{k+1/2} - \frac{\Delta t}{2}\nabla_q V(q^{k+1}), \end{aligned}$$

where $\{\eta^k\}$ are n-dimensional normal random variables with mean zero and variance 1. A method same as above was studied in [85] and was shown to be quasi-symplectic and geometrically ergodic. It is also first-order strongly convergent [85].

Another method is obtained by splitting Hamiltonian part into kinetic and potential

$$H(q,p) = H_1 + H_2, \quad H_1(q,p) = \frac{p^T M^{-1} p}{2} \text{ and } H_2(q,p) = V(q).$$

Let

$$\Phi_{\Delta t, H_1}(q,p) := (q + \Delta t M^{-1}p, p) \text{ and } \Phi_{\Delta t, H_2}(q,p) := (q, p - \Delta t \nabla_q V(q))$$

be the discrete maps for solutions of H_1 and H_2. The composition

$$(q^{k+1}, p^{k+1}) := \Phi_{\Delta t/2, H_1} \circ \Theta_{\Delta t/2} \circ \Phi_{\Delta t, H_2} \circ \Phi_{\Delta t/2, H_1} \circ \Theta_{\Delta t/2}(q^k, p^k)$$

gives an integrator for Langevin dynamics, given by

$$\begin{aligned} p^{k+1/2} :=& e^{-\gamma\Delta t/2}p^k - \frac{\Delta t}{2}\nabla_q V(q^k) + \sqrt{\frac{m(1-e^{-\gamma\Delta t})}{\beta}}\eta^k, \\ q^{k+1} =& q^k + \Delta t M^{-1}p^{k+1/2}, \\ p^{k+1} =& e^{-\gamma\Delta t/2}p^{k+1/2} - \frac{\Delta t}{2}\nabla_q V(q^{k+1}) + \sqrt{\frac{m(1-e^{-\gamma\Delta t})}{\beta}}\zeta^k, \end{aligned}$$

where $\{\eta^k\}$ and $\{\zeta^k\}$ are independent sets of n-dimensional normal random variables. A method for rigid body dynamics that would simplifies to the above was studied in [86] and was shown to be quasi-symplectic and second-order (in the weak sense).

The BBK Method

The BBK method proposed by Brünger, Brooks and Karplus [87], is a generalisation

of Störmer-Verlet method to Langevin equations (2.20)-(2.21). BBK have been used in many molecular simulations and it was shown to preform well for small values of γ [88, 89], for large values of γ impulse integrator [90, 91] or second order method proposed in [92] is recommended [93]. BBK is given by

$$p^{k+1/2} = p^k - \frac{\Delta t}{2}\nabla_q V(q^k) - \frac{\Delta t}{2}\gamma p^k + \sigma\frac{\sqrt{\Delta t}}{2}\eta^k, \tag{2.28}$$

$$q^{k+1} = q^k + \Delta t M^{-1} p^{k+1/2}, \tag{2.29}$$

$$p^{k+1} = \frac{p^{k+1/2} - \frac{\Delta t}{2}\nabla_q V(q^{k+1}) + \sigma\frac{\sqrt{\Delta t}}{2}\eta^k}{1 + \Delta t\gamma/2}, \tag{2.30}$$

where $\{\eta^k\}$ are n-dimensional normal random variables. The original BBK uses a different random variable in (2.30), our version above is similar to method proposed in [94], different random variables introduces bias in average kinetic energy [93]. In the absence of noise (i.e., $\gamma = 0$) BBK simply becomes Störmer-Verlet, and the implementation is very simple, perhaps this is the reason for its popularity.

Chapter 3

The Approach to Equilibrium

In many applications modelling requires understanding the kinetic and long-time behaviour of systems composed of large number of interacting particles. It is known that such systems have a tendency to go to their equilibrium as time increases. In thermodynamics the approach to equilibrium is explained by the second law of thermodynamics. Let $f(q,p,t)$ be the density of position $q \in \mathcal{M} \subseteq \mathbb{R}^n$ and momenta $p \in \mathbb{R}^n$ of particles in phase space $\mathbb{X} = \mathcal{M} \times \mathbb{R}^n$. It was discovered by Boltzmann in the 1870's that the functional (entropy)

$$S(f) = -\int_{\mathbb{X}} f(q,p,t) \log f(q,p,t)\, \mathrm{d}q\, \mathrm{d}p, \tag{3.1}$$

is increasing in time. Later Gibbs showed that the equilibrium distribution is the one which achieves the maximum entropy under the constraints imposed by conservation laws (i.e., conservation of mass and kinetic energy). Since the maximiser of (3.1) is a Gaussian distribution we expect f to become nearly Gaussian as $t \to \infty$.

The object of this chapter is to study the rate of convergence to equilibrium for solutions of Fokker-Planck equations arising from molecular dynamics applications. The Fokker-Planck operators that we study are elliptic or hypoelliptic, hence the solution f is always continuous with respect to the Lebesgue measure.

Let $\mathrm{d}\rho = f\,\mathrm{d}x$, and let $\mathrm{d}\rho_\infty = f_\infty\,\mathrm{d}x$ be the equilibrium measure. Since the entropy attains its maximum at ρ_∞ we can measure the distance of ρ from ρ_∞ using the *relative entropy* [95] $H(\rho|\rho_\infty)$ defined by

$$H(\rho|\rho_\infty) = \int_{\mathbb{X}} \log \frac{\mathrm{d}\rho}{\mathrm{d}\rho_\infty}\, \mathrm{d}\rho = \int_{\mathbb{X}} \frac{\mathrm{d}\rho}{\mathrm{d}\rho_\infty} \log \frac{\mathrm{d}\rho}{\mathrm{d}\rho_\infty}\, \mathrm{d}\rho_\infty,$$

or equivalently by

$$H(f|f_\infty) = \int_{\mathbb{X}} f \log \frac{f}{f_\infty} \, \mathrm{d}x. \tag{3.2}$$

We also define the relative *Fisher information* [95] by

$$I(\rho|\rho_\infty) = \int_{\mathbb{X}} \left| \nabla \log \frac{\mathrm{d}\rho}{\mathrm{d}\rho_\infty} \right|^2 \mathrm{d}\rho = 4 \int_{\mathbb{X}} \left| \nabla \sqrt{\frac{\mathrm{d}\rho}{\mathrm{d}\rho_\infty}} \right|^2 \mathrm{d}\rho_\infty$$

or equivalently by

$$I(f|f_\infty) = \int_{\mathbb{X}} f \left| \nabla \log \frac{f}{f_\infty} \right|^2 \mathrm{d}x, \tag{3.3}$$

where $|x| = \sqrt{x \cdot x}$ denotes the square norm on $\mathbb{X}$, and ∇ is the gradient on $\mathbb{X}$.

Thus, we we avoid proving directly that ρ converges to ρ_∞ and instead we show that $H(\rho|\rho_\infty)$ converges to zero which is dubbed "convergence in relative entropy". Using the *Csiszár-Kullback-Pinsker* inequality [96, 97, 98]

$$\|\rho - \rho_\infty\|_{L^1} = \int_{\mathbb{X}} |\rho - \rho_\infty| \, \mathrm{d}\rho_\infty \leq \sqrt{2 \int_{\mathbb{X}} \log \frac{\mathrm{d}\rho}{\mathrm{d}\rho_\infty} \, \mathrm{d}\rho_\infty} = \sqrt{2H(\rho|\rho_\infty)}, \tag{3.4}$$

convergence in relative entropy implies convergence of ρ to ρ_∞ in the L^1 norm, this is why relative entropy is a good way of controlling the distance between probability measures.

In order to prove that $H(\rho|\rho_\infty)$ converges to zero we study the entropy dissipation which is the negative time derivative of the entropy $-\mathrm{d}H(f|f_\infty)/\mathrm{d}t$. The idea is to find a functional inequality of type

$$-\frac{\mathrm{d}}{\mathrm{d}t} H(f|f_\infty) \geq \Theta(H(f|f_\infty)), \tag{3.5}$$

if Θ is known, then it is possible to find an explicit bound for the rate of convergence to equilibrium. In particular if $\Theta(H(f|f_\infty)) = \lambda H(f|f_\infty)$, then Equation (3.5) implies exponential convergence to equilibrium with the speed given by λ.

Another way to measure the distance between two probability measures is the Wasserstein distance [95], or transportation distance with quadratic cost

$$W(\rho, \rho_\infty) = \sqrt{\inf_{\pi \in \Pi(\rho, \rho_\infty)} \int_{\Omega \times \Omega} \mathrm{d}_\Omega(x, y)^2 \, \mathrm{d}\pi(x, y)}, \tag{3.6}$$

where Ω is a smooth complete Riemannian manifold of dimension n with geodesic

distance

$$\mathrm{d}_\Omega(x,y) = \inf\left\{\sqrt{\int_0^1 |\dot{w}(t)|^2\,\mathrm{d}t}\,;\ w\in C^1((0,1);\Omega),\ w(0)=x,\ w(1)=y\right\},$$

$\Pi(\rho,\rho_\infty)$ denotes the set of probability measure on $\Omega\times\Omega$ such that their marginals are ρ and ρ_∞, that is for all bounded continuous functions h and g on Ω

$$\int_\Omega [h(x)+g(y)]\ \mathrm{d}\pi(x,y) = \int_\Omega h\ \mathrm{d}\rho + \int_\Omega g\ \mathrm{d}\rho_\infty.$$

The Wasserstein distance is well established in probability theory and statistics, and its application to entropy dissipation and convergence to equilibrium was shown in works by Marton [99] and Talagrand [100]. Let the reference measure be the standard Gaussian measure

$$\mathrm{d}\rho_\infty = \frac{e^{-\frac{1}{2}|x|^2}}{(2\pi)^{n/2}},$$

Talagrand [100] proved that

$$W(\rho,\rho_\infty) \le \sqrt{2H(\rho|\rho_\infty)}.$$

3.1 Some Functional Inequalities

Definition 3 (Poincaré Inequality [95]). *We say that a probability measure ρ, on $\mathbb{R}^n$ satisfies a Poincaré inequality with constant λ, if for all smooth functions u*

$$\int_{\mathbb{R}^n} u^2\,\mathrm{d}\rho - \left(\int_{\mathbb{R}^n} u\,\mathrm{d}\rho\right)^2 \le \frac{1}{\lambda}\int_{\mathbb{R}^n} |\nabla u|^2\,\mathrm{d}\rho \tag{3.7}$$

We say that ρ admits a spectral gap with constant λ if for all smooth functions u on $\mathbb{R}^n$ with $\int_{\mathbb{R}^n} u\,\mathrm{d}\rho = 0$, the following Poincaré inequality holds:

$$\int_{\mathbb{R}^n} u^2\,\mathrm{d}\rho \le \frac{1}{\lambda}\int_{\mathbb{R}^n} |\nabla u|^2\,\mathrm{d}\rho. \tag{3.8}$$

Definition 4 (Weak Poincaré Inequality [95]). *We say that a probability measure ρ on $\mathbb{R}^n$ satisfies a weak Poincaré inequality, if for all smooth functions u, $s>0$ and a*

non-deceasing function $b(s)$

$$\int_{\mathbb{R}^n} u^2 \,\mathrm{d}\rho - \left(\int_{\mathbb{R}^n} u \,\mathrm{d}\rho\right)^2 \leq b(s) \int_{\mathbb{R}^n} |\nabla u|^2 \,\mathrm{d}\rho + s \,\mathrm{osc}(u)^2, \tag{3.9}$$

where $\mathrm{osc}(u) = \sup(u) - \inf(u)$.

Let us define the Sobolev space

$$W^{1,p}(\mathbb{R}^n) = \{u \in L^p(\mathbb{R}^n) \,;\, \nabla u \in L^p(\mathbb{R}^n)\}\,, \tag{3.10}$$

where $n \geq 1$ is an integer and $p \geq 1$ is a real number. When $p \in [1, n)$ define $p^* = \frac{np}{n-p}$, the classical Sobolev inequality states that whenever u is in $W^{1,p}(\mathbb{R}^n)$ then it is also in $L^{p^*}(\mathbb{R}^n)$.

Definition 5 (Sobolev Inequality [95])**.** *Let* $u \in W^{1,p}(\mathbb{R}^n)$ *then* $u \in L^{p^*}(\mathbb{R}^n)$ *and there exists a constant* $C_n(p) > 0$ *which depends on* n *and* p *such that*

$$\|u\|_{L^{p^*}} \leq C_n(p) \|\nabla u\|_{L^p}. \tag{3.11}$$

This result is known as the Sobolev embedding theorem [101] since it asserts that

$$W^{1,p}(\mathbb{R}^n) \subset L^{p^*}(\mathbb{R}^n).$$

Definition 6 (Logarithmic Sobolev Inequality [102, 103, 104])**.** *Let* ρ_∞ *be a reference probability measure on* $\mathbb{R}^n$*, absolutely continuous with respect to Lebesgue measure.* ρ_∞ *satisfies a logarithmic Sobolev inequality with constant* $\lambda > 0$ *(in short: LSI(*λ*)) if for all probability measures* ρ *absolutely continuous with respect to* ρ_∞

$$H(\rho|\rho_\infty) \leq \frac{1}{2\lambda} I(\rho|\rho_\infty). \tag{3.12}$$

It is called logarithmic Sobolev inequality because (3.12) can be rewritten as

$$\int |u|^2 \log |u|^2 \,\mathrm{d}\rho_\infty \leq 2\lambda \int |\nabla u|^2 \,\mathrm{d}\rho_\infty + \left(\int |u|^2 \,\mathrm{d}\rho_\infty\right) \log \left(\int |u|^2 \,\mathrm{d}\rho_\infty\right) \tag{3.13}$$

which asserts the embedding of the weighted Sobolev space

$$W^{1,2}(\,\mathrm{d}\rho_\infty) = \left\{u \in L^2(\,\mathrm{d}\rho_\infty) \,;\, \nabla u \in L^2(\,\mathrm{d}\rho_\infty)\right\}$$

into the Orlicz space

$$L^2 \log L(\,\mathrm{d}\rho_\infty) = \left\{ u \in L^2(\,\mathrm{d}\rho_\infty)\,;\, \int |u|^2 \log |u|\,\mathrm{d}\rho_\infty < \infty \right\}.$$

Logarithmic Sobolev inequality shares the characteristic of all above inequalities. Comparing the logarithmic Sobolev embedding

$$W^{1,2}(\,\mathrm{d}\rho_\infty) \subset L^2 \log L(\,\mathrm{d}\rho_\infty) \tag{3.14}$$

with the Sobolev embedding

$$W^{1,2}(\mathbb{R}^n) \subset L^{\frac{2n}{n-2}}(\mathbb{R}^n), \quad n \geq 3. \tag{3.15}$$

We first note that (3.14) is taken with respect of a probability measure (e.g. Gaussian) whereas (3.15) does not hold in this case. Secondly, both the embedding space and the constant of embedding are independent of the dimension. On the other hand, the exponent $2n/(n-2)$ tends to 2 as $n \to \infty$ but at the same limit the constant of embedding blows up in the classical Sobolev inequality (3.11). In this sense logarithmic Sobolev inequality is stronger than the classical Sobolev inequality. It has been shown by Beckner [105] that (3.14) can be approximated by a version of (3.15) on n-dimensional sphere, with sharp constants, as $n \to \infty$. Hence in some sense the logarithmic Sobolev inequality can be seen as an infinite dimensional version of the classical Sobolev inequality.

Theorem 1 (Rothaus [106])**.** *Let the probability measure ρ satisfies the logarithmic Sobolev inequality (3.12) with constant λ. Then ρ also satisfies the Poincaré inequality (3.8) with constant λ.*

This is an important result, since it signifies that we lose nothing working in more general framework of the logarithmic Sobolev inequality.

The Poincaré inequality (3.8) can be seen as a linearised version of the logarithmic Sobolev inequality. Let g be smooth function such that $\int g\,\mathrm{d}\rho_\infty = 0$, and set $\rho = (1+\epsilon g)\rho_\infty$, then as $\epsilon \to 0$,

$$H(\rho|\rho_\infty) \simeq \frac{\epsilon^2}{2} \int g^2\,\mathrm{d}\rho_\infty, \quad I(\rho|\rho_\infty) \simeq \epsilon^2 \int |\nabla g|^2\,\mathrm{d}\rho_\infty.$$

Theorem 2 (Bakry and Emery [107]). *Let* $\mathrm{d}\rho_\infty = e^{-V}\,\mathrm{d}x$ *be a probability measure on* $\mathbb{R}^n$ *(resp. a Riemannian manifold* $\mathcal{M}$*), such that* $D^2V \geq \lambda I_n$ *(resp.* $D^2V + \mathrm{Ric} \geq \lambda I_n$*). Then* ρ_∞ *satisfies the logarithmic Sobolev inequality (3.12) with constant* λ*.*

In the above V is the potential function, D^2V stands for Hessian of V, I_n denotes the identity matrix of dimension n and Ric stands for Ricci curvature tensor on $\mathcal{M}$.

Theorem 3 (Holley and Stroock [108]). *Let* $V = V_0 + g$*, where* $g \in L^\infty$*, if* e^{-V_0} *satisfies the logarithmic Sobolev inequality with constant* λ*, then* e^{-V} *also satisfies the logarithmic Sobolev inequality, with constant* $\lambda e^{-\mathrm{osc}(g)}$*.*

The combination of Theorems 2 and 3 enables us to apply logarithmic Sobolev inequality to a wider class of potentials in statistical physics, such a double-well potential $V(x) = ax^4 - bx^2$.

Definition 7 (Talagrand Inequality [95]). *The probability measure* ρ_∞ *satisfies the Talagrand inequality with constant* $\lambda > 0$ *(in short* $T(\lambda)$*) if for all probability measures* ρ *absolutely continuous with respect to* ρ_∞ *and with finite moments of order 2*

$$W(\rho_\infty, \rho) \leq \sqrt{\frac{2H(\rho_\infty|\rho)}{\lambda}}. \tag{3.16}$$

Definition 8. *The probability measure* ρ_∞ *satisfies* $LSI + T(\lambda)$ *if for all probability measures* ρ *absolutely continuous with respect to* ρ_∞*, with finite moments of order 2*

$$W(\rho_\infty, \rho) \leq \frac{1}{\lambda}\sqrt{I(\rho_\infty|\rho)}. \tag{3.17}$$

The following theorem due to Villani and Otto [109] shows that the logarithmic Sobolev inequality (3.12) is stronger than the Talagrand inequality (3.16).

Theorem 4 (Villani and Otto [109]). *Let* $\mathrm{d}\rho_\infty = e^{-V}\,\mathrm{d}x$ *be a probability measure with finite moment of order 2, such that* $V \in C^2(\mathbb{R}^n)$ *and* $D^2V \geq CI_n$*,* $C \in \mathbb{R}$*. If* ρ_∞ *satisfies* $LSI(\lambda)$ *for some* $\lambda > 0$*, then it also satisfies* $T(\lambda)$*, and thus* $LSI + T(\lambda)$*.*

Using results of Theorem 2 and Theorem 4 we obtain the following corollary.

Corollary 1. *Let* $\mathrm{d}\rho_\infty = e^{-V}\,\mathrm{d}x$ *be a probability measure with finite moment of order 2, such that* $V \in C^2(\mathbb{R}^n)$ *and* $D^2V \geq \lambda I_n$*,* $\lambda > 0$*. Then* $T(\lambda)$ *holds.*

Since $LSI + T(\lambda)$ is a weaker inequality, it is natural to ask, what can we gain from $LSI + T(\lambda)$. This question was answered in [109] by finding a general interpolation between the functionals H, W and I.

Theorem 5 (Villani and Otto [109]). *Let* $\mathrm{d}\rho_\infty = e^{-V}\,\mathrm{d}x$ *be a probability measure with finite moment of order 2, such that* $V \in C^2(\mathbb{R}^n)$ *and* $D^2V \geq CI_n$, $K \in \mathbb{R}$. *Then, for all probability measures* ρ *on* $\mathbb{R}^n$, *absolutely continuous with respect to* ρ_∞, *hold the following "HWI inequality":*

$$H(\rho|\rho_\infty) \leq W(\rho,\rho_\infty)\sqrt{I(\rho|\rho_\infty)} - \frac{K}{2}W(\rho|\rho_\infty)^2. \tag{3.18}$$

This is a nice general result that can be used to find a relation between different inequalities. Note that

- In the case where V is convex, we have $D^2V \geq 0$ which implies

$$H(\rho|\rho_\infty) \leq W(\rho,\rho_\infty)\sqrt{I(\rho|\rho_\infty)}.$$

- In the case $K > 0$, using Young's inequality (e.g. $ab \leq \frac{1}{2}a^2 + \frac{1}{2}b^2$, see [3]) (3.18) implies $LSI(K)$, thus Theorem 5 contains the result of Theorem 2.

- In any case, we have, for any $\lambda > 0$

$$H(\rho|\rho_\infty) \leq \frac{1}{2\lambda}I(\rho|\rho_\infty) + \frac{\lambda - K}{2}W(\rho,\rho_\infty)^2.$$

  Thus $LSI(\lambda)$ is always satisfied (for any λ), up to an error term of second order in the *weak topology*.

For more details on entropy techniques for proving convergence see [95, 110, 111, 112].

3.2 Ergodicity and Hypoellipticity

We briefly review sufficient conditions that imply geometric ergodicity (see Definition 2 in Chapter 2) for the Markov process $x(t,\omega;x_0)$ satisfying a stochastic differential equation (SDE) of the form

$$\mathrm{d}x = b(x)\,\mathrm{d}t + \sigma(x)\,\mathrm{d}W, \quad x(0) = x_0, \tag{3.19}$$

where $x \in \mathbb{R}^n$, $b : \mathbb{R}^n \to \mathbb{R}^n$, $\sigma : \mathbb{R}^n \to \mathbb{R}^{n\times m}$ and W is m-dimensional Brownian motion. We also require b and σ to be Lipschitz continuous, hence there exists a constant K such that

$$||b(x) - b(y)|| + ||\sigma(x) - \sigma(y)|| \leq K||x - y|| \quad x, y \in \mathbb{R}^n.$$

Establishing the uniqueness of invariant probability measure for the solution of (3.19) and its rate of convergence can be done by studying its generator. The generator $\mathcal{L}$ of (3.19) is known as the Kolmogorov backward operator and is defined by

$$\mathcal{L}f = \sum_{i}^{n} b_i \frac{\partial f}{\partial x_i} + \tfrac{1}{2} \sum_{i,j}^{n} \{\sigma\sigma^T\}_{ij} \frac{\partial^2 f}{\partial x_i \partial x_j}, \quad f \in C^2(\mathbb{R}^n). \tag{3.20}$$

Let $g \in C_0^2(\mathbb{R}^n)$ and define u to be the expectation of g with respect to the transition probability of the solution x:

$$u(t,x) = \mathbf{E}[g(x(t))] = \int g(x)\,\mathrm{d}\rho(x) = \int g(x) f(x,t)\,\mathrm{d}x,$$

where $\mathrm{d}\rho = f(x,t)\,\mathrm{d}x$ is the distribution induced by x on $\mathbb{R}^n$ and f is the density of ρ. The Kolmogorov backward operator describes how u changes along the solution x:

$$\frac{\partial u}{\partial t} = \mathbf{E}[\mathcal{L}g(x)].$$

Thus, we have

$$\int_{\mathbb{R}^n} g(x) f(x,t)\,\mathrm{d}x = g(x_0) + \int_0^t \int_{\mathbb{R}^n} \mathcal{L}g\, f(x,s)\,\mathrm{d}x\,\mathrm{d}s,$$

differentiating with respect to t and using the identity

$$\langle \mathcal{L}f, g\rangle = \langle f, \mathcal{L}^* g\rangle, \quad \text{for } f \in C_0^2,\ g \in C^2,$$

we obtain

$$\frac{\partial f}{\partial t} = \mathcal{L}^* f = -\sum_{i}^{n} \frac{\partial}{\partial x_i}(b_i f) + \tfrac{1}{2} \sum_{i,j}^{n} \frac{\partial^2}{\partial x_i \partial x_j}(\{\sigma\sigma^T\}_{ij} f), \quad f \in C^2(\mathbb{R}^n). \tag{3.21}$$

Proving uniqueness of the probability measure amount to show that all distributional solution of $\mathcal{L}^* f = 0$ are continuous, where f is a density of a probability measure and $\mathcal{L}^*$ is the adjoint of $\mathcal{L}$ known as Kolmogorov forward operator (Fokker-Planck operator).

Now we state two main conditions that imply geometric ergodicity [23, 84].

Condition 1. *Let $U \subset \mathbb{R}^n$ be open, connected and invariant under (3.19) i.e.,*

$$x(t) \in U \text{ for all } t \text{ whenever } x(0) \in U.$$

The transition probabilities $P(t, x_0, A)$, $t > 0, x_0 \in U, A \in \mathcal{B}(U)$ of Markov process solving (3.19) are positive and have smooth densities, more precisely the following:

(i) for some $y^* \in \operatorname{int}(U)$ and for any $\delta > 0$, there exist a time $t_1 = t_1(\delta)$ such that

$$P(t_1, x_0, B_\delta(y^*)) > 0 \quad \forall x_0 \in U,$$

(ii) $P(t, x_0, y)$ is jointly continuous in $((0, \infty), U \times U)$.

Condition 1 implies that the process generated by (3.19) is ergodic on U.

Theorem 6. *Suppose there exist a set $U \subset \mathbb{R}^n$ such that the Condition 1 hold, then solution of (3.19) has a unique invariant measure $\mathrm{d}\rho_\infty = f_\infty \, \mathrm{d}x$ on U.*

Proof. Suppose there exist more than one invariant measure, then by Birkhoff's ergodic theorem [113] for each pair of densities f, g, either $\operatorname{int}(\operatorname{supp}(f)) \cap \operatorname{int}(\operatorname{supp}(g)) = \emptyset$ or $f = g$. Let $f \neq g$, by decomposition theorem for invariant measures we have $f_\infty = af + bg$, for weights $a, b \in [0, 1]$.

Now suppose $a > 0$ and there exists $z \in \partial\operatorname{supp}(f)$. Then, by continuity of f for every $\varepsilon > 0$ there exists $\delta > 0$ such that $f(z') < \varepsilon$ for all $|z - z'| < \delta$. But this is impossible since $\inf_{|z-z'|<1} f_\infty(z') > 0$ and $f_\infty(z') = af(z')$ for all $z' \in \operatorname{int}(\operatorname{supp}(f))$.

Therefore, $\partial\operatorname{supp}(f) = \emptyset$ and $\partial\operatorname{supp}(g) = \emptyset$. The connectedness of U implies that either $\operatorname{supp}(f) = U$ or $\operatorname{supp}(f) = \emptyset$. This implies that there exists precisely one density with nonzero weight.

□

Let $\mathcal{F}_n$ be the σ-algebra of the events up to and including the time t_n, to control the return time to U we use the following

Condition 2 (Drift Condition)**.** *There exist a measurable function $\mathcal{V} : U \to [1, \infty)$ with $\mathcal{V}(x) \to \infty$ as $x \to \infty$ and positive real numbers $\alpha \in (0, 1)$, $c < \infty$ such that*

$$\mathbf{E}[\mathcal{V}(x(t_{n+1}))|\mathcal{F}_n] \leq \alpha\mathcal{V}(x(t_n)) + c.$$

For continuous Markov process, the drift condition is verified by finding a similar bound for $\mathcal{L}\mathcal{V}$.

Lemma 1. *Suppose there exist a measurable fucntion* $\mathcal{V} : U \to [1, \infty)$ *with* $\mathcal{V}(x) \to \infty$ as $x \to \infty$ *and* $a \in (0, \infty)$, $d \in (0, \infty)$ *such that*

$$\mathcal{L}\mathcal{V}(x) \leq -a\mathcal{V}(x) + d, \quad \forall x \in U,$$

then the Drift condition holds.

This is a known result and a proof can be found in [84].

Theorem 7 (Theorem 16.0.1 [23] or Theorem 2.5 [84])**.** *Assume that Condition 1 and Condition 2 hold for some set* U*. Then the process solving (3.19) is geometrically ergodic. More precisely, it possesses a unique invariant probability measure* ρ_∞ *and furthermore there exist constants* $\lambda, C > 0$ *such that for all measurable functions* $g : \mathbb{R}^n \to \mathbb{R}$ *with* $|g(x)| \leq \mathcal{V}(x)$*:*

$$|\mathbf{E}\left[g(x(t))\right] - \rho_\infty(g)| \leq C\mathcal{V}(x_0)e^{-\lambda t} \quad \forall x_0 \in \mathbb{R}^n.$$

Next we introduce an appropriate notion for regularity [53, 54, 55].

Definition 9 (Hypoelliptic Operator)**.** *Let* $\mathcal{L}^*$ *be a linear operator. We say that* $\mathcal{L}^*$ *is hypoelliptic if all distributional solutions* f *of* $\mathcal{L}^* f = g$ *are* C^∞ *whenever* g *is* C^∞*.*

Let X and Y be two C^∞ real vector fields, the bracket of X and Y, denoted by $[X, Y]$:

$$[X, Y]f = X(Yf) - Y(Xf),$$

is a new vector field. We are interested in the case when Hörmander's condition is satisfied.

Definition 10 (Hörmander's Condition)**.** *Let* $U \subset \mathbb{R}^n$ *be open, the vector fields* $X_0, \ldots, X_r : U \to \mathbb{R}^n$ *satisfy Hörmander's condition at* $z \in U$ *if the vector space generated by the iterated brackets*

$$X_0(z), \ldots, X_r(z), [X_i, X_j](z), \ [X_i, [X_j, X_k]](z) \ldots$$

is $\mathbb{R}^n$*.*

The main application of the Hörmander's condition is Hörmander's theorem. [54, 53].

Theorem 8. *Let $U \subset \mathbb{R}^n$ be an open set. If $X_0, X_1, X_2, \cdots, X_d : U \to \mathbb{R}^n$ are vector fields that satisfy Hörmander's condition at every $z \in U$, then the operator $\mathcal{L}^*$ which is defined by*

$$\mathcal{L}^* f(z) := -\sum_{i=1}^{n} \frac{\partial}{\partial z_i}(f(z)X_{0,i}(z)) + \frac{1}{2}\sum_{k=1}^{d}\sum_{i,j=1}^{n} \frac{\partial^2}{\partial z_i \partial z_j}(f(z)X_{k,i}(z)X_{k,j}(z))$$

is hypoelliptic.

Note that to satisfy Condition 1(ii) is sufficient to show that $\mathcal{L}^*$ is hypoelliptic, since, hypoellipticity effectively implies that the transition probabilities of the process solving (3.19) have smooth densities:

$$P(t, x, y) \in C^\infty([0, \infty) \times U \times U).$$

Since the existence of a Lyapunov function satisfying Condition 2 and a Poincaré inequality both imply exponential rate of convergence, it is natural to look for a relation between them. Indeed, this was studied in recent papers by Bakry et. al. [114, 115], where they found that if a probability measure ρ satisfies Condition 2, then ρ also satisfies Poincaré inequality.

In the following sections we use techniques discussed here to study ergodicity and convergence rate of three different dynamics: the gradient flow system, whose generator is self-adjoint in a suitable separable Hilbert space, hence its convergence rate is equivalent to the spectral gap of its generator and can be studied by spectral techniques; a homogeneous heat bath which has an elliptic generator; Langevin dynamics whose generator is not elliptic but is hypoelliptic.

3.3 Gradient Flows

Consider the following stochastic differential equation

$$\mathrm{d}q = -\nabla V(q)\,\mathrm{d}t + \sqrt{2\beta^{-1}}\,\mathrm{d}w, \tag{3.22}$$

where the potential $V(q)$ here and throughout this thesis is a smooth function such that

$$\lim_{q\to\infty} V(q) = +\infty.$$

The differential equation (3.22) describes a set of particles experiencing both diffusion and drift. The interplay between these two processes is fundamental to the long-time behaviour of its solution. The corresponding Fokker-Planck equation is

$$\frac{\partial f}{\partial t} = \nabla \cdot \left(\beta^{-1}\nabla f + f\nabla V\right). \tag{3.23}$$

The equation (3.23) is elliptic, hence the existence and uniqueness of the classical solution is guaranteed [116]. The challenge is that for most potentials it is not possible to calculate the time dependent solution. On the other hand we know that the stationary solution is $f_V(q) = \frac{1}{Z_V}e^{-\beta V(q)}$, in fact substituting f_V in (3.23) we have

$$\frac{\partial f_V}{\partial t} = \nabla \cdot (-\nabla V f_V + f_V \nabla V) = 0.$$

Thus our aim is to study how fast f converges to f_V in time.

Let assume that the time dependent solution of (3.23) is of the form

$$f(q,t) = h(q,t)f_V(q).$$

From (3.23) we have

$$\begin{aligned} f_V\frac{\partial h}{\partial t} =& \nabla \cdot \left(\beta^{-1} f_V \nabla h - h f_V \nabla V + h f_V \nabla V\right) \\ =& \nabla \cdot \left(\beta^{-1} f_V \nabla h\right) \\ =& f_V \beta^{-1}\Delta h - f_V \nabla V \cdot \nabla h. \end{aligned}$$

Hence $h(q,t)$ satisfies an equation of the form

$$\frac{\partial h}{\partial t} = \mathcal{A}h = \beta^{-1}\Delta h - \nabla V \cdot \nabla h. \tag{3.24}$$

Next we define the weighted L^2 space $L^2_{f_V}$:

$$L^2_{f_V} = \{u : \int_{\mathbb{R}^n} |u|^2 f_V(q)\, \mathrm{d}q < \infty\}.$$

This is a Hilbert space with inner product

$$\langle u, g\rangle_{f_V} = \int_{\mathbb{R}^n} u g f_V(q)\, \mathrm{d}q.$$

Note that

$$\begin{aligned}\int_{\mathbb{R}^n} \mathcal{A}h\, g f_V \,\mathrm{d}q &= \int_{\mathbb{R}^n} \left(\beta^{-1}\Delta h - \nabla V\cdot\nabla h\right) g f_V \,\mathrm{d}q \\ &= \int_{\mathbb{R}^n} \nabla\cdot\left(\beta^{-1} f_V \nabla h\right) g \,\mathrm{d}q \\ &= -\int_{\mathbb{R}^n} \beta^{-1}\nabla h\cdot\nabla g f_V \,\mathrm{d}q = \int_{\mathbb{R}^n} \left(\beta^{-1}\Delta g - \nabla V\cdot\nabla g\right) h f_V \,\mathrm{d}q.\end{aligned}$$

Thus we have

$$\langle \mathcal{A}h, g\rangle_{f_V} = -\beta^{-1}\langle \nabla h, \nabla g\rangle_{f_V} = \langle h, \mathcal{A}g\rangle_{f_V}.$$

This signifies that, the operator

$$\mathcal{A} = \beta^{-1}\Delta - \nabla V\cdot\nabla,$$

is self-adjoint in $L^2_{f_V}$. Moreover, if we set $g = h$ in the above we get

$$\langle \mathcal{A}h, h\rangle_{f_V} = -\beta^{-1}\left\|\nabla h\right\|^2_{L^2_{f_V}},$$

which implies that $\mathcal{A}$ is a non-positive operator, whose kernel consist of constants. Thus the only acceptable equilibria for (3.23) are constant multiple of f_V and constant are determined by the norm of h in $L^2_{f_V}$. It is worth noting that the Fokker-Planck of a diffusion process is self-adjoint if and only if the drift term is the gradient of the potential. A Markov process whose generator is self-adjoint is reversible. As we mentioned in Chapter 2, reversibility implies that f_V is invariant, but the existence of an invariant measure does not imply reversibility, in this sense reversibility is a stronger condition than having invariant measure with density f_V, see [117] on reversibility of diffusion processes.

We want to study the rate of convergence to equilibirum for (3.23) with initial condition

$$f(q,0) = f_0; \quad f_0 \geq 0, \ \int_{\mathbb{R}^n} f_0 \,\mathrm{d}q = 1.$$

Let assume that $f_0 \in L^2_{f_V^{-1}}$, and consider the Equation (3.24) with initial condition $h_0 = f_0 f_V^{-1}$. Since $\mathcal{A}$ is self-adjoint and non-positive, it can be shown using spectral analysis that $h(q,t)$ converges exponentially fast to 1. The existence of spectral gap (i.e. the smallest non-zero eigenvalue) of size λ is equivalent to f_V satisfying Poincaré inequality (3.7) with constant λ. Let $\int_{\mathbb{R}^n}(h-1)f_V \,\mathrm{d}q = 0$, then using (3.24) and

Poincaré inequality (3.7) we have

$$\begin{aligned}\frac{\mathrm{d}}{\mathrm{d}t}\int_{\mathbb{R}^n}(h-1)^2 f_V\,\mathrm{d}q =& 2\int_{\mathbb{R}^n}(h-1)\mathcal{A}h f_V\,\mathrm{d}q\\ =& 2\int_{\mathbb{R}^n}\nabla\cdot(\beta^{-1}f_V\nabla h)(h-1)\,\mathrm{d}q\\ =& -2\beta^{-1}\int_{\mathbb{R}^n}|\nabla h|^2 f_V\,\mathrm{d}q\\ \leq& -2\lambda\beta^{-1}\int_{\mathbb{R}^n}(h-1)^2 f_V\,\mathrm{d}q.\end{aligned}$$

Solving the above inequality yields

$$\int_{\mathbb{R}^n}(h-1)^2 f_V\,\mathrm{d}q \leq e^{-2\lambda\beta^{-1}t}\int_{\mathbb{R}^n}(h_0-1)^2 f_V\,\mathrm{d}q.$$

Thus, if h solves (3.24) with initial condition $h_0 \in L^2_{f_V}$, then

$$\|h(q,t)-1\|_{L^2_{f_V}} \leq e^{-\lambda\beta^{-1}t}\,\|h(q,0)-1\|_{L^2_{f_V}}.$$

Equivalently, if f solves (3.23) with initial condition $f_0 \in L^2_{f_V^{-1}}$, then

$$\|f(q,t)-f_V\|_{L^2_{f_V^{-1}}} \leq e^{-\lambda\beta^{-1}t}\,\|f(q,0)-1\|_{L^2_{f_V^{-1}}}.$$

Note that the assumption $f_0 \in L^2_{f_V^{-1}}$ is very restrictive. For physical purposes we should only assume that f is integrable, ideally we would like to prove convergence in L^1. Using relative entropy and logarithmic Sobolev inequality (3.12) we can prove convergence in L^1. Let

$$H(f|f_V) = \int_{\mathbb{R}^n} f\log\left(\frac{f}{f_V}\right)\mathrm{d}q, \tag{3.25}$$

and assume that $D^2V \geq \lambda I_n$, then by Theorem 2, f_V satisfies $LSI(\lambda)$. Thus we have

$$\begin{aligned}\frac{\mathrm{d}}{\mathrm{d}t}H(f|f_V) =& \int_{\mathbb{R}^n}\frac{\partial f}{\partial t}\log\left(\frac{f}{f_V}\right)\mathrm{d}q + \int_{\mathbb{R}^n}\frac{\partial f}{\partial t}\,\mathrm{d}q\\ =& \int_{\mathbb{R}^n}\nabla\cdot\left(\beta^{-1}\nabla f + f\nabla V\right)\log\left(\frac{f}{f_V}\right)\mathrm{d}q\\ =& -\beta^{-1}\int_{\mathbb{R}^n}\left(\nabla f + \beta f\nabla V\right)\nabla\log\left(\frac{f}{f_V}\right)\mathrm{d}q\\ =& -\beta^{-1}\int_{\mathbb{R}^n} f\left|\nabla\log\left(\frac{f}{f_V}\right)\right|^2\mathrm{d}q\\ \leq& -2\beta^{-1}\lambda H(f|f_V),\end{aligned}$$

which implies

$$H(f|f_V) \leq e^{-2\beta^{-1}\lambda t} H(f_0|f_V).$$

Using Csiszár-Kullback-Pinsker inequality (3.4), we obtain

$$\|f - f_V\|_{L^1} \leq \sqrt{2H(f_0|f_V)} e^{-\beta^{-1}\lambda t}.$$

3.4 Homogeneous Heat Bath

Consider a system of n interacting particles given by Hamiltonian function

$$H(q,p) = \frac{p^T M^{-1} p}{2} + V(q). \tag{3.26}$$

We are interested in the case when the system is in contact with an infinite heat bath system at temperature $\frac{1}{\beta}$, the effective equations are

$$\mathrm{d}q = M^{-1} p \,\mathrm{d}t - \gamma_q(p) \nabla_q V \,\mathrm{d}t + \sigma_q(p) \,\mathrm{d}W_q, \tag{3.27}$$

$$\mathrm{d}p = -\nabla_q V \,\mathrm{d}t - \gamma_p(q) M^{-1} p \,\mathrm{d}t + \sigma_p(q) \,\mathrm{d}W_p, \tag{3.28}$$

where $\gamma_l : \mathbb{R}^n \to \mathbb{R}^{n\times n}$, $\sigma_l : \mathbb{R}^n \to \mathbb{R}^{n\times n}$, and W_l is n dimensional Brownian motion, with $l = q, p$.

Let $x = (q, p)$,

$$\Gamma = \begin{pmatrix} \gamma_q(p) & 0 \\ 0 & \gamma_p(q) \end{pmatrix}, \qquad \Sigma = \begin{pmatrix} \sigma_q(p) & 0 \\ 0 & \sigma_p(q) \end{pmatrix},$$

then, (3.27)-(3.28) can be written as

$$\mathrm{d}x = J\nabla H(x) - \Gamma(x)\nabla H(x) \,\mathrm{d}t + \Sigma(x) \,\mathrm{d}W, \tag{3.29}$$

where W is $2n$ family of independent Brownian motion and

$$J = \begin{pmatrix} 0 & I_n \\ -I_n & 0 \end{pmatrix}.$$

It can be seen from (3.29) that the homogeneous heat bath (3.27)-(3.28) is a particular case of the gradient flow. We assume that the dissipation and diffusion matrices satisfy

the fluctuation dissipation relation:

$$\sigma_q \sigma_q^T = \frac{2}{\beta}\gamma_q \text{ and } \sigma_p \sigma_p^T = \frac{2}{\beta}\gamma_p.$$

Hence the Boltzmann-Gibbs measure with density

$$f_\beta(q,p) = \frac{1}{Z} e^{-\beta H(q,p)}$$

is the invariant measure of the Markov process x solving (3.29). The Fokker-Planck equation is

$$\begin{aligned}\frac{\partial f}{\partial t} = \mathcal{L}^* f = -M^{-1}p \cdot \nabla_q f + \nabla_q V \cdot \nabla_p f + \\ \nabla_q \cdot \left(\frac{1}{\beta}\gamma_q \nabla_q f + \gamma_q \nabla_q V f\right) + \nabla_p \cdot \left(\frac{1}{\beta}\gamma_p \nabla_p f + \gamma_p M^{-1} p f\right). \quad (3.30)\end{aligned}$$

Indeed f_β is the stationary solution of (3.30), substituting f_β in (3.30) the nonzero terms are

$$\begin{aligned}-M^{-1}p \cdot \nabla_q f_\beta =& f_\beta \left[\beta M^{-1} p \cdot \nabla_q V\right], \\ \nabla_q V \cdot \nabla_p f_\beta =& - f_\beta \left[\beta M^{-1} p \cdot \nabla_q V\right], \\ \nabla_q \cdot \left(\frac{1}{\beta}\gamma_q \nabla_q f_\beta + \gamma_q \nabla_q V f_\beta\right) =& \nabla_q \cdot \left(\gamma_q \nabla_q V f_\beta - \gamma_q \nabla_q V f_\beta\right), \\ \nabla_p \cdot \left(\frac{1}{\beta}\gamma_p f_\beta + \gamma_p M^{-1} p f_\beta\right) =& \nabla_p \cdot \left(\gamma_p M^{-1} p f_\beta - \gamma_p M^{-1} p f_\beta\right),\end{aligned}$$

which add to zero.

Note that the principal part of $\mathcal{L}^*$ is

$$\nabla_q \cdot \left(\frac{1}{\beta}\gamma_q \nabla_q f\right) + \nabla_p \cdot \left(\frac{1}{\beta}\gamma_p \nabla_p f\right),$$

and its characteristic polynomial is

$$Q(q,p) = \frac{1}{\beta}\left(q^T \gamma_q q + p^T \gamma_p p\right).$$

Thus $\mathcal{L}^*$ is elliptic as long as γ_q and γ_p are positive definite:

$$x^T \gamma_q x > 0 \text{ and } x^T \gamma_p x > 0 \ \forall x \in \mathbb{R}^n \ x \neq 0.$$

Ellipticity of $\mathcal{L}^*$ implies existence and uniqueness of solution for the Fokker-Planck equation (3.30), and consequently ergodicity of the Markov process x solving (3.29).

We have already mentioned that for most potentials V, it is not possible to explicitly calculate the time dependent solution of (3.30), therefore, to overcome this problem, we need to find information on the rate of convergence of the time dependent solution denoted by $f(q,p,t)$ to the stationary Boltzmann-Gibbs density $f_\beta(q,p)$.

Without loss of generality we assume that $M = I_n$, $\gamma_q = c_1 I_n$, $\gamma_p = c_2 I_n$, where c_1 and c_2 are positive constant. The Fokker-Planck equation becomes

$$\frac{\partial f}{\partial t} = \mathcal{L}^* f = -p \cdot \nabla_q f + \nabla_q V \cdot \nabla_p f + c_1 \nabla_q \cdot \left(\frac{1}{\beta} \nabla_q f + \nabla_q V f \right) + c_2 \nabla_p \cdot \left(\frac{1}{\beta} \nabla_p f + p f \right). \tag{3.31}$$

Note that

$$f_\beta(q,p) = \frac{1}{Z_V} \exp(-\beta V(q)) \frac{1}{Z_M} \exp\left(-\beta \frac{\|p\|^2}{2} \right),$$

where Z_V and Z_M are normalization constant given by

$$Z_V = \int \exp(-\beta V(q)) \, \mathrm{d}q \quad \text{and} \quad Z_M = \int \exp\left(-\beta \frac{\|p\|^2}{2} \right) \mathrm{d}p.$$

This signifies the fact that the probability of events in positions are independent of events in momenta. Hence, we let

$$\rho_q(q,t) = \int f(q,p,t) \, \mathrm{d}p, \quad \rho_p(p,t) = \int f(q,p,t) \, \mathrm{d}q. \tag{3.32}$$

Next, we define local equilibria as $\rho_q f_M$ and $\rho_p f_V$ where

$$f_M = \frac{1}{Z_M} \exp\left(-\beta \frac{\|p\|^2}{2} \right), \quad f_V = \frac{1}{Z_V} \exp\left(-\beta V(q) \right). \tag{3.33}$$

The relative entropy is

$$H(f|f_\beta) = \int f \log \frac{f}{f_\beta} \, \mathrm{d}q \, \mathrm{d}p = \int f (\log f + H) \, \mathrm{d}q \, \mathrm{d}p. \tag{3.34}$$

We have

$$\frac{\mathrm{d}}{\mathrm{d}t} H(f|f_\beta) = \int \frac{\partial f}{\partial t} (\log \frac{f}{f_\beta}) \, \mathrm{d}q \, \mathrm{d}p + \int \frac{\partial f}{\partial t} \, \mathrm{d}q \, \mathrm{d}p,$$

where

$$\int \frac{\partial f}{\partial t}(\log \frac{f}{f_\beta})\,\mathrm{d}q\,\mathrm{d}p = \int (-p\cdot\nabla_q f + \nabla_q V\cdot\nabla_p f)(\log f + \beta H)\,\mathrm{d}q\,\mathrm{d}p$$
$$+ c_1\int \nabla_q\cdot(\frac{1}{\beta}\nabla_q f + \nabla_q V f)\log\frac{f}{f_\beta}\,\mathrm{d}q\,\mathrm{d}p + c_2\int \nabla_p\cdot(\frac{1}{\beta}\nabla_p f + pf)\log\frac{f}{f_\beta}\,\mathrm{d}q\,\mathrm{d}p.$$

After some integration by parts and using the fact that f is zero on boundary, we have for each term

$$\begin{aligned}\int (-p\cdot\nabla_q f + \nabla_q V\cdot\nabla_p f)(\log f + \beta H)\,\mathrm{d}q\,\mathrm{d}p &= -\int (\nabla_q V\cdot\nabla_p f - p\cdot\nabla_q f)\,\mathrm{d}q\,\mathrm{d}p\\ &\quad + \beta\int (\nabla_q V\cdot p - \nabla_q V\cdot p) f\,\mathrm{d}q\,\mathrm{d}p\\ &= -\int (\nabla_q V\cdot\nabla_p f - p\cdot\nabla_q f)\,\mathrm{d}q\,\mathrm{d}p,\end{aligned}$$

$$\begin{aligned}c_1\int \nabla_q\cdot(\frac{1}{\beta}\nabla_q f + \nabla_q V f)\log\left(\frac{f}{f_\beta}\right)\,\mathrm{d}q\,\mathrm{d}p&\\ = -c_1\int (\frac{1}{\beta}\nabla_q f + \nabla_q V f)\cdot\left(\frac{\nabla_q f}{f} + \beta\nabla_q V\right)\,\mathrm{d}q\,\mathrm{d}p&\\ = -\frac{c_1}{\beta}\int f\nabla_q(\log f - \log f_V - \log\rho_p)\cdot\nabla_q(\log f - \log f_V - \log\rho_p)\,\mathrm{d}q\,\mathrm{d}p&\\ = -\frac{c_1}{\beta}\int f\left|\nabla_q\log\left(\frac{f}{\rho_p f_V}\right)\right|^2\,\mathrm{d}q\,\mathrm{d}p,&\end{aligned}$$

$$\begin{aligned}c_2\int \nabla_p\cdot(\frac{1}{\beta}\nabla_p f + pf)\log\left(\frac{f}{f_\beta}\right)\,\mathrm{d}q\,\mathrm{d}p&\\ = -c_2\int (\frac{1}{\beta}\nabla_p f + pf)\cdot\left(\frac{\nabla_p f}{f} + \beta p\right)\,\mathrm{d}q\,\mathrm{d}p&\\ = -\frac{c_2}{\beta}\int f\nabla_p(\log f - \log f_M - \log\rho_q)\cdot\nabla_p(\log f - \log f_M - \log\rho_q)\,\mathrm{d}q\,\mathrm{d}p&\\ = -\frac{c_2}{\beta}\int f\left|\nabla_p\log\left(\frac{f}{\rho_q f_M}\right)\right|^2\,\mathrm{d}q\,\mathrm{d}p,&\end{aligned}$$

where we used the fact that $\nabla_q\rho_p = 0$ and $\nabla_p\rho_q = 0$, the last term is

$$\int \frac{\partial f}{\partial t}\,\mathrm{d}q\,\mathrm{d}p = \int (-p\cdot\nabla_q f + \nabla_q V\cdot\nabla_p f)\,\mathrm{d}q\,\mathrm{d}p.$$

Putting all together we get

$$\frac{\mathrm{d}}{\mathrm{d}t}H(f|f_\beta) = -\frac{c_2}{\beta}\int f\left|\nabla_p \log\left(\frac{f}{\rho_q f_M}\right)\right|^2 \mathrm{d}q\,\mathrm{d}p - \frac{c_1}{\beta}\int f\left|\nabla_q \log\left(\frac{f}{\rho_p f_V}\right)\right|^2 \mathrm{d}q\,\mathrm{d}p.$$

Now, if we assume that the potential V satisfies $D^2V \geq \lambda I_n$, for some $\lambda > 0$, then by Theorem 2, $\rho_p f_V$ satisfies the logarithmic Sobolev inequality

$$2\lambda H(f|\rho_p f_V) \leq \int f\left|\nabla_q \log\left(\frac{f}{\rho_p f_V}\right)\right|^2 \mathrm{d}q\,\mathrm{d}p.$$

Thus we obtain

$$\frac{\mathrm{d}}{\mathrm{d}t}H(f|f_\beta) \leq -\frac{2c_2}{\beta}H(f|\rho_q f_M) - \frac{2\lambda c_1}{\beta}H(f|\rho_p f_V)$$

Let $r := \min\{c_2, \lambda c_1\}$, then we have

$$\begin{aligned}
\frac{\mathrm{d}}{\mathrm{d}t}H(f|f_\beta) &\leq -\frac{2r}{\beta}\left(H(f|\rho_q f_M) + H(f|\rho_p f_V)\right) \\
&= -\frac{2r}{\beta}\left(\int f \log\left(\frac{f f}{\rho_q f_M \rho_p f_V}\right)\mathrm{d}q\,\mathrm{d}p\right) \\
&= -\frac{2r}{\beta}\left(\int f\left(\log\left(\frac{f}{f_V f_M}\right) + \log\left(\frac{f}{\rho_q \rho_p}\right)\right)\mathrm{d}q\,\mathrm{d}p\right) \\
&= -\frac{2r}{\beta}\left(H(f|f_\beta) + H(f|\rho_q\rho_p)\right).
\end{aligned}$$

Note that $H(f|\rho_q\rho_p) \geq 0$ for all time, indeed using Gibbs inequality we have

$$-\int f \log f\,\mathrm{d}q\,\mathrm{d}p \leq -\int f \log(\rho_q\rho_p)\,\mathrm{d}q\,\mathrm{d}p,$$

which implies $H(f|\rho_q\rho_p) \geq 0$. Thus we obtain a close differential inequality

$$\frac{\mathrm{d}}{\mathrm{d}t}H(f|f_\beta) \leq -\frac{2r}{\beta}H(f|f_\beta)$$

which yeilds

$$H(f|f_\beta) \leq e^{-2r\beta^{-1}t}H(f_0|f_\beta).$$

Using Csiszár-Kullback-Pinsker inequality (3.4), we obtain

$$\|f - f_\beta\|_{L^1} \leq \sqrt{2H(f_0|f_\beta)}e^{-r\beta^{-1}t}.$$

3.5 Langevin Dynamics

Consider the following stochastic differential equations

$$\mathrm{d}q = M^{-1}p\,\mathrm{d}t, \tag{3.35}$$

$$\mathrm{d}p = -\nabla_q V(q)\,\mathrm{d}t - \gamma(q)p\,\mathrm{d}t + \sigma(q)\,\mathrm{d}W, \tag{3.36}$$

where $\gamma : \mathbb{R}^n \to \mathbb{R}^{n\times n}$ is the dissipation matrix, $\sigma : \mathbb{R}^n \to \mathbb{R}^{n\times n}$ is the diffusion matrix and we assume the fluctuation-dissipation relation $\sigma\sigma^T = \frac{2}{\beta}\gamma M$, which implies that the Boltzmann-Gibbs measure is the invariant measure. We also assume that $V(q)$ and σ are smooth, and γ is positive definite, i.e., for some $\gamma^- > 0$

$$\gamma^-\|z\|^2 \le \langle z, \gamma(q)z\rangle \quad \forall q \in \mathbb{R}^n,\ z \in \mathbb{R}^n. \tag{3.37}$$

Under the above assumptions, it is possible to obtain an implicit exponential rate of convergence to the Boltzmann-Gibbs measure, see the work on geometric ergodicity of Langevin [84]. For earlier results on ergodicity and convergence to equilibrium of Langevin dynamics see [25, 118].

The corresponding Fokker-Planck equation is

$$\frac{\partial f}{\partial t} = \mathcal{L}^* f = -M^{-1}p\cdot\nabla_q f + \nabla_q V\cdot\nabla_p f + \nabla_p\cdot\left(\frac{1}{2}\sigma\sigma^T\nabla_p f + \gamma p f\right), \tag{3.38}$$

where $\mathcal{L}^*$ is the adjoint of the generator

$$\mathcal{L} = M^{-1}p\cdot\nabla_q - \nabla_q V\cdot\nabla_p - \gamma p\nabla_p + \nabla_p\cdot\left(\frac{1}{2}\sigma\sigma^T\Delta_p\right).$$

Let $\mathcal{L}^* f = \mathcal{L}_T f + \mathcal{L}_C f$, where

$$\mathcal{L}_C = \nabla_p\cdot\left(\frac{1}{2}\sigma\sigma^T\nabla_p f + \gamma p f\right) \text{ and } \mathcal{L}_T = -M^{-1}p\cdot\nabla_q f + \nabla_q V\cdot\nabla_p f,$$

are the collision and transport operators. The tansport operator $\mathcal{L}_T$ is antisymmetric and the collision operator $\mathcal{L}_C$ becomes self-adjoint in the weighted L^2 space $L^2_{\rho_\beta}$:

$$L^2_{\rho_\beta} = \{u\,;\, \int_{\mathbb{R}^{2n}} |u|^2 f_\beta\,\mathrm{d}q\,\mathrm{d}p < \infty\}, \tag{3.39}$$

with inner product

$$\langle u, g\rangle_{\rho_\beta} = \int_{\mathbb{R}^{2n}} ug\, f_\beta \,\mathrm{d}q\,\mathrm{d}p.$$

In particular if $f(q,p,t) = h(q,p,t)f_\beta$ then we have

$$\begin{aligned}\mathcal{L}_C(hf_\beta) =& \nabla_p \cdot (\frac{1}{2}\sigma\sigma^T\nabla_p(hf_\beta) + \gamma p h f_\beta)\\ =& \nabla_p \cdot (\frac{1}{2}\sigma\sigma^T\nabla_p H f_\beta - \frac{\beta}{2}\sigma\sigma^T M^{-1} h f_\beta + \gamma p h f_\beta)\\ =& (\nabla_p \cdot (\frac{1}{\beta}\gamma M\nabla_p h) - \gamma p\cdot\nabla_p h) f_\beta,\end{aligned}$$

which is self-adjoint in $L^2_{\rho_\beta}$. Thus in $L^2_{\rho_\beta}$ space we might use spectral techniques to study long time behaviour of (3.35)-(3.36). However $L^2_{\rho_\beta}$ implies that f should satisfy:

$$\int \frac{f^2}{f_\beta}\,\mathrm{d}q\,\mathrm{d}p < \infty \tag{3.40}$$

which is a much more strong assumption than just assuming that f is integrable. Indeed it is possible that for some potential V convergence to equilibrium is exponential under Assumption (3.40) but not for general L^1- type assumption (that is assuming integrability). In this regrad, L^1 results are stronger than L^2 results.

Let $x = (q,p)$ and

$$Y = \begin{pmatrix} M^{-1}p \\ -\nabla_q V - \gamma p \end{pmatrix}, \quad X_i = \begin{pmatrix} 0 \\ \sigma_i \end{pmatrix}, \tag{3.41}$$

where σ_i is the ith column of σ, then (3.38) can be written as

$$\mathcal{L}^* f = -\sum_{i=1}^{2n}\frac{\partial}{\partial x_i}(fY^i) + \frac{1}{2}\sum_{k=1}^{n}\sum_{i,j=1}^{2n}(fX_k^i X_k^j). \tag{3.42}$$

The Condition (3.37) implies that σ_i's are linearly independent, thus the vectors

$$X_i = \begin{pmatrix} 0 \\ \sigma_i \end{pmatrix} \text{ and } [X_i, Y] = \begin{pmatrix} \sigma_i(q) \\ -\nabla_q\sigma_i(q)p - \gamma(q)\sigma_i(q) \end{pmatrix},$$

are linearly independent and we have

$$\mathrm{span}\{X_1,\ldots,X_n,[X_1,Y],\ldots,[X_n,Y]\} = \mathbb{R}^{2n}, \quad \text{for every } q \text{ and } p.$$

This concludes that the operator $\mathcal{L}^*$ is hypoelliptic which implies that (3.38) is well-posed and has a unique solution, consequently by Theorem 6 the Langevin dynamics is ergodic.

Without loss of generality we assume that $M = I_n$, $\gamma(q) = cI_n$, so $\mathcal{L}_C$ and $\mathcal{L}_T$ are

$$\mathcal{L}_C = c\nabla_p \cdot (\frac{1}{\beta}\nabla_p f + pf) \text{ and } \mathcal{L}_T = -p \cdot \nabla_q f + \nabla_q V \cdot \nabla_p f.$$

The collision operator $\mathcal{L}_C$ only acts on momenta, hence (3.35)-(3.36) can be viewed as a system in contact with a heat bath where the collisions are not homogeneous in space. Similar to the concept of hypoellipticity where regularity in some directions leads regularity in all direction, we would like to show that collisions on momenta is sufficient to converge to the global equilibrium.

The relative entropy is

$$H(f|f_\beta) = \int f \log \frac{f}{f_\beta} \,\mathrm{d}q \,\mathrm{d}p.$$

Its time derivative is

$$\begin{aligned}
\frac{\mathrm{d}}{\mathrm{d}t} H(f|f_\beta) &= \int \frac{\partial f}{\partial t} \log \frac{f}{f_\beta} \,\mathrm{d}q \,\mathrm{d}p + \int \frac{\partial f}{\partial t} \,\mathrm{d}q \,\mathrm{d}p \\
&= \int \mathcal{L}_T f \log \frac{f}{f_\beta} \,\mathrm{d}q \,\mathrm{d}p + \int \mathcal{L}_C f \log \frac{f}{f_\beta} \,\mathrm{d}q \,\mathrm{d}p \\
&= -\frac{c}{\beta} \int (\nabla_p f + \beta p f) \cdot (\frac{\nabla_p f}{f} + \beta p f) \,\mathrm{d}q \,\mathrm{d}p \\
&= -\frac{c}{\beta} \int f \left| \nabla_p \log \left(\frac{f}{\rho_q f_M} \right) \right|^2 \,\mathrm{d}q \,\mathrm{d}p.
\end{aligned}$$

Using logarithmic Sobolev inequality yields

$$\frac{\mathrm{d}}{\mathrm{d}t} H(f|f_\beta) \leq -\frac{2c}{\beta} H(f|\rho_q f_M). \tag{3.43}$$

This only gives us information about the equilibration in momenta, but not much about positions. In fact, our conjecture is that $\mathcal{L}_C$ forces the distribution of momenta to become close to its equilibrium (i.e., Maxwellian) faster than distribution of positions. Note that

$$H(f|f_\beta) = H(f|\rho_q f_M) + H(\rho_q|f_V),$$

hence, if we assume that the system is close to equilibrium such that $H(\rho_q|f_V)$ is a

linear function of $H(f|f_\beta)$, then we have

$$\frac{\mathrm{d}H(f|f_\beta)}{\mathrm{d}H(f|\rho_q f_M)} = k,$$

where k is some constant. Thus, using (3.43) we have

$$\frac{\mathrm{d}}{\mathrm{d}t}H(f|\rho_q f_M) \leq -\frac{2c}{\beta k}H(f|\rho_q f_M)$$

which signifies that momenta converges to its Maxwellian distribution if we are not far from equilibrium.

Calculating the general convergence rate to global equilibrium is very difficult, Villani and Desvillettes in [119] obtained a decay rate to equilibrium faster than $t^{-1/\epsilon}$, $\epsilon > 0$. Another result (with quite complicated analysis) on convergence rate is [120], where under assumption of local regularity and $V(x) \to \infty$ as $x \to \infty$ explicit rate of convergence in terms of M, γ, β and V was obtained in some weighted Sobolev space.

3.5.1 Harmonic Potential

In general it is very difficult or not possible to calculate the eigenvalues and eigenfunction of the operator (3.38). One example where the calculation can be done explicitly is the harmonic oscillator:

$$H(q,p) = \frac{p^2}{2} + \omega_0^2\frac{q^2}{2},$$

where $q \in \mathbb{R}$, $p \in \mathbb{R}$ and $k > 0$ is a constant. This was done in the book by Risken [121], but our exposition here is close to [122]. Langevin dynamics for the harmonic oscillator is

$$\begin{aligned}\mathrm{d}q =& p\,\mathrm{d}t,\\ \mathrm{d}p =& -\omega_0^2 q\,\mathrm{d}t - \gamma p\,\mathrm{d}t + \sigma\,\mathrm{d}W.\end{aligned}$$

This can be written as

$$\mathrm{d}\begin{pmatrix} q \\ p \end{pmatrix} = \begin{pmatrix} 0 & 1 \\ -\omega_0^2 & -\gamma \end{pmatrix}\begin{pmatrix} q \\ p \end{pmatrix}\mathrm{d}t + \begin{pmatrix} 0 & 0 \\ 0 & \sigma \end{pmatrix}\mathrm{d}W$$

which is a particular case of an Ornstein-Uhlenbeck process.

Let $f(q,p,t) = h(q,p,t)f_\beta(q,p)$, hence h solves

$$\frac{\partial h}{\partial t} = \mathcal{A}h,$$

where

$$\mathcal{A} = -p\frac{\partial}{\partial q} + kq\frac{\partial}{\partial p} + \gamma\left[\frac{1}{\beta}\frac{\partial^2}{\partial p^2} - p\frac{\partial}{\partial p}\right].$$

let us define the operators

$$\begin{aligned} a^- =& \beta^{-1/2}\frac{\partial}{\partial p}, \quad a^+ = -\beta^{-1/2}\frac{\partial}{\partial p} + \beta^{1/2}p, \\ b^- =& \omega_0^{-1}\beta^{-1/2}\frac{\partial}{\partial q}, \quad b^+ = -\omega_0^{-1}\beta^{-1/2}\frac{\partial}{\partial q} + \omega_0\beta^{1/2}q. \end{aligned}$$

The operators $a^\pm$, $b^\pm$ satisfy the commutation relations

$$[a^+, a^-] = -1, \quad [b^+, b^-] = -1, \quad [a^\pm, b^\pm] = 0$$

and we may write $\mathcal{A}$ as

$$\mathcal{A} = -\gamma a^+a^- - \omega_0(b^+a^- - a^+b^-). \tag{3.44}$$

We want to find operators $c^\pm$, $d^\pm$ that are linear combinations of $a^\pm$, $b^\pm$, such that, for some constants C and D,

$$\mathcal{A} = -Cc^+c^- - Dd^+d^-, \tag{3.45}$$

and

$$[c^+, c^-] = -1, \quad [d^+, d^-] = -1, \quad [c^\pm, d^\pm] = 0. \tag{3.46}$$

Using (3.44), (3.45) and the relations (3.46), we find

$$\begin{aligned} c^+ =& \delta^{-1/2}\left(\sqrt{\lambda_1}a^+ + \sqrt{\lambda_2}b^+\right), \\ c^- =& \delta^{-1/2}\left(\sqrt{\lambda_1}a^- - \sqrt{\lambda_2}b^-\right), \\ d^+ =& \delta^{-1/2}\left(\sqrt{\lambda_2}a^+ + \sqrt{\lambda_1}b^+\right), \\ d^- =& \delta^{-1/2}\left(\sqrt{\lambda_1}b^- - \sqrt{\lambda_2}a^-\right), \end{aligned}$$

where λ_1 and λ_2, with $\lambda_1 \neq \lambda_2$ (we do not consider the case when $\lambda_1 = \lambda_2$) are the

eigenvalues of the deterministic problem:

$$\frac{\mathrm{d}^2 q}{\mathrm{d}t^2} = -\gamma \frac{\mathrm{d}q}{\mathrm{d}t} - \omega_0^2 q,$$

with solution

$$q(t) = C_1 e^{-\lambda_1 t} + c_2 e^{-\lambda_2 t},$$

where

$$\lambda_{1,2} = \frac{\gamma \pm \delta}{2}, \quad \delta = \sqrt{\gamma^2 - 4\omega_0^2} > 0.$$

Now the operator $\mathcal{A}$ can be written as

$$\mathcal{A} = -\lambda_1 c^+ c^- - \lambda_2 d^+ d^-.$$

We also have

$$\begin{aligned}
[\mathcal{A}, c^+] =& (-\lambda_1 c^+ c^- c^+ + \lambda_1 c^+ c^+ c^-) + \lambda_2 (c^+ d^+ d^- - d^+ d^- c^+) \\
=& -\lambda_1 c^+ ([c^-, c^+] + c^+ c^-) + \lambda_1 c^+ c^+ c^-) + \lambda_2 (c^+ d^+ d^- - d^+ ([d^-, c^+] + c^+ d^-)) \\
=& -\lambda_1 c^+ + \lambda_2 (c^+ d^+ d^- - ([d^+, c^+] + c^+ d^+) d^-) \\
=& -\lambda_1 c^+.
\end{aligned}$$

In fact it can be checked that

$$[\mathcal{A}, c^\pm] = -\lambda_1 c^\pm, \quad [\mathcal{A}, d^\pm] = -\lambda_2 d^\pm.$$

Using the above relations we have

$$\begin{aligned}
[\mathcal{A}, (c^+)^2] =& \mathcal{A}(c^+)^2 - (c^+)^2 \mathcal{A} \\
=& ([\mathcal{A}, c^+] + c^+ \mathcal{A}) - c^+ ([c^+, \mathcal{A}] + \mathcal{A} c^+) \\
=& -2\lambda_1 (c^+)^2.
\end{aligned}$$

Indeed, by induction we have

$$[\mathcal{A}, (c^\pm)^n] = -n\lambda_1 (c^\pm)^n, \quad [\mathcal{A}, (d^\pm)^m] = -m\lambda_2 (d^\pm)^m. \tag{3.47}$$

Now we can use (3.47) to calculate

$$\begin{aligned}
\mathcal{A}(c^+)^n(d^+)^m 1 =&([\mathcal{A},(c^+)^n]+(c^+)^n\mathcal{A})(d^+)^m 1\\
=&(-n\lambda_1(c^+)^n+(c^+)^n\mathcal{A})(d^+)^m 1\\
=&-n\lambda_1(c^+)^n(d^+)^m 1+(c^+)^n([\mathcal{A},(d^+)^m]+(d^+)^m\mathcal{A})1\\
=&-n\lambda_1(c^+)^n(d^+)^m 1-m\lambda_2(c^+)^n(d^+)^m 1+(c^+)^n(d^+)^m\mathcal{A}1\\
=&-n\lambda_1(c^+)^n(d^+)^m 1-m\lambda_2(c^+)^n(d^+)^m 1.
\end{aligned}$$

Hence the eigenvalues and normalised eigenfunctions of $\mathcal{A}$ are

$$\lambda_{nm}=n\lambda_1+m\lambda_2=\frac{1}{2}\gamma(n+m)+\frac{1}{2}\delta(n-m),\quad n,m=0,1,\cdots \tag{3.48}$$

and

$$\phi_{nm}(q,p)=\frac{1}{\sqrt{n!m!}}(c^+)^n(d^+)^m 1,\quad n,m=0,1,\cdots \tag{3.49}$$

Since $\mathcal{A}$ is not self-adjoint the eigenvalues are not real, for the *underdamped* regime, $\gamma<2\omega_0$ the dynamic is dominated by the deterministic part and the eigenvalues are complex:

$$\lambda_{nm}=\frac{1}{2}\gamma(n+m)+\frac{1}{2}i\sqrt{-\gamma^2+4\omega_0^2}(n-m).$$

The *overdamped* regime $\gamma>2\omega_0$ is dominated by collision operator $\gamma\left[\frac{1}{\beta}\frac{\partial^2}{\partial p^2}-p\frac{\partial}{\partial p}\right]$ and the eigenvalues are real:

$$\lambda_{nm}=\frac{1}{2}\gamma(n+m)+\frac{1}{2}\sqrt{\gamma^2-4\omega_0^2}(n-m).$$

Indeed in the limit $\gamma\to\infty$ the Langevin dynamics is equivalent to the gradient flow.

In this chapter, we have studied two different dynamics for sampling the canonical ensemble, namely the homogeneous heat bath and Langevin dynamics. The homogeneous heat bath is uniformly elliptic and we did find an explicit rate of convergence to equilibrium. Langevin dynamics is degenerate and we could only find the exact rate of convergence for the harmonic potential. The interesting point is that for the harmonic potential both methods have the same rate of convergence. Naturally we asked if this is true for other potential. It is desirable to do a numerical experiment for a system with complex potential, such as a single butane molecule, and examine the rate of equilibration for each method. However for now, we leave this for future work.

Chapter 4

Highly Degenerate Thermostat

To calculate averages with respect to the Boltzmann-Gibbs measure , we introduce a thermostat, a perturbation of Hamiltonian dynamics which generates trajectories $(q(t), p(t))$, $t \geq 0$, such that, for an observable $O = O(q, p)$

$$\lim_{t\to\infty} t^{-1} \int_0^t O(q(s), p(s))\, \mathrm{d}s = \int_{\mathbb{X}} O(q, p)\, \mathrm{d}\rho_\beta(q, p).$$

Many such thermostats have been proposed [123, 124, 125, 126, 58, 56]. In practice, it has been observed that these thermostats vary considerably in the extent to which they alter the dynamics of the system. The standard stochastic thermostats such as Langevin dynamics perturb every momentum, hence they decorrelate the dynamics much faster than deterministic thermostats such as Nosé-Hoover. The advantage of stochastic method is that it is possible to prove ergodicity. In particular, Langevin dynamics is ergodic and we have shown in Chapter 3 that it converges exponentially fast to its unique measure. However Nosé-Hoover has been used successfully in many MD simulations, its success is due to its control of kinetic energy and the fact that its perturbation to the dynamics is milder than stochastic thermostats such as Langevin [59], but it has a flaw that its evolution is not ergodic, see [61, 58, 62].

In this chapter we propose a method that is a combination of Nosé-Hoover and Langevin, similar formulation has also been given in [127]. We add a stochastic perturbation to the auxiliary variable of the Nosé-Hoover to improve its ergodicity. The aim is to achieve the virtue of Langevin while keeping the virtue of Nosé-hoover that is the disturbance to the dynamics is small.

Some recent articles have used a similar combination of stochastic and deterministic dynamics. Bussi *et al* [128] developed a sampling method introducing a stochastic

perturbation of velocities, while reducing the extent of random perturbation of the system compare to the Langevin dynamics. On the other hand their method relies on an auxiliary dynamics for kinetic energy and there is no clear case that it can improve the ergodicity. A method related to ours was also suggested by Quigley and Probert [129] for integration in the isothermal-isobaric ensemble. The primary distinction between our approach and others in the literature is that we provide not only a new method (which generalizes all the ones of which we are aware) but also an analysis of ergodicity, making use of the concept of *hypoellipticity* with respect to the operator defining the right hand side of the Fokker-Planck equations.

4.1 The Effective Equations

With intuition from Nosé-Hoover thermostat [56, 58, 65] we introduce *empirical temperature* as

$$\theta = \frac{\nabla_p H \cdot G(q,p)}{\nabla_p \cdot G(q,p)},$$

where, in general $G : \mathbb{X} \to \mathbb{R}^n$ is a function of q and p which we choose to control the ensemble. Next we replace Nosé-Hoover equations with the following family of stochastic differential equation

$$\frac{\mathrm{d}q}{\mathrm{d}t} = M^{-1}p, \tag{4.1}$$

$$\frac{\mathrm{d}p}{\mathrm{d}t} = -\nabla V(q) - \xi G(q,p), \tag{4.2}$$

$$\mathrm{d}\xi = \frac{1}{\mu}\left(\nabla_p H \cdot G(q,p) - \frac{1}{\beta}\nabla_p \cdot G(q,p)\right)\mathrm{d}t - \gamma(q,p)\xi\,\mathrm{d}t + \sigma(q,p)\,\mathrm{d}W, \tag{4.3}$$

where W is a one dimensional Brownian motion (not a family of n Brownian motion as in the case of Langevin), $\gamma(q,p) > 0$ and $\sigma(q,p) > 0$ are dissipation and diffusion coefficients. We also assume fluctuation-dissipation relation $\sigma^2 = \frac{2}{\beta\mu}\gamma$. Here the system is augmented by an auxiliary variable ξ which governs the dissipation, assuming that the empirical temperature θ converges to $\frac{1}{\beta}$ then, the mean value of ξ converges to zero with the rate γ:

$$\mathbf{E}[\xi] = \xi_0 e^{-\gamma t}.$$

Therefore, we expect ξ to be small and fluctuating around zero, consequently the perturbation to the system is small. We refer to the method defined by (4.1)-(4.3) as Nosé-Hoover-Langevin (NHL).

The augmented Boltzmann-Gibbs measure ρ_{NHL} with density

$$f_{NHL}(q,p,\xi) = \frac{1}{Z_{NHL}} \exp\left(-\beta\left(H(q,p) + \tfrac{\mu}{2}\xi^2\right)\right), \tag{4.4}$$

where

$$Z_{NHL} = \int \exp\left(-\beta\left(H(q,p) + \tfrac{1}{2}\xi^2\right)\right)\, \mathrm{d}q\, \mathrm{d}p\, \mathrm{d}\xi, \tag{4.5}$$

is invaraint for process $x = (q,p,\xi)$ solving (4.1)-(4.3), that is f_{NHL} satisfies the stationary Fokker-Planck equation $\mathcal{L}^* f_{NHL} = 0$ where

$$\begin{aligned}\mathcal{L}^* f_{NHL} = &-\mathcal{L}_H f_{NHL} + \nabla_p \cdot [\xi G(q,p) f_{NHL}] - \\ &\frac{\partial}{\partial \xi}\left[\frac{1}{\mu}\left(\nabla_p H \cdot G(q,p) - \frac{1}{\beta}\nabla_p \cdot G(q,p)\right) f_{NHL}\right] + \gamma \frac{\partial}{\partial \xi}(\xi f_{NHL}) + \frac{1}{2}\sigma^2 \frac{\partial^2 f_{NHL}}{\partial \xi^2}\end{aligned}$$

The $\mathcal{L}_H f_{NHL}$ on the right hand side is zero since $\mathcal{L}_H$ is Liouville's operator

$$\mathcal{L}_H f_{NHL} = \nabla_p H \cdot \nabla_q f_{NHL} - \nabla_q H \cdot \nabla_p f_{NHL},$$

for the other terms we have

$$\begin{aligned}\nabla_p \cdot [\xi G f_{NHL}] =& f_{NHL}\left[\xi \nabla_p \cdot G - \beta \xi \nabla_p H \cdot G\right], \\ -\frac{\partial}{\partial \xi}\left[\frac{1}{\mu}\left(\nabla_p H \cdot G - \frac{1}{\beta}\nabla_p \cdot G\right) f_{NHL}\right] =& f_{NHL}\left[\beta \xi \nabla_p H \cdot G - \xi \nabla_p G\right], \\ \gamma \frac{\partial}{\partial \xi}(\xi f_{NHL}) =& f_{NHL}\left[\gamma - \gamma\beta\mu\xi^2\right], \\ \frac{1}{2}\sigma^2 \frac{\partial^2 f_{NHL}}{\partial \xi^2} =& f_{NHL}\left[-\gamma + \gamma\beta\mu\xi^2\right],\end{aligned}$$

which sum up to zero.

A simplified version of (4.1)-(4.3) with $G(q,p) = p$ and constant γ is of the form:

$$\frac{\mathrm{d}q}{\mathrm{d}t} = M^{-1}p, \tag{4.6}$$

$$\frac{\mathrm{d}p}{\mathrm{d}t} = -\nabla V(q) - \xi p, \tag{4.7}$$

$$\mathrm{d}\xi = \frac{1}{\mu}\left(p^T M^{-1} p - \frac{n}{\beta}\right)\mathrm{d}t - \gamma\xi\,\mathrm{d}t + \sigma\,\mathrm{d}W. \tag{4.8}$$

In what follows we study (4.6)-(4.8).

4.2 Ergodicity and Convergence

In this section we study the ergodicity and convergence of NHL dynamics (4.6)-(4.8). We start by writing (4.6)-(4.8) in an abstract form:

$$\mathrm{d}x = X_0(x)\,\mathrm{d}t + X_1(x)\,\mathrm{d}W,\ x(0) = x_0, \tag{4.9}$$

where

$$x = \begin{pmatrix} q \\ p \\ \xi \end{pmatrix} \in \mathbb{R}^N, \quad N = 2n+1,$$

W is one dimensional standard Brownian motion, and

$$X_0(x) = \begin{pmatrix} M^{-1}p \\ -\nabla_q V(q) - \xi p \\ \frac{1}{\mu}\left(p^T M^{-1} p - \frac{n}{\beta}\right) - \gamma\xi \end{pmatrix}, \quad X_1(x) = \begin{pmatrix} 0 \\ 0 \\ \sigma \end{pmatrix}.$$

Since $V : \mathcal{M} \subseteq \mathbb{R}^n \to [0,\infty)$ is smooth, for some constant K we have

$$||X_0(x) - X_0(y)|| + ||X_1(x) - X_1(y)|| \leq K||x-y|| \quad x, y \in \mathbb{R}^N,$$

i.e., X_0 and X_1 are Lipschitz continuous which also implies that (4.9) is time-homogeneous.

The generator $\mathcal{L}$ of (4.9) is defined by

$$\mathcal{L}f = \sum_i^N X_{0,i}\frac{\partial f}{\partial x_i} + \tfrac{1}{2}\sum_{i,j}^N \{X_1 X_1^T\}_{ij}\frac{\partial^2 f}{\partial x_i \partial x_j}, \quad f \in C^2(\mathbb{R}^N). \tag{4.10}$$

Its corrsponding Fokker-Planck operator $\mathcal{L}^*$ is

$$\mathcal{L}^* f = -\sum_{i=1}^N \frac{\partial}{\partial x_i}(f X_{0,i}) + \frac{1}{2}\sum_{i,j=1}^N \frac{\partial^2}{\partial x_i \partial x_j}(f\{X_1 X_1^T\}_{ij}), \quad f \in C^2(\mathbb{R}^N). \tag{4.11}$$

Hypoellipticity clearly provides smoothness of densities required by Condition 1 (see Chapter 3 Section 3.2), hence the first step is to find an open, connected set U such that the vector fields X_0 and X_1 satisfy Hörmander's condition (see Chapter 3 Section 3.2) at every $x \in U$.

A simple case where this can be done is given by quadratic Hamiltonians, where

$$H(q,p) = \frac{1}{2}p^T M^{-1} p + \frac{1}{2}q^T B q.$$

Only a mild assumption on the spectrum of B is needed. For general forces we conjecture that $\mathcal{L}^*$ remains hypoelliptic, but it is difficult to verify this analytically due to the long calculation of iterated Lie brackets and the requirement to show that they are linearly independent. However, in the case of Langevin dynamics it is possible to verify hypoellipticity for bounded Lipschitz forces since there are n family of Brownian motion and therefore we don't need to iterate brackets [130, 84, 131].

Theorem 9 (Geometric Ergodicity of NHL)**.** *Let $M, B \in \mathbb{R}^{n\times n}$ be two symmetric and positive definite matrices such that*

$$\omega_k \neq \omega_l \text{ for all } k \neq l, \tag{4.12}$$

where $\omega_k = \varphi_k^T M^{-1} B \varphi_k$ are the eigenvalues and $\varphi_1, \ldots, \varphi_n \in \mathbb{R}^n$ are the normalized eigenvectors of $M^{-1}B$. If $H(q,p) = \frac{1}{2}p^T M^{-1} p + \frac{1}{2}q^T B q$ and

$$U = \left\{ (q,p) \;\middle|\; q \in \mathcal{M} \subseteq \mathbb{R}^n,\, p \in \mathbb{R}^n,\, \prod_{k=1}^{n} \left((q\cdot\varphi_k)^2 + (p\cdot\varphi_k)^2 \right) \neq 0 \right\} \times \mathbb{R}, \tag{4.13}$$

then the process solving (4.9) is ergodic on U with augmented Boltzmann-Gibbs measure ρ_{NHL}. Furthermore there exist a function $\mathcal{V} : \mathbb{R}^N \to [1,\infty)$ and constants $C > 0$, $r > 0$ such that for any measurable function $g : U \to \mathbb{R}$ with $|g(x)| \leq \mathcal{V}(x)$ the following hold

$$|\mathbf{E}^{x_0}\left[g(x(t))\right] - \rho_{NHL}(g)| \leq C\mathcal{V}(x_0)e^{-rt} \quad \forall x(0) = x_0 \in \mathbb{R}^n.$$

The theorem is sharp in the sense that if one of the Assumption (4.12), (4.13) is violated, then the dynamics generated by (4.9) is not ergodic. Indeed, assume that B is a diagonal matrix and $q_i(t=0) = p_i(t=0) = 0$ for some i. Clearly $q_i(t), p_i(t) = 0$ for all t and thus the evolution is not ergodic.

Assume next that $n = 3$ and $M = B = \mathrm{Id}$ (the identity matrix). Define the subspace

$$\mathcal{S} = \mathrm{span}\{(q_0,0),(p_0,0),(0,q_0),(0,p_0)\} \subset \mathbb{R}^6,$$

where q_0 and p_0 are the initial values of q and p. Again, it can be seen easily that $\mathcal{S}$ is

invariant. Since $\mathcal{S}$ is 4-dimensional the evolution is not ergodic.

A nontrivial quadratic Hamiltonian that satisfies (4.12) is a harmonic chain with clamped end-particles where $V(q) = \frac{1}{2}\sum_{i=0}^{n}(q_{i+1} - q_i)^2$ and $q_0 = q_{n+1} = 0$. Then $\partial V(q)/\partial q_i = -q_{i-1} + 2q_i - q_{i+1}$ if $i \in \{1, \ldots, n\}$. Without the clamping assumption the Hamiltonian H is translation invariant and $Z = \int_{\mathbb{R}^{2(n+2)}} \mathrm{d}q\ \mathrm{d}p\ \exp(-\beta H)$ does not exist. Define the discrete sine-transform as follows: $(\mathcal{F}q)_k = \hat{q}_k = \frac{2}{n+1}\sum_{i=1}^{n}\sin(\pi ik/(n+1))q_i$, such that $q_i = \sum_{k=1}^{n}\hat{q}_k \sin(\pi ik/(n+1))$. One obtains that $|\hat{q}| = |q|$ and

$$\mathcal{F}(-q_{i-1} + 2q_i - q_{i+1})(k) = 2(1 - \cos(\pi k/(n+1)))\hat{q} = \omega_k \hat{q}(k).$$

Since the dispersion relation ω is strictly increasing with k, inequality (4.12) is satisfied.

We conjecture that if Equation (4.8) of NHL dynamics is replaced by

$$\frac{\mathrm{d}p}{\mathrm{d}t} = -\nabla V(q) - A(\xi)p, \tag{4.14}$$

where $A : \mathbb{R} \to \mathbb{R}^{n\times n}$ is random, then Theorem 9 holds almost surely without the non-resonance Assumption (4.12).

Conjecture 1. *Let M be diagonal matrix and B be symmetric, positive definite matrix. If*

$$H(q,p) = \frac{1}{2}(p^T M^{-1} p + q^T B q),$$

$A = \xi I_n + SM$ where $S = G - G^T$ and $G \in \mathbb{R}^{n\times n}$ is a random matrix with iid Gaussian entries, then for almost every realization of S the flow generated by Equations (4.9) is ergodic on U (defined by (4.13)).

Note that A leaves ρ_{NHL} invariant, indeed, since S is skew-symmetric we have $p^T S p = 0$ and $\nabla_p \cdot (SMp) = 0$. Thus, we have

$$\begin{aligned}
\nabla_p \cdot (A(\xi)p f_{NHL}) =& f_{NHL}\left[n\xi + \nabla_p \cdot (SMp) - \beta p^T(\xi I_n + SM)M^{-1}p\right] \\
=& f_{NHL}\left[n\xi - \beta\xi p^T M^{-1} p - \beta p^T S p\right] \\
=& f_{NHL}\left[n\xi - \beta\xi p^T M^{-1} p\right].
\end{aligned}$$

Proof of Theorem 9. The proof follows from application of Theorem 7 (see Section 3.2 of Chapter 3) and consists of three steps. First we show that $\mathcal{L}^*$ is hypoelliptic, hence Condition 1(ii) is satisfied. Second we verfiy Condition 1(i) and third we verify

Condition 2. Finally we apply Theorem 7 to get the desired result.

We can assume without loss of generality that $\gamma = \mu = \beta = 1$ and $M = \mathrm{Id}$. Furthermore, we assume that B is diagonal, hence

$$H(q,p) = \frac{1}{2}\sum_{k=1}^{n}(\omega_k q_k^2 + p_k^2).$$

This assumption does not involve any loss of generality since it amounts to choosing the coordinate system which is created by the eigenvectors $\varphi_1 \dots \varphi_n$.

Step 1: hypoellipticity of $\mathcal{L}^*$. After the above simplifications the vector fields X_0 and X_1 assume the form

$$X_0 = \left(p, -Bq - \xi p, (\|p\|^2 - n) - \xi\right), \quad X_1 = \left(0, 0, \sqrt{2}\right).$$

Next, we define recursively the following sequence of vector fields:

$$Z_k = \tfrac{1}{2}[Y_k, X_3], \quad Y_{k+1} = -\tfrac{1}{2}[Z_k, X_3],$$

where

$$\begin{aligned}
\tilde{X}_1 &= \tfrac{1}{\sqrt{2}} X_1 = (0,0,1)\,,\\
\tilde{X}_0 &= X_0 - \left((\|p\|^2 - n) - \xi\right)\tilde{X}_1 = (p, -Bq - \xi p, 0),\\
X_2 &= [\tilde{X}_0, \tilde{X}_1] = (0, p, 0),\\
X_3 &= \tilde{X}_0 + \xi X_2 = (p, -Bq, 0),\\
Y_1 &= [X_2, X_3] = (p, Bq, 0).
\end{aligned}$$

Induction yields that

$$Y_k = (B^{k-1}p, B^k q, 0), \quad Z_k = (B^k q, -B^k p, 0), \quad k = 1, 2, \dots, n$$

After these preparations we can show that the vectors $X_1, Y_1, Z_1, \dots Y_{n-1}, Z_{n-1}, Y_n, Z_n$ span $\mathbb{R}^{2n+1}$. Clearly, it suffices to demonstrate that for each $\eta, \mu \in \mathbb{R}^n$ there exist coefficients $a_1, b_1 \dots, a_n, b_n \in \mathbb{R}$ such that

$$\sum_{k=1}^{n}(a_k Y_k + b_k Z_k) = \sum_{k=1}^{n}(a_k B^{k-1}p + b_k B^k q,\ a_k B^k q - b_k B^k p) = (\eta, \mu). \tag{4.15}$$

Since the matrix B is diagonal, Equation (4.15) is equivalent to

$$\begin{pmatrix} \mathrm{diag}(B^{-1}p) & \mathrm{diag}(q) \\ \mathrm{diag}(q) & -\mathrm{diag}(p) \end{pmatrix} \begin{pmatrix} \mathcal{V}a \\ \mathcal{V}b \end{pmatrix} = \begin{pmatrix} \eta \\ \mu \end{pmatrix},$$

where $\mathcal{V}_{kl} = \omega_k^l$, $k, l = 1 \dots n$ is a Vandermonde matrix with determinant

$$\det(\mathcal{V}) = \prod_k \omega_k \prod_{k>l} (\omega_k - \omega_l).$$

Set now

$$\tilde{a} = \mathcal{V}a, \quad \tilde{b} = \mathcal{V}b, \tag{4.16}$$

then the k-th components of $\tilde{a}, \tilde{b}$ solve of the linear system

$$\begin{pmatrix} \omega_k^{-1} p_k & q_k \\ q_k & -p_k \end{pmatrix} \begin{pmatrix} \tilde{a}_k \\ \tilde{b}_k \end{pmatrix} = \begin{pmatrix} \eta_k \\ \mu_k \end{pmatrix},$$

i.e. $\begin{pmatrix} \tilde{a}_k \\ \tilde{b}_k \end{pmatrix} = \frac{1}{\omega_k^{-1} p_k^2 + q_k^2} \begin{pmatrix} p_k & q_k \\ q_k & -\omega_k^{-1} p_k \end{pmatrix} \begin{pmatrix} \eta_k \\ \mu_k \end{pmatrix}$.

The coefficient vectors a and b are obtained by inverting the relation (4.16) which is possible since we have assumed that the eigenvalues ω_i are pairwise different from each other and bigger than zero, thus the determinant of $\mathcal{V}$ is nonzero. Thus $\mathcal{L}^*$ is hypoelliptic.

Step 2: verification of Condition 1(i). In principle Condition 1(i) is satisfied whenever the coefficient of the SDE are Lipschitz continuous and the diffusion matrix is invertible. We use a technique from [84] to verify Condition 1(i). It suffices to show that for any x_0, $y \in \mathbb{R}^N$, the solution of (4.9) starting at x_0 will reach an arbitrary small neighbourhood of y.

Consider $\mathcal{W} \in C^1([0,t], \mathbb{R})$ such that

$$\frac{\mathrm{d}z}{\mathrm{d}t} = X_0(z) + X_1(z) \frac{\mathrm{d}\mathcal{W}}{\mathrm{d}t}$$

satisfies $z(0) = x_0$ and $z(t) = y$. Note that it is possible to find such $\mathcal{W}$, since we can construct smooth curve $z(t)$ using polynomial interpolation between the end points.

Hence we have,

$$x(t) = x_0 + \int_0^t X_0(x(s))\,\mathrm{d}s + \int_0^t X_1(x(s))\,\mathrm{d}W_s,$$
$$z(t) = x_0 + \int_0^t X_0(z(s))\,\mathrm{d}s + \int_0^t X_1(z(s))\,\mathrm{d}\mathcal{W}_s.$$

This gives

$$||x(t) - z(t)|| \leq \int_0^t ||X_0(x(s)) - X_0(z(s))||\,\mathrm{d}s + \int_0^t ||X_1(x(s)) - X_1(z(s))||\,\mathrm{d}\mathcal{W}_s + \left\| \int_0^t X_1(x(s))\,\mathrm{d}\left(W_s - \mathcal{W}_s\right) \right\|.$$

Integrating by parts and using the fact that X_0 and X_1 are Lipschitz, we get

$$\begin{aligned} ||x(t) - z(t)|| &\leq K \int_0^t \|x(s) - z(s)\|\,\mathrm{d}s + \\ &\qquad \left\| X_1(x(t))(W_t - \mathcal{W}_t) - \int_0^t (W_s - \mathcal{W}_s)\,\mathrm{d}X_1(x(s)) \right\|, \\ &\leq K \int_0^t \|x(s) - z(s)\|\,\mathrm{d}s + K \sup_{0\leq s\leq t} \|W_s - \mathcal{W}_s\|. \end{aligned}$$

Using the Gronwall's lemma we obtain

$$||x(t) - z(t)|| \leq K e^{Kt} \sup_{0\leq s\leq t} \|W_s - \mathcal{W}_s\|.$$

Now suppose that

$$\sup_{0\leq s\leq t} \|W_s - \mathcal{W}_s\| \leq \epsilon = \frac{\delta}{K e^{Kt}}, \tag{4.17}$$

since

$$0 < \int_{-\epsilon}^{+\epsilon} e^{-(u-\mathcal{W})^2}\,\mathrm{d}u,$$

the probability that the event (4.17) occurs is also positive. Thus

$$||x(t) - y|| \leq \delta,$$

as required.

Step 3: verification of Condition 2. Let $\mathcal{V} : U \to [1, \infty)$:

$$\mathcal{V}(x) = \tfrac{1}{2} p^T M^{-1} p + V(q) + \tfrac{1}{2}\left(\xi - a\right)^2, \tag{4.18}$$

by Lemma 1 (see Section 3.2 of Chapter 3) it is sufficient to find constant $\lambda \in (0, \infty)$ and $\Lambda \in (0, \infty)$ such that

$$\mathcal{L}\mathcal{V}(x) \leq -\lambda \mathcal{V}(x) + \Lambda.$$

We start by calculating

$$\mathcal{L}\mathcal{V} = \sum_{i=1}^{n} \frac{p_i}{m_i} \frac{\partial \mathcal{V}}{\partial q_i} - \sum_{i=1}^{n} \frac{\partial V}{\partial q_i} \frac{\partial \mathcal{V}}{\partial p_i} - \xi \sum_{i=1}^{n} p_i \frac{\partial \mathcal{V}}{\partial p_i} + \frac{1}{\mu} \left(\sum_{i=1}^{n} \frac{p_i^2}{m_i} - \frac{n}{\beta} \right) \frac{\partial \mathcal{V}}{\partial \xi} - \gamma \xi \frac{\partial \mathcal{V}}{\partial \xi} + \frac{1}{2} \sigma^2 \frac{\partial^2 \mathcal{V}}{\partial \xi^2},$$

where $\mathcal{L}$ is the generator of (3.19), we have

$$\begin{aligned} \mathcal{L}\mathcal{V} =& \langle M^{-1}p, Bq \rangle - \langle M^{-1}p, Bq \rangle - \xi \langle p, M^{-1}p \rangle + \xi \langle p, M^{-1}p \rangle \\ & - \frac{n}{\beta}\xi - a\langle p, M^{-1}p \rangle + \frac{na}{\beta} - \gamma\mu\xi^2 + \gamma\mu a\xi + \frac{1}{2}\sigma^2 \\ =& - a\langle p, M^{-1}p \rangle - \gamma\mu\xi^2 + \left(\gamma\mu a - \frac{n}{\beta} \right) \xi + \frac{na}{\beta} + \frac{1}{2}\sigma^2 \end{aligned}$$

Let define a by

$$\gamma\mu a - \frac{n}{\beta} = 0,$$

which gives $a = \frac{n}{\gamma\mu\beta}$, hence we get,

$$\mathcal{L}\mathcal{V} = -a p^T M^{-1} p - \gamma\mu\xi^2 - \gamma\mu a^2 + \gamma\mu a^2 + \left(\frac{na}{\beta} + \frac{1}{2}\sigma^2 \right),$$

using the fact that $(x - y)^2 \leq 2x^2 + 2y^2$, we get

$$\mathcal{L}\mathcal{V} \leq -2a \left[\frac{p^T M^{-1} p}{2} \right] - \gamma\mu \left[\frac{(\xi - a)^2}{2} \right] + \left(\gamma\mu a^2 + \frac{na}{\beta} + \frac{1}{2}\sigma^2 \right).$$

Let,

$$\lambda = \min\{2a, \gamma\mu\} = \min\left\{ \frac{n}{\gamma\mu\beta}, \gamma\mu \right\}, \tag{4.19}$$

then we obtain

$$\begin{aligned} \mathcal{L}\mathcal{V} \leq& - \lambda\mathcal{V} + \lambda V(q) + \left(\gamma\mu a^2 + \frac{na}{\beta} + \frac{1}{2}\sigma^2 \right) \\ \leq& - \lambda\mathcal{V} + \Lambda, \end{aligned}$$

where

$$\Lambda = \sup\left\{\lambda V(q) + \gamma\mu a^2 + \frac{na}{\beta} + \frac{1}{2}\sigma^2\right\}.$$

Thus, for a finite system $n < \infty$, if we choose μ to be of order n so that $a^2 < \infty$, and if we let $\mathcal{M} = \mathbb{T}^n \subset \mathbb{R}^n$, where $\mathbb{T}^n$ is n-dimensional torus, which is the case in most of MD simulations since we often use periodic boundary conditions, or $\mathcal{M} = \{q : V(q) < \infty\}$, then since $V(q)$ is smooth and bounded below by zero, we have $\Lambda < \infty$. □

4.3 Numerical Integrators for NHL

In this section we proposed some numerical methods to obtain a discrete solution of NHL. In general the sampling result is dependent on the integrator we use to solve (4.6)-(4.8). More precisely we want the discrete Markov chain which is the numerical solution of NHL to have the same distribution and convergence rate as the continuous solution.

One way to design numerical integrator for NHL is to split equations (4.6)-(4.8) into

$$\frac{\mathrm{d}q}{\mathrm{d}t} = M^{-1}p, \tag{4.20}$$
$$\frac{\mathrm{d}p}{\mathrm{d}t} = 0, \tag{4.21}$$
$$\frac{\mathrm{d}\xi}{\mathrm{d}t} = 0, \tag{4.22}$$

$$\frac{\mathrm{d}q}{\mathrm{d}t} = 0, \tag{4.23}$$
$$\frac{\mathrm{d}p}{\mathrm{d}t} = -\nabla_q V(q), \tag{4.24}$$
$$\frac{\mathrm{d}\xi}{\mathrm{d}t} = 0, \tag{4.25}$$

$$\frac{\mathrm{d}q}{\mathrm{d}t} = 0, \tag{4.26}$$
$$\frac{\mathrm{d}p}{\mathrm{d}t} = -\xi p, \tag{4.27}$$
$$\frac{\mathrm{d}\xi}{\mathrm{d}t} = \frac{1}{\mu}\left(p^T M^{-1} p - \frac{n}{\beta}\right), \tag{4.28}$$

$$\frac{\mathrm{d}q}{\mathrm{d}t} = 0, \tag{4.29}$$

$$\frac{\mathrm{d}p}{\mathrm{d}t} = 0, \tag{4.30}$$

$$\mathrm{d}\xi = -\gamma\xi\,\mathrm{d}t + \sigma\,\mathrm{d}W. \tag{4.31}$$

Let

$$\Phi_{\Delta t,H_1}(q,p,\xi) := (q + \Delta t M^{-1}p, p, \xi) \text{ and } \Phi_{\Delta t,H_2}(q,p,\xi) := (q, p - \Delta t \nabla_q V(q), \xi)$$

be the discrete maps for solutions of (4.20)-(4.22) and (4.23)-(4.25). Similarly, we define numerical solution of (4.26)-(4.28) by the composition

$$\Phi_{\Delta t,NH}(q^{k+1},p^{k+1},\xi^{k+1}) := \Phi_{\Delta t/2,NH_2} \circ \Phi_{\Delta t,NH_1} \circ \Phi_{\Delta t/2,NH_2}(q^k,p^k,\xi^k)$$

given by

$$\begin{aligned}
p^{k+1/2} &= p^k - \frac{\Delta t}{2}(\xi^k p^{k+1/2}),\\
\xi^{k+1} &= \xi^k + \frac{\Delta t}{\mu}\left((p^{k+1/2})^T M^{-1} p^{k+1/2} - \frac{n}{\beta}\right),\\
p^{k+1} &= p^{k+1/2} - \frac{\Delta t}{2}(\xi^{k+1} p^{k+1/2}).
\end{aligned}$$

The discrete solution of Ornstein-Uhlenbeck process (4.31) is given by

$$\Phi_{\Delta t,OU}(q,p,\xi) := (q,p, e^{-\gamma\Delta t}\xi + \sqrt{\frac{(1-e^{-2\gamma\Delta t})}{\mu\beta}}\eta),$$

where η is a normal random variable with mean zero and variance 1.

A numerical solution of NHL is obtained by the composition

$$\Phi_{\Delta t/2,H_2} \circ \Phi_{\Delta t/2,NH_2} \circ \Phi_{\Delta t,NH_1} \circ \Phi_{\Delta t,OU} \circ \Phi_{\Delta t,H_1} \circ \Phi_{\Delta t/2,NH_2} \circ \Phi_{\Delta t/2,H_2}(q^k,p^k,\xi^k)$$

which is given by

$$\begin{aligned}
p^{k+1/2} =& p^k - \frac{\Delta t}{2}\nabla_q V(q^k) - \frac{\Delta t}{2}(\xi^k p^{k+1/2}),\\
q^{k+1} =& q^k + \Delta t p^{k+1/2},\\
\xi^{k+1} =& e^{-\gamma\Delta t}\xi^k + \frac{\Delta t}{\mu}\left((p^{k+1/2})^T M^{-1} p^{k+1/2} - \frac{n}{\beta}\right) + \sqrt{\frac{(1-e^{-2\gamma\Delta t})}{\mu\beta}}\eta^k,\\
p^{k+1} =& p^{k+1/2} - \frac{\Delta t}{2}\nabla_q V(q^{k+1}) - \frac{\Delta t}{2}(\xi^{k+1} p^{k+1/2}),
\end{aligned}$$

where $\{\eta^k\}$ are normal random variables $\mathcal{N}(0,1)$. One can follow the procedure for proving Theorem 9 and the technique used in [85, 84] to show that the Markov process generated by the above method is geometrically ergodic with the same assumptions that we used to prove the ergodicity for continuous solution. It can also be shown that the above method is second-order (in weak sense) by comparing it to the standard second-order weak method for SDEs with additive noise from [132](p. 113).

Next, integrating the Nosé-Hoover part, that is (4.26)-(4.28) we obtain

$$\begin{aligned}
p(t+\Delta t) =& p(t)\exp\left(-\int_t^{t+\Delta t}\xi(s)\,\mathrm{d}s\right),\\
\xi(t+\Delta t) =& \xi(t) + \frac{1}{\mu}\int_t^{t+\Delta t} p(s)^T M^{-1} p(s)\,\mathrm{d}s - \frac{n}{\mu\beta}\Delta t.
\end{aligned}$$

Using the approximations

$$\int_t^{t+\Delta t}\xi(s)\,\mathrm{d}s = \Delta t\xi(t)+\mathcal{O}(\Delta t^2) \text{ and } \int_t^{t+\Delta t} p(s)^T M^{-1} p(s)\,\mathrm{d}s = \Delta t(p(t)^T M^{-1} p(t))+\mathcal{O}(\Delta t^2),$$

gives

$$p(t+\Delta t) = p(t)e^{-\Delta t\xi(t)} + \mathcal{O}(\Delta t^2), \tag{4.32}$$

$$\xi(t+\Delta t) = \xi(t) + \frac{\Delta t}{\mu}\left(\left(p(t)^T M^{-1} p(t)\right) - \frac{n}{\beta}\right) + \mathcal{O}(\Delta t^2). \tag{4.33}$$

Equation (4.31) can be written as the integral equation

$$\xi(t+\Delta t) = \xi(t) - \gamma\int_t^{t+\Delta t}\xi(s)\,\mathrm{d}s + \sigma\int_t^{t+\Delta t}\mathrm{d}W(s),$$

where $\int_t^{t+\Delta t} \mathrm{d}W(s)$ is Gaussian with mean zero and variance

$$\mathbf{E}\left[\left(\int_t^{t+\Delta t} \mathrm{d}W(s)\right)^2\right] = \Delta t.$$

Hence, using the approximation

$$\int_t^{t+\Delta t} \xi(s)\,\mathrm{d}s = \frac{\Delta t}{2}(\xi(t) + \xi(t+\Delta t)) + \mathcal{O}(\Delta t^2)$$

we can approximate the Ornstein-Uhlenbeck process (4.31) by

$$\xi(t+\Delta t) = \xi(t) - \frac{\gamma \Delta t}{2}(\xi(t) + \xi(t+\Delta t)) + \sigma\sqrt{\Delta t}\eta, \tag{4.34}$$

where η is a normal random variable (i.e. $\eta \sim \mathcal{N}(0,1)$). Using $\Phi_{\Delta t,H_1}$, $\Phi_{\Delta t,H_2}$, (4.32)-(4.33) and (4.34), we obtain the following discretization:

$$\begin{aligned}
P :=& p^k - \frac{\Delta t}{2}\nabla_q V(q^k),\\
Q :=& q^k + \frac{\Delta t}{2}P,\\
P :=& \exp\left(-\frac{\Delta t}{2}\xi^k\right)P,\\
\xi^{k+1} :=& \xi^k + \frac{\Delta t}{\mu}\left(\left(P^T M^{-1} P\right) - \frac{n}{\beta}\right) - \frac{\gamma \Delta t}{2}(\xi^n + \xi^{k+1}) + \sqrt{\frac{2\gamma\Delta t}{\mu\beta}}\eta^k,\\
P :=& \exp\left(-\frac{\Delta t}{2}\xi^{k+1}\right)P,\\
q^{k+1} =& Q + \frac{\Delta t}{2}P,\\
p^{k+1} =& P - \frac{\Delta t}{2}\nabla_q V(q^{k+1}).
\end{aligned}$$

A discretization of NHL which we used in this chapter for our numerical experiment

is

$$
\begin{aligned}
q^{k+1/2} =& q^k + \frac{\Delta t}{2} p^k, \\
\bar{p} =& p^k - \frac{\Delta t}{2} \nabla V(q^{k+1/2}) - \frac{\Delta t}{2} \bar{\xi} \bar{p}, \\
\bar{\xi} =& \xi^k + \frac{\Delta t}{2} \mu^{-1} \left(\bar{p}^T M^{-1} \bar{p} - \frac{n}{\beta} \right) - \frac{\Delta t}{2} \gamma \bar{\xi} + \frac{1}{2} \sqrt{\frac{2\gamma \Delta t}{\mu \beta}} \eta^k, \\
p^{k+1} =& 2\bar{p} - p^k, \\
\xi^{k+1} =& 2\bar{\xi} - \xi^k, \\
q^{k+1} =& q^{k+1/2} + \frac{\Delta t}{2} p^{k+1}.
\end{aligned}
$$

This method is semi-implicit (requiring an iteration to solve at each step), but it is important to note that only one force evaluation is required at each time step. Hence, in practice the method has the cost of an explicit integrator such as comparable methods [87, 77, 76, 92] for Langevin dynamics. We expect both above methods to be second-order (in weak sense). This can be checked by following the procedures in [86], that is by comparing the above methods with the standard second-order weak method for SDEs with additive noise from [132] (p. 113) and assuming that the forces are globally Lipschitz.

Alternative discretization may be obtained by following the procedures described in [90, 132, 76, 77, 92, 81, 78].

4.4 Numerical Results

In this section we run a series of tests on the system (4.6)-(4.8) to investigate the validity of the invariant measure ρ_{NHL} and its applications.

4.4.1 Harmonic Oscillator

First we investigate the dynamics of (4.6)-(4.8) for the case where the energy of the system is given by a Hamiltonian of the form

$$H(q,p) = \frac{p^2}{2m} + \omega^2 \frac{q^2}{2}.$$

In our experiment we chose $\omega = m = 1$, $\beta = 1.0$, $\mu = 0.5$, $\sigma = 5.0$ and $\Delta t = 0.01$. The parameter μ influences the control on temperature and σ influences the coupling be-

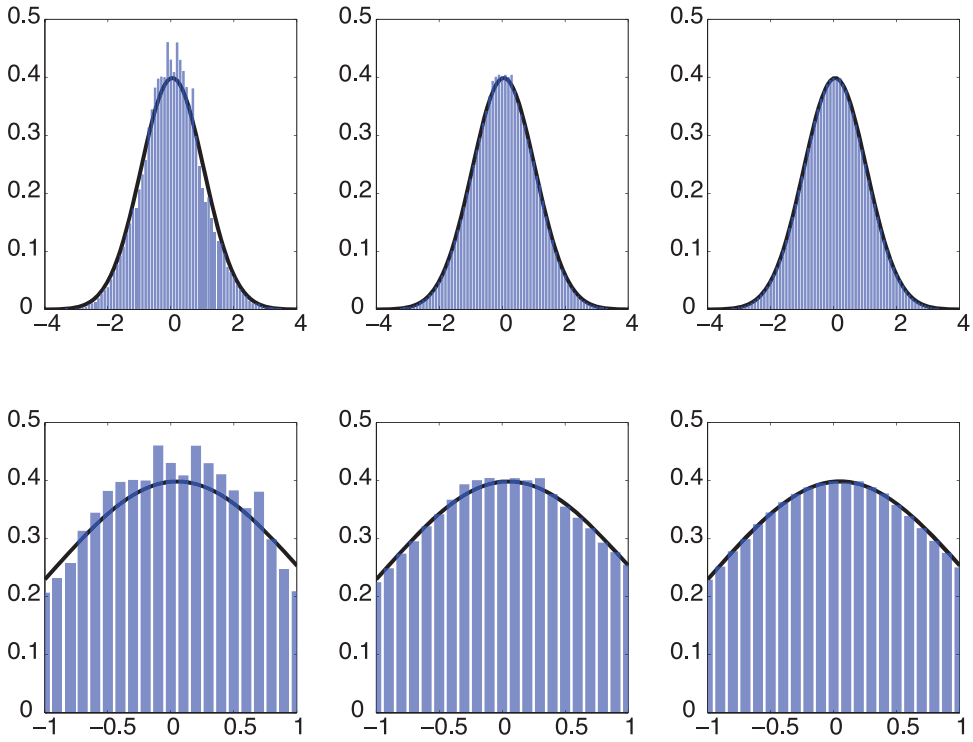

Figure 4.1: Convergence of momentum distribution is verified for the harmonic oscillator. The solid line is the exact density and the approximated density is in bar style. The (left) column 10^5 steps, the (middle) column 10^6 of steps and the (right) column 10^7 steps, each step of size $\Delta t = 0.01$.

tween system and the heat bath. To verify that our dynamics generates the Boltzmann-Gibbs distribution, the distribution of momentum is compared to $\sqrt{\frac{\beta}{2\pi m}}e^{-\beta\frac{p^2}{2m}}$. This is demonstrated in Figure 4.1.

In order to quantify the error in the distribution generated by (4.6)-(4.8), we define the following norm. For a given interval (a, b), define

$$D_n(x) = \left(\frac{1}{M}\sum_{i=1}^{M}\left(\phi_{K_i}(x) - \int_{K_i} \mathrm{d}\rho_\beta\right)^2\right)^{\frac{1}{2}}, \tag{4.35}$$

where x is a set of size n samples generated by the dynamics, $(K_1, \ldots, K_M)$ are M partitions of (a, b) and $\phi_{K_i}(x)$ is the observed density of samples in x which belong to the partition K_i.

In Figure 4.2, we compare the error norm $D_n(x)$ for the new dynamics (Hoover-Langevin) with other widely used sampling methods namely Nosé-Hoover chains (NHC) [62] (an extension of Nosé-Hoover where a chain of thermostats ξ_i with thermostat coefficient Q_i are attached to the system) and Langevin dynamics to investigate the

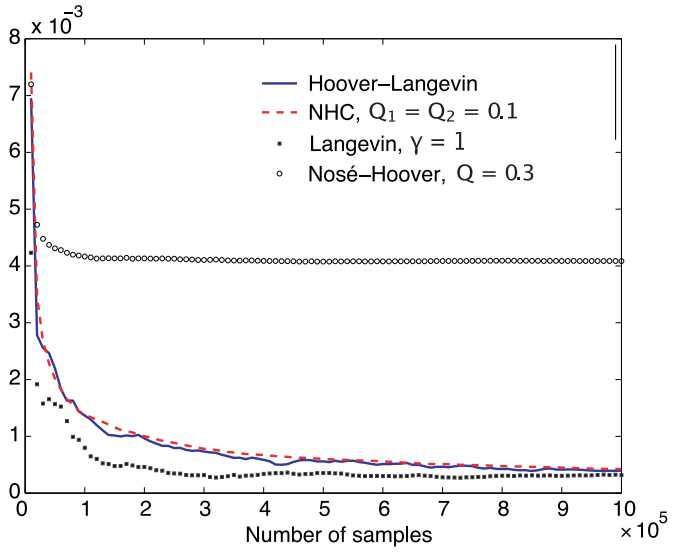

Figure 4.2: The graph shows the error $D_n(x)$ in the approximated density of momentum against the number of samples n. The rate of convergence of the distribution of Hoover-Langevin is similar to Nosé-Hoover chain (NHC) and Langevin dynamics for the case of harmonic oscillator.

Table 4.1: Error (4.35) in distribution for p, p^2 and p^4 using Hoover-Langevin.

	Error for 10^5 evolutions	Error for 10^6 evolutions	Error for 10^7 evolutions
p	0.201035×10^{-2}	0.454371×10^{-3}	0.167924×10^{-3}
p^2	0.912343×10^{-3}	0.207135×10^{-3}	0.444854×10^{-6}
p^4	0.130941×10^{-2}	0.251866×10^{-3}	0.487444×10^{-6}

rate of convergence. We chose $\gamma = 1$ for Langevin and $Q_1 = Q_2 = 0.1$ for NHC which we observed to be optimal parameters for these methods. The time step $\Delta t = 0.01$ was used for all simulations. In order to reduce the inconsistency in the results due to the random noise, for each method, 100 different simulations with different initial conditions have been performed and the result illustrated in Figure 4.2 is the mean of the 100 different results.

We also computed the errors (4.35) in distribution for p^2 and p^4, which are presented in Table 4.1.

4.4.2 Discrepancy In The Dynamics

One important aspect of molecular dynamics (MD) is to capture macroscopic information from the dynamics of atoms or small constituent parts that form a material. Therefore it is essential to take care that the algorithm used in MD is not changing the

dynamics of the physical system significantly. The new dynamics is designed to generate the canonical distribution by introducing a minimal perturbation to the system so that the dynamics of the thermostated system is close to the unperturbed system.

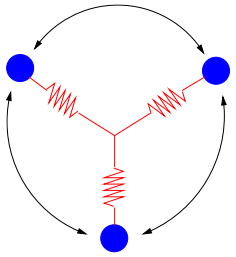

Figure 4.3: Three particles of mass m are connected by springs to the origin and interacting with each other through Lennard-Jones (LJ) potential.

Consider a two dimensional system consisting of three particles which are connected by springs with rest length to a fixed point at the origin (Figure 4.3). The interaction between particles is modelled by Lennard-Jones potential,

$$U_{LJ}(r) = 4\epsilon \left[\left(\frac{\alpha}{r}\right)^{12} - \left(\frac{\alpha}{r}\right)^{6} \right].$$

The Hamiltonian of the system is

$$H(q,p) = \sum_{i=1}^{3} \tfrac{1}{2m_i} p_i^2 + \sum_{i=1}^{3} \tfrac{1}{2} k \left(L - \parallel q_i \parallel\right)^2 + \sum_{i=1}^{2} \sum_{j=i+1}^{3} U_{LJ}(r_{ij}), \tag{4.36}$$

where L is the spring rest length, k is the spring constant, $r_{ij} = \parallel q_j - q_i \parallel$ and U_{LJ} is the Lennard-Jones potential. This is a challenging problem in terms of equilibration due to the locking of energy in springs. x

In our simulation we took $\alpha = \epsilon = 1$, $k = 10$, $L = 1$, $m_i = 1$ for $i = 1, 2, 3$ and set the target temperature $T = 1$, $k_B = 1$. In order to measure the changes in the dynamics we look at the velocity autocorrelation function of the radial component of velocity,

$$v_{ri}(t) = \frac{\dot{q}_i \cdot q_i}{\parallel q_i \parallel}, \tag{4.37}$$

To calculate the canonically weighted VAF function we first construct a set of 1000 random initial conditions $\{z_i\}$ from a canonical distribution at the target temperature. From each z_i we run a microcanonical simulation and calculate its VAF, the correct

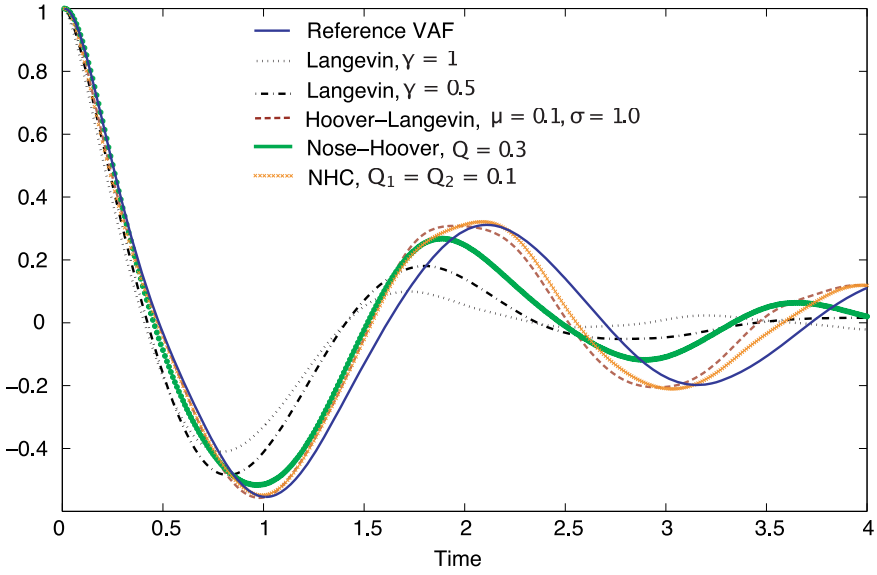

Figure 4.4: Autocorrelation function $c_1(\tau)$, computed using Hoover-Langevin, Langevin, Nose-Hoover and NHC, and compared to the velocity autocorrelation of canonically averaged microcanonical ($\bar{c}_1(\tau)$) dynamics.

VAF is then obtained as a weighted average of VAFs from different initial conditions:

$$\bar{c}(\tau) = \frac{\sum_i c(\tau; z_i)\rho_\beta(z_i)}{\sum_i \rho_\beta(z_i)}, \tag{4.38}$$

where

$$c(\tau; z) = \lim_{T\to+\infty} \frac{1}{T} \int_0^T \frac{v_{r_1}(t; z)v_{r_1}(t+\tau; z)}{v_{r_1}(t; z)v_{r_1}(t; z)}\, \mathrm{d}t, \tag{4.39}$$

with v_{r_1} representing, in this case, the radial velocity of the first particle of the system. Figure 4.4 compares the radial VAF for Hoover-Langevin with those obtained by other methods. The parameters are chosen with the criteria to achieve a correct distribution: $\mu = 0.1$, $\sigma = 1$ for Hoover-Langevin, $\gamma = 1$ and $\gamma = 0.5$ for Langevin, $Q = 0.3$ for Nosé-Hoover and $Q_1 = Q_2 = 0.1$ for NHC. We used these values of the Langevin parameter so that the error in its distribution is of the same size of the error in the distribution for Hoover-Langevin. Moreover, we observed that for $\gamma < 0.5$ the temperature fails to reach its target value within the simulation time, we elaborate more on temperature in the next subsection. As can be seen from Figure 4.4, Hoover-Langevin follows the VAF of microcanonical (unperturbed dynamics) very closely, whereas the Langevin dynamics for $\gamma = 1.0$ and $\gamma = 0.5$ profoundly changes the VAF, since it perturbs every degree of freedom by adding random noise. Using smaller values of γ

Table 4.2: Comparison of root mean square of error on $[0, 4]$ of VAF and the error in distribution using (4.35) for 10^6 of $\Delta t = 0.01$ evaluations.

Method	Parameters	Error in distribution	Error on $[0, 4]$ of VAF
Hoover-Langevin	$\mu = 0.1$, $\sigma = 1$	0.270198×10^{-3}	0.0675
Hoover-Langevin	$\mu = 0.1$, $\sigma = 10$	0.232064×10^{-3}	0.0578
Langevin	$\gamma = 0.5$	0.252864×10^{-3}	0.1018
Langevin	$\gamma = 1$	0.228635×10^{-3}	0.1383
NHC	$Q_1 = Q_2 = 0.1$	0.275997×10^{-3}	0.0603
Nos e-Hoover	$Q = 0.3$	0.165209×10^{-2}	0.0807

would improve the result for the VAF for Langevin dynamics, albeit at the expense of further perturbing the distribution obtained on a fixed time interval. Hence we compare the VAF of Langevin and Hoover-Langevin for the same level of perturbation needed for each method to approximate the Gibbs measure with the same accuracy, with a given amount of computational effort, Table 4.2 shows that Langevin dynamics and Hoover-Langevin approximate the Gibbs measure with very close accuracy for the chosen values of parameters. This illustrates that the dynamics of Hoover-Langevin has the characteristic of deterministic thermostats of being close to the original dynamics despite the fact that it is a stochastic method.

The error in VAF and the error in distribution for Hoover-Langevin, Nose-Hoover, NHC and Langevin method are shown in Table. 4.2. It worth noting that Langevin fails to produce the correct qualitative approximation of VAF as is visible in Figure 4.4.

4.4.3 Temperature Control

One important feature of the new dynamics is the control feedback loop in the dynamics which stabilizes the cumulative average kinetic energy of the system near the target temperature. Cumulative average kinetic energy is defined by

$$K(t) = \frac{1}{t} \int_0^t n^{-1} p^T(s) M^{-1} p(s) \, \mathrm{d}s.$$

In Figure 4.5 we compare the $K(t)$ of the Hoover-Langevin with the Langevin dynamics for the system (4.36). We used $\mu = 0.1$, $\sigma = 1$ for Hoover-Langevin and $\gamma = 1$ and $\gamma = 0.5$ for Langevin, both methods produce correct Gibbs measure in the long term, but the convergence of $K(t)$ is much slower for Langevin dynamics. Note that this

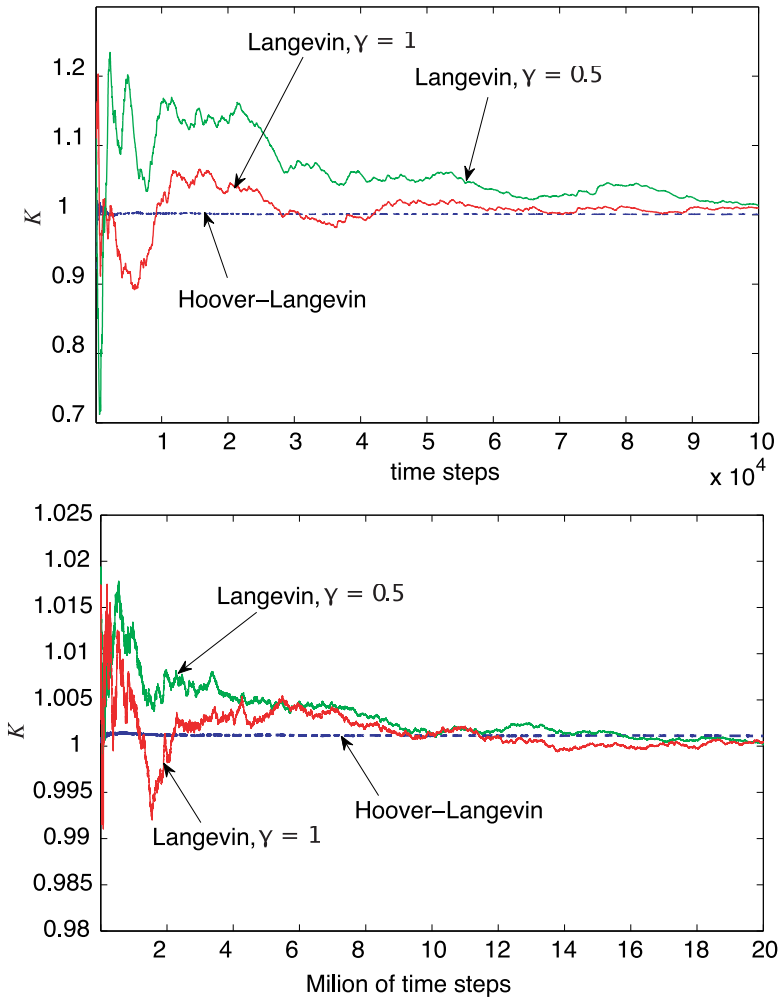

Figure 4.5: The (top) panel shows cumulative kinetic energy during 10^5 of time steps ($\Delta t = 0.01$) simulation. $K(t)$ computed by Hoover-Langevin dynamics reaches 1 (the target temperature) and stays close to 1, whereas it takes longer for Langevin dynamics to reaches the target temperature and the deviation is greater. The (lower) panel shows the slow convergence of temperature over twenty million time steps.

experiment does not demonstrate convergence to equilibrium; for general convergence to equilibrium one needs to compare the spectral gaps of the generator of the process (see [95]), which is difficult to do for Hoover-Langevin because it highly degenerate.

4.5 Adaptive Langevin Dynamics

In many applications it is desirable to reduce the disturbance to the dynamics. Intuitively one may argue that using small values for γ is the way forward. However, for Langevin dynamics the rate of relaxation to equilibrium and the rate at which the disturbance to the dynamics is growing, are both proportional to γ. Thus, small γ slows down the convergence. This suggest that we should search for a thermostat whose rate

of convergence to equilibrium is faster than the rate at which it perturbs the dynamics. Another solution would be to adaptively control the dissipation parameter in the Langevin dynamics. Indeed this is what we try here.

We propose the following stochastic differential equations

$$\mathrm{d}q = M^{-1}p\ \mathrm{d}t, \tag{4.40}$$

$$\mathrm{d}p = -\nabla_q V(q)\ \mathrm{d}t - \xi p\ \mathrm{d}t + \sigma\ \mathrm{d}W, \tag{4.41}$$

$$\mathrm{d}\xi = \frac{1}{\mu}\left(p^T M^{-1}p - \frac{n}{\beta}\right)\ \mathrm{d}t, \tag{4.42}$$

where W is n-dimensional Brownian motion, $\sigma \in \mathbb{R}^{n\times n}$ is a positive definite matrix, and we assume the fluctuation-dissipation relation $\sigma\sigma^T = \frac{2}{\beta}\gamma M$, where $\gamma \in \mathbb{R}^+$. The corresponding Fokker-Planck equation is

$$\begin{aligned}\frac{\partial f}{\partial t} = \mathcal{L}^* f = &-\nabla_q \cdot (M^{-1}pf) + \nabla_p \cdot (\nabla_q V(q) f) + \nabla_p \cdot (\xi p f) \\ &+ \frac{1}{2}\nabla_p \cdot (\sigma\sigma^T \nabla_p f) - \frac{\partial}{\partial \xi}\left(\frac{1}{\mu}\left(p^T M^{-1}p - \frac{n}{\beta}\right) f\right).\end{aligned} \tag{4.43}$$

The augmented Boltzmann-Gibbs measure with density is

$$f_{LNH}(q,p,\xi) = \frac{1}{Z_{LNH}} \exp\left(-\beta\left(H(q,p) + \frac{\mu}{2}(\xi-\gamma)^2\right)\right), \tag{4.44}$$

where $Z_{LNH} = \int f_{LNH}\ \mathrm{d}q\,\mathrm{d}p\,\mathrm{d}\xi$ is the stationary solution of the Fokker-Planck equation $\mathcal{L}^* f_{LNH} = 0$. Indeed, substituting f_{LNH} in (4.43) we have

$$\begin{aligned}-\nabla_q \cdot (M^{-1}p f_{LNH}) =& f_{LNH}\left(\beta M^{-1}p \cdot \nabla_q V\right), \\ \nabla_p \cdot (\nabla_q V f_{LNH}) =& -f_{LNH}\left(\beta \nabla_q V \cdot M^{-1}p\right), \\ \nabla_p \cdot (\xi p f_{LNH}) =& f_{LNH}\left(n\xi - \beta\xi p^T M^{-1}p\right), \\ \frac{1}{2}\nabla_p \cdot (\sigma\sigma^T \nabla_p f_{LNH}) =& f_{LNH}\left(-n\gamma + \beta\gamma P^T M^{-1}p\right), \\ -\frac{\partial}{\partial\xi}\left(\frac{1}{\mu}\left(p^T M^{-1}p\right) f_{LNH}\right) =& f_{LNH}\left(\beta\xi p^T M^{-1}p - n\xi\right) + \\ & f_{LNH}\left(-\beta\gamma p^T M^{-1}p + n\gamma\right),\end{aligned}$$

which sum up to zero.

The dynamics of (4.40)-(4.42) is adaptive in the sense that we only fix the average value of dissipation coefficient, that is $\mathbf{E}[\xi] = \gamma$. In this way we can effectively choose

small γ and still converge rapidly to the right Maxwellian distribution for momenta.

Remark

The following can be used as an alternative to the above method:

$$\begin{aligned}
\frac{\mathrm{d}q}{\mathrm{d}t} =& M^{-1}p\,\mathrm{d}t,\\
\frac{\mathrm{d}p}{\mathrm{d}t} =& -\nabla_q V(q) - \xi p + \eta,\\
\frac{\mathrm{d}\xi}{\mathrm{d}t} =& \frac{1}{\mu}\left(p^T M^{-1} p - \frac{n}{\beta}\right),\\
\mathrm{d}\eta =& -M^{-1}p\,\mathrm{d}t - \gamma(q,p)\eta\,\mathrm{d}t + \sigma(q,p)\,\mathrm{d}W,
\end{aligned}$$

where W is n-dimensional Brownian motion, $\gamma : \mathbb{R}^n \times \mathbb{R}^n \to \mathbb{R}^{n\times n}$ is the dissipation matrix, $\sigma : \mathbb{R}^n \times \mathbb{R}^n \to \mathbb{R}^{n\times n}$ is the diffusion matrix and we assume the fluctuation-dissipation relation $\sigma\sigma^T = \frac{2}{\beta}\gamma$, which implies that the augmented Boltzmann-Gibbs measure, with density proportional to

$$\exp\left(-\beta\left(H(q,p) + \frac{\mu}{2}\xi^2 + \frac{1}{2}\eta^2\right)\right),$$

is invariant under the evolution of the above SDE.

4.6 Discussion and Conclusion

We have presented a new thermostat for generating the canonical distribution in molecular dynamics simulations. This thermostat is derived by combining Nosé-Hoover and Langevin dynamics together with the aim to achieve a provable correct distribution and at the same time minimizing the effect on the dynamics. The new method should be of interest in cases where one is concerned with computing the average of local observables which depend on small number of degrees of freedom. For instance for calculating free energy of activated processes where the process occurs along a reaction coordinate which can be described as a function of the degrees of freedom of the system. This new thermostat is likely to be preferable for some non-equilibrium molecular dynamics simulations than the Langevin method, since it is close to the dynamics of the unperturbed system, and therefore interacts weakly with a non-equilibrium force acting on the system.

The new dynamics has an invariant probability measure ρ_{NHL} which is proportional

to the Boltzmann-Gibbs distribution and we have proved analytically that under a non-resonance assumption, an open, connected set U with full measure can be constructed such that ρ_{NHL} is ergodic on U. Thus, when the new thermostat is applied to Hamiltonians without resonances the dynamics is ergodic. This has been checked in several simple examples.

Chapter 5

A Measure of Efficiency for Heat Bath in Molecular Dynamics

This chapter is concerned with the question of how efficiently molecular dynamics can calculate time dependent properties such as autocorrelation functions in the canonical ensemble. A heat bath (a thermostat) is a modified Hamiltonian dynamics

$$\frac{\mathrm{d}}{\mathrm{d}t}\tilde{\varphi}_t(x) = \mathbb{J}\nabla H(\tilde{\varphi}_t(x)) + \varepsilon(\tilde{\varphi}_t(x)), \tag{5.1}$$

such that for a function of phase space $O : \mathbb{X} \to \mathbb{R}$

$$\lim_{t\to\infty} t^{-1} \int_0^t O(\tilde{\varphi}_s(x))\,\mathrm{d}s = \int_{\mathbb{X}} O(x)\,\mathrm{d}\rho_\beta(x). \tag{5.2}$$

In principle ε should be small perturbations to the dynamics and yet large enough to achieve the equality in (5.2). Indeed, a given method will typically have parameters that allow adjustment of the degree of perturbations introduced, usually balanced against the need for a rapid thermalisation of the system. Here we provide a first attempt to quantify this relationship, by calculating a quantity we call the *efficiency* of a heat bath: the ratio of the rate of convergence to equilibrium to the *rate of growth* of the dynamical perturbations.

To clarify this, let η be the efficiency of a heat bath, and let r be the rate of convergence to equilibrium, so that the rate at which the error in dynamics grows is r/η. Now, suppose we want to measure an equilibrium correlation function that decays in time τ. To do this with only a small error, we need $\tau(r/\eta) \ll 1$ which implies $1/r \gg \tau/\eta$. Thus the time to reach equilibrium, which is of order $1/r$, is $\gg \tau/\eta$. Any

simulation to measure equilibrium properties will last at least as long as the time to reach equilibrium (i.e., it will last a time that is $\gg \tau/\eta$). So the larger η, the more efficient the method, in the sense that we can compute accurately correlation functions for longer time (i.e., for larger τ).

We calculate the efficiency for Langevin dynamics (2.20)-(2.21) and Nosé-Hoover-Langevin (NHL) (4.6)-(4.8). We see that, for a system with many degrees of freedom, NHL is more efficient than Langevin.

5.1 The Rate of Growth of Perturbations

We define the rate of growth of perturbation as the rate at which the relative error

$$\frac{\left(\mathbf{E}\left[\|\varphi_t(x) - \tilde{\varphi}_t(x)\|^2\right]\right)^{1/2}}{\left(\mathbf{E}\left[\|\varphi_t(x)\|^2\right]\right)^{1/2}} \tag{5.3}$$

grows in time, where $\tilde{\varphi}_t$ is the solution of the perturbed equation (5.1) and φ_t is the unperturbed Hamiltonian flow map. The expectation $\mathbf{E}$ in (5.3) means average over equilibrium set of initial conditions.

5.1.1 Growth of Perturbations for NHL

Let us repeat the equations (4.6)-(4.8) for NHL dynamics:

$$\frac{\mathrm{d}q}{\mathrm{d}t} = M^{-1}p, \tag{5.4}$$

$$\frac{\mathrm{d}p}{\mathrm{d}t} = -\nabla V(q) - \xi p, \tag{5.5}$$

$$\mathrm{d}\xi = \frac{1}{\mu}\left(p^T M^{-1} p - \frac{n}{\beta}\right)\mathrm{d}t - \gamma\xi\,\mathrm{d}t + \sigma\,\mathrm{d}W. \tag{5.6}$$

Note that here and in Section 5.1.2, we are only interested in the growth of perturbations during a short time $t \ll \frac{1}{\lambda}$, where λ is the largest Lyapunov exponent of the system. Therefore we can assume that the changes in forces are negligible. Thus the main perturbation in momenta is:

$$\delta p(t) = -\int_0^t \xi(s)p(s)\,\mathrm{d}s.$$

The variance of this quantity (average over equilibrium set of initial conditions [1]) is

$$\mathbf{E}\left[\|\delta p(t)\|^2\right] = \sum_{i=1}^{n} \mathbf{E}\left[(\delta p_i(t))^2\right].$$

Its rate of change is

$$\frac{\mathrm{d}}{\mathrm{d}t}\mathbf{E}\left[\|\delta p(t)\|^2\right] = \sum_{i=1}^{n} \frac{\mathrm{d}}{\mathrm{d}t}\mathbf{E}\left[(\delta p_i(t))^2\right],$$

for each term in the sum, we have

$$\begin{aligned}\frac{\mathrm{d}}{\mathrm{d}t}\mathbf{E}\left[(\delta p_i(t))^2\right] =& 2\mathbf{E}\left[\xi p_i\left(\int_0^t \xi(s)p_i(s)\ \mathrm{d}s\right)\right] \\ \leq& 2\sqrt{\mathbf{E}[\xi^2 p_i^2]}\sqrt{\mathbf{E}\left[(\delta p_i(t))^2\right]},\end{aligned}$$

thus

$$\begin{aligned}\frac{\mathrm{d}}{\mathrm{d}t}\sqrt{\mathbf{E}\left[(\delta p_i(t))^2\right]} \leq& \sqrt{\mathbf{E}\left[\xi^2 p_i^2\right]} \\ \leq& \frac{1}{\beta}\sqrt{\frac{m}{\mu}},\end{aligned}$$

which gives

$$\sqrt{\mathbf{E}\left[\|\delta p(t)\|^2\right]} \leq \frac{1}{\beta}\sqrt{\frac{nm}{\mu}}t.$$

Hence the rate of growth in the standard deviation of the perturbations in p is at most $\frac{1}{\beta}\sqrt{\frac{nm}{\mu}}$, and the rate of growth in the relative error, i.e.,

$$\frac{\sqrt{\mathbf{E}\left[\|\delta p(t)\|^2\right]}}{\sqrt{\mathbf{E}\left[\|p\|^2\right]}},$$

is at most $\sqrt{\frac{1}{\beta\mu}}$.

[1] Here $\mathbf{E}$ is the expectation with respect to the stationary density f_{NHL}

5.1.2 Growth of Perturbations for Langevin

We repeat the equations (2.20)-(2.21) for Langevin dynamics:

$$\mathrm{d}q = M^{-1}p\,\mathrm{d}t, \tag{5.7}$$

$$\mathrm{d}p = -\nabla_q V(q)\,\mathrm{d}t - \gamma p\,\mathrm{d}t + \sigma\,\mathrm{d}W, \tag{5.8}$$

where the mass matrix $M = mI_n$, $\gamma \in \mathbb{R}$ is a positive constant and $\sigma^2 = \frac{2m}{\beta}\gamma$. In the Langevin dynamics the perturbations appear only in momenta. Over any short time ($t \ll \frac{1}{\lambda}$, where λ is the largest Lyapunov exponent of the system) the second term in equation (5.8) introduces an error $-\gamma p$ and the third term intriduces a random error whose mean is zero. Thus the growth of perturbations can be find by looking at

$$\delta p(t) = -\int_0^t \gamma p(s)\ \mathrm{d}s.$$

The variance of this quantity (average over equilibrium set of initial conditions [1]) is

$$\begin{aligned}\mathbf{E}\left[\|\delta p(t)\|^2\right] =& \sum_{i=1}^{n} \mathbf{E}\left[(\delta p_i(t))^2\right] \\ =& \sum_{i=1}^{n} \mathbf{E}\left[\left(\int_0^t \gamma p_i(s)\,\mathrm{d}s\right)^2\right].\end{aligned}$$

Its rate of change is

$$\frac{\mathrm{d}}{\mathrm{d}t}\mathbf{E}\left[\|\delta p(t)\|^2\right] = \sum_{i=1}^{n} \frac{\mathrm{d}}{\mathrm{d}t}\mathbf{E}\left[\left(\int_0^t \gamma p_i(s)\,\mathrm{d}s\right)^2\right],$$

for each term in the sum, we have

$$\begin{aligned}\frac{\mathrm{d}}{\mathrm{d}t}\mathbf{E}\left[\left(\int_0^t \gamma p_i(s)\,\mathrm{d}s\right)^2\right] =& 2\mathbf{E}\left[\gamma p_i\left(\int_0^t \gamma p_i(s)\ \mathrm{d}s\right)\right] \\ \leq& 2\sqrt{\mathbf{E}\left[\gamma^2 p_i^2\right]}\sqrt{\mathbf{E}\left[\left(\int_0^t \gamma p_i(s)\,\mathrm{d}s\right)^2\right]}.\end{aligned}$$

[1] Here $\mathbf{E}$ is the expectation with respect to the stationary density f_β

Thus

$$\frac{\mathrm{d}}{\mathrm{d}t}\sqrt{\mathbf{E}\left[\left(\int_0^t \gamma p_i(s)\,\mathrm{d}s\right)^2\right]} \leq \sqrt{\mathbf{E}\left[\gamma^2 p_i^2\right]} \leq \gamma\sqrt{\frac{m}{\beta}},$$

which implies

$$\sqrt{\mathbf{E}\left[\|\delta p(t)\|^2\right]} \leq \sqrt{\frac{nm}{\beta}}\gamma t.$$

Hence the rate of growth in the standard deviation of the perturbations in p is at most $\sqrt{\frac{nm}{\beta}}\gamma$, and the rate of growth in the relative error is at most γ.

5.2 The Rate of Convergence to Equilibrium

In this section we estimate the time it takes for each method to reach Maxwellian distribution for momenta. Our estimates are valid for systems not far from equilibrium, for systems far from equilibrium one should study the spectral gap of the generator for each method which is not always possible. The motivation for looking at the convergence in momenta comes from simulations, where usually the system is said to be equilibrated when the temperature converges to its limit.

5.2.1 Equilibration Rate for NHL

The rate of convergence to equilibrium can be seen as a rate at which the system converges to the absolute temperature T. Let $M = mI_n$, the generator $\mathcal{L}$ of NHL dynamics is

$$\mathcal{L} = M^{-1}p\cdot\nabla_q - \nabla_q V(q)\cdot\nabla_p - \xi p\cdot\nabla_p + \frac{1}{\mu}\left(p^T M^{-1}p\frac{n}{\beta}\right)\frac{\partial}{\partial\xi} - \gamma\xi\frac{\partial}{\partial\xi} + \frac{1}{2}\sigma^2\frac{\partial^2}{\partial\xi^2}.$$

The rate of change of the expectation of the energy $H(q,p)$ is

$$\begin{aligned}\frac{\mathrm{d}}{\mathrm{d}t}\mathbf{E}\left[H(q,p)\right] =& \mathbf{E}\left[\mathcal{L}H(q,p)\right]\\ =& \mathbf{E}\left[M^{-1}p\cdot\nabla_q V(q) - \nabla_q V(q)\cdot M^{-1}p - \xi p^T M^{-1}p\right]\\ =& -\mathbf{E}\left[\xi\left(p^T M^{-1}p\right)\right].\end{aligned}$$

The rate of change of the expectation of ξ can be calculated by taking expectation of equation (5.6):

$$\frac{\mathrm{d}}{\mathrm{d}t}\mathbf{E}[\xi(t)] = -\gamma\mathbf{E}[\xi(t)] + \frac{n}{\mu}\left(\theta - \frac{1}{\beta}\right),$$

where we defined the empirical temperature θ as

$$n\theta = \mathbf{E}\left[p^T M^{-1} p\right].$$

We use the following assumption to find a closed system in terms of θ and $\mathbf{E}[\xi]$.

Assumption 1 (Quasi-Equilibrium)**.**

- *We assume that starting from equilibrium initial conditions, the empirical temperature and the expectation of energy are linked by the same relation as in equilibrium:*

  $$C_V = \frac{\partial \rho_{NHL}(H)}{\partial T} \approx \frac{\partial E[H]}{\partial \theta},$$

  where C_V is the heat capacity at constant volume.

- *The random variables ξ and $\left(p^T M^{-1} p\right)$ that are uncorrelated initially at time $t = 0$, remain uncorrelated for all $t > 0$:*

  $$\mathbf{E}\left[\xi\left(p^T M^{-1} p\right)\right] \approx \mathbf{E}\left[\xi\right]\mathbf{E}\left[p^T M^{-1} p\right].$$

Using Assumption 1 we obtain

$$\begin{aligned} C_V\frac{\mathrm{d}\theta}{\mathrm{d}t} &= -\,n\theta\mathbf{E}[\xi], \\ \frac{\mathrm{d}}{\mathrm{d}t}\mathbf{E}[\xi] &= -\,\gamma\mathbf{E}[\xi] + \frac{n}{\mu}\left(\theta - \frac{1}{\beta}\right), \end{aligned}$$

The equilibrium of the above system is when $\theta = \frac{1}{\beta}$ and $\xi = 0$, hence we can study the decay to equilibrium by looking at the corresponding linearised system around this equilibrium:

$$\begin{aligned} C_V\frac{\mathrm{d}\delta}{\mathrm{d}t} &= -\,\frac{n}{\beta}\mathbf{E}[\xi], \\ \frac{\mathrm{d}}{\mathrm{d}t}\mathbf{E}[\xi] &= -\,\gamma\mathbf{E}[\xi] + \frac{n}{\mu}\delta, \end{aligned}$$

where we used $\theta = \frac{1}{\beta} + \delta$. The linearised system can be written as

$$\begin{bmatrix} \mathrm{d}\delta/\,\mathrm{d}t \\ \mathrm{d}\mathbf{E}[\xi]/\,\mathrm{d}t \end{bmatrix} = \begin{bmatrix} 0 & -n/(C_V\beta) \\ n/\mu & -\gamma \end{bmatrix} \begin{bmatrix} \delta \\ \mathbf{E}[\xi] \end{bmatrix}. \tag{5.9}$$

Its eigenvalues are

$$\lambda_{1,2} = -\frac{\gamma}{2} \pm \frac{1}{2}\sqrt{\gamma^2 - 4\frac{n^2}{\mu C_V \beta}}. \tag{5.10}$$

It is worth noting that the constant volume specific heat is of order n, indeed for a system with quadratic potential $C_V = nk$, where k is the Boltzmann constant. Hence if we choose μ to be of order n, then $\frac{n^2}{\mu C_V \beta} \approx \frac{1}{\beta}$. The underdamped regime is when $\gamma^2 < 4\frac{n^2}{\mu C_V \beta}$ and all eigenvalues are complex, the damped regime is when $\gamma^2 \geq 4\frac{n^2}{\mu C_V \beta}$ and the critical damping is when $\gamma^2 = 4\frac{n^2}{\mu C_V \beta}$, which gives the most rapid convergence to equilibrium. It is worth noting that Nosé-Hoover dynamics corresponds to $\gamma = 0$, which implies that the eigenvalues are complex with no real part so that the system oscillates indefinitely, this may be an indication that Nosé-Hoover is not ergodic.

The equilibration rate for Langevin dynamics in the case of quadratic potential is γ (see Chapter 3, Section 3.5.1).

5.2.2 Summary of Results

The main results can be summarized in a table:

	Convergence Rate	Growth Rate	Efficiency
Langevin	γ	γ	1
NHL	$\leq \sqrt{\frac{n}{\mu\beta}}$	$\sqrt{\frac{1}{\mu\beta}}$	$\leq \sqrt{n}$

Thus, for the NHL process, the estimated rate of growth of the perturbations, as they affect the molecular motions, is smaller then the temperature relaxation rate by a factor $n^{1/2}$, whereas for standard Langevin the two rates are approximately equal. This suggests that for large systems, with (say) 100 or more degrees of freedom, the NHL process will be significantly better than standard Langevin for estimating things like autocorrelation functions.

Numerical experiments to validate our results is desirable but is left for future works.

Chapter 6

An Adaptive Method for Kinetic Energy Control

Under standard assumptions, microcanonical and canonical ensembles agree in the thermodynamic limit. In many applications, the correction of sampling by Nosé dynamics and other schemes is less important than obtaining the correct temperature, i.e. that

$$\lim_{t\to\infty} \frac{1}{t} \int_0^t p^T(s) M^{-1} p(s)\, \mathrm{d}s \to \frac{n}{\beta}.$$

We have seen already that thermostat introduces persistent artificial perturbations to the Newtonian dynamics, which is sometimes severe [133, 134, 135, 136]. For example, the thermostat may inhibit large local fluctuations of temperature which are important in stimulating a transition. In many applications it would be more appropriate to use Newtonian dynamics, at an energy consistent with the desired target temperature.

Consider Nosé-Hoover dynamics (NHD):

$$\frac{\mathrm{d}q}{\mathrm{d}t} = M^{-1} p, \tag{6.1}$$

$$\frac{\mathrm{d}p}{\mathrm{d}t} = -\nabla_q V(q) - \xi p, \tag{6.2}$$

$$\frac{\mathrm{d}\xi}{\mathrm{d}t} = \frac{1}{\mu}\left(p^T M^{-1} p - \frac{n}{\beta}\right). \tag{6.3}$$

The idea considered here is to replace the control equation (6.3) by an alternative differential equation:

$$\frac{\mathrm{d}}{\mathrm{d}t}\xi = \alpha(t)\left(p^T M^{-1} p - \frac{n}{\beta}\right) - \gamma(t)\xi, \tag{6.4}$$

where the coefficient functions α and $\gamma > 0$ are (for the moment) arbitrary bounded functions. The purpose of this equation is to (i) control the temperature of the system, while (ii) reducing the influence of the artificial device on the system dynamics once equilibrium is achieved.

Traditionally the concept of temperature–and the idea of a thermostat–is meaningful for systems in or near thermal equilibrium. In the nonequilibrium setting, we share the perspective of D. Ruelle [137] " To keep a finite system outside of equilibrium we subject it to non-Hamiltonian forces...This means that the system will heat up. Indeed, this is what is observed experimentally: dissipative systems produce heat. An experimentalist will eliminate excess heat by use of a thermostat, and if we want to study nonequilibrium steady states we have to introduce the mathematical equivalent of a thermostat. " Thus we interpret a thermostat in the nonequilibrium context as a practical device: a (mild as possible) perturbation of dynamics which removes excess heat induced by non-equilibrium forces.

In the following sections, we describe the motivation for (6.4), propose specific choices for the functions $\alpha(t)$ and $\gamma(t)$ that appear in this equation, and discuss numerical experiments which include comparison with standard (equilibrium) thermostats such as Nosé dynamics and Langevin dynamics.

6.1 Temperature Regulated Molecular Dynamics

Instead of a differential temperature control law as in (6.3), consider the following algebraic formula to define ξ:

$$\mu\xi = \frac{1}{t}\int_0^t \frac{1}{n}K(s)\,\mathrm{d}s - \frac{1}{\beta}, \tag{6.5}$$

where $K = \sum_{i=1}^n m_i^{-1}p_i^2$. If we assume the cumulative average kinetic energy per degree of freedom were to converge to $\frac{1}{\beta}$ with time, then ξ would tend to zero so that the perturbation of constant energy dynamics would be expected to diminish with time. Effective numerical methods for (6.1), (6.2), (6.5) are cumbersome to design and analyse, since the equations are in the form of a delay-differential system. We therefore

differentiate (6.5) with respect to time to obtain:

$$\begin{aligned} \mu\frac{d}{dt}\xi &= \frac{1}{t}\left(\frac{K}{n}\right) - \frac{1}{t^2}\int_0^t \frac{1}{n}K(s)\,\mathrm{d}s \\ &= \frac{1}{t}\left(\frac{K}{n} - \frac{1}{\beta}\right) - \frac{1}{t}\mu\xi, \end{aligned} \tag{6.6}$$

which we recognise to be in the form (6.4) with $\alpha(t) = (\mu t)^{-1}$, $\gamma(t) = t^{-1}$. If the term proportional to ξ were absent from (6.6), the equation would look similar to the usual Nosé-Hoover formula, but with a t^{-1} scaling. The t^{-1} term thus acts as a coefficient of damping which becomes weaker with time, even as the effect of the thermostat is similarly reduced. We implemented a numerical method for the system (6.1), (6.2), (6.6) with positive results. However, as described the method has an obvious flaw: since the control is effectively scaled by $1/t$, the control will be less responsive to a change in state occurring later in the simulation. In nonequilibrium modelling, it is necessary to consider the potential need for re-equilibration during simulation.

The idea this suggests is to introduce a time-localised weight function in the computation of the average temperature:

$$\mu\xi = \frac{1}{\hat{\phi}(t)}\int_0^t \phi(t-s)\frac{K(s)}{n}\,\mathrm{d}s - \frac{1}{\beta}, \tag{6.7}$$

where $\phi(t)$ is the prescribed weight function, and $\hat{\phi}(t)$ its integral on $[0,t]$. Note that (6.5) can be recovered as a special case of (6.7), with the choice $\phi(t) \equiv 1$. This approach has again the drawback of requiring the design of a numerical method for delay differential equations. Introduce a new variable $\Phi = \int_0^t \phi(t-s)\frac{K(s)}{n}\,\mathrm{d}s$, and set $\mu\xi = \frac{\Phi}{\hat{\phi}(t)} - \frac{1}{\beta}$. Then, if $\phi(t) = \exp(-t/\tau)$, we have

$$\frac{\mathrm{d}}{\mathrm{d}t}\Phi = \phi(0)\frac{K(t)}{n} + \int_0^t \phi'(t-s)\frac{K(s)}{n}\,\mathrm{d}s = \frac{K(t)}{n} - \frac{\Phi}{\tau}.$$

We thus arrive at an elegant closed differential equation for the controlled system

(temperature regulated molecular dynamics, or TRMD for short):

$$\frac{\mathrm{d}q}{\mathrm{d}t} = M^{-1}p, \tag{6.8}$$

$$\frac{\mathrm{d}p}{\mathrm{d}t} = -\nabla_q V(q) - \xi p, \tag{6.9}$$

$$\frac{\mathrm{d}}{\mathrm{d}t}\Phi = \tfrac{1}{n}K(t) - \tfrac{1}{\tau}\Phi, \tag{6.10}$$

$$\mu\xi = \hat{\phi}^{-1}\Phi - \beta^{-1}, \tag{6.11}$$

where $\hat{\phi}(t) = \tau(1 - \exp(-t/\tau))$. In the limit $\tau \to +\infty$, we see that $\phi(t)$ becomes constant and equal to 1, and the exponential relaxation system formally becomes the average temperature control system (6.1), (6.2), (6.6) that we considered previously.

In our experiments we obtained good results by use of the following discretization scheme:

$$\begin{aligned}
q_i^{k+1} &= q_i^k + \Delta t m_i^{-1} p_i^{k+\frac{1}{2}}, \\
p_i^{k+\frac{1}{2}} &= p_i^k - \frac{\Delta t}{2}\frac{\partial V(q^k)}{\partial q_i} - \frac{\Delta t}{2}\xi^k p_i^{k+\frac{1}{2}}, \\
\Phi^{k+1} &= \Phi^k + \Delta t \frac{1}{n} K^{k+\frac{1}{2}} - \frac{\Delta t}{2\tau}(\Phi^k + \Phi^{k+1}), \\
\mu\xi^{k+1} &= \frac{\Phi^{k+1}}{\hat{\phi}(t_{k+1})} - \frac{1}{\beta}, \\
p_i^{k+1} &= p_i^{k+\frac{1}{2}} - \frac{\Delta t}{2}\frac{\partial V(q^{k+1})}{\partial q_i} - \frac{\Delta t}{2}\xi^{k+1} p_i^{k+\frac{1}{2}}.
\end{aligned}$$

The TRMD dynamics are not Hamiltonian or time-reversible and have no apparent conserved quantities, thus it does not make sense to talk about the preservation of these properties under discretization. Nonetheless, we expect that in simulation ξ will become small in the long term (cf. following sections), and it is useful to observe that the above discretization reduces in the limit $\xi \to 0$ to the symplectic-reversible Verlet method for the constant energy model. Our experience is that the method is highly stable. As a simple illustration of the method, we performed a simulation of a dense liquid MD model consisting of 108 atoms initialised on a simple cubic lattice moving in a Lennard-Jones potential with periodic boundary conditions. Parameters were, in reduced units (i.e., $\sigma_{LJ} = 1.0$, $\epsilon_{LJ} = 1.0$), $\frac{1}{\beta} = 1.31$ and initial density $\rho = 0.9184$. We took $\tau = 1$, $\mu = 1$, in our simulations (regarding these as arbitrary parameters that would need to be selected experimentation for realistic systems). One million timesteps of size $\Delta t = 0.01$ were taken. As we see in Figure 6.1, ξ remains small and, judging

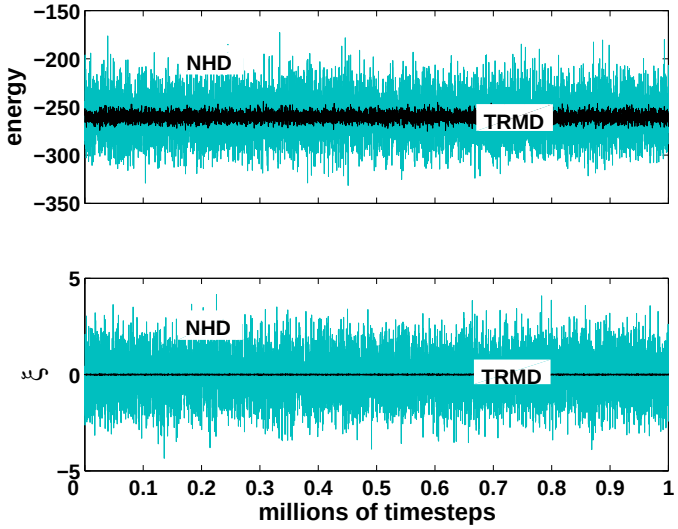

Figure 6.1: Comparison of energy conservation (upper panel) and long term stability of ξ (lower panel) for the TRMD method (dark) and Nosé-Hoover (light).

from the lack of drift in the energy, the method appears to be quite stable.

6.2 Long Time Behaviour

It is possible to perform a partial analysis of the behaviour of TRD dynamics in the long time limit. In order to study the long time behaviour we compute the divergence of the TRD vector field: $\kappa = -n\xi - 1/\tau$. From its definition, it is apparent that Φ is a positive function, and thus $\xi(t) \geqq -\frac{1}{\beta\mu}$, hence it follows that

$$\kappa \leqq \frac{n}{\beta\mu} - \frac{1}{\tau}.$$

Thus one can choose μ such that $\kappa \leqq -\kappa_c < 0$, in which case the phase space volume is contracting: for any set of initial conditions occupying a positive volume, the volume v_t occupied by the corresponding set after some time t goes to 0 as t goes to infinity. In our simulation (see Figure 6.1), we verify that ξ remains small ($|\xi(t)| \leq 0.05$) and that the trajectory stays on (or close to) a constant energy surface. In Figure 6.2 we illustrate a trajectory of the TRMD extension for a harmonic oscillator compared with a corresponding Nosé-Hoover trajectory. The Nosé-Hoover trajectory (light) apparently covers the surface of a torus in the (3-dimensional) phase space, and its projection onto the qp-plane fills an annulus. The TRMD trajectory (dark) converges to the

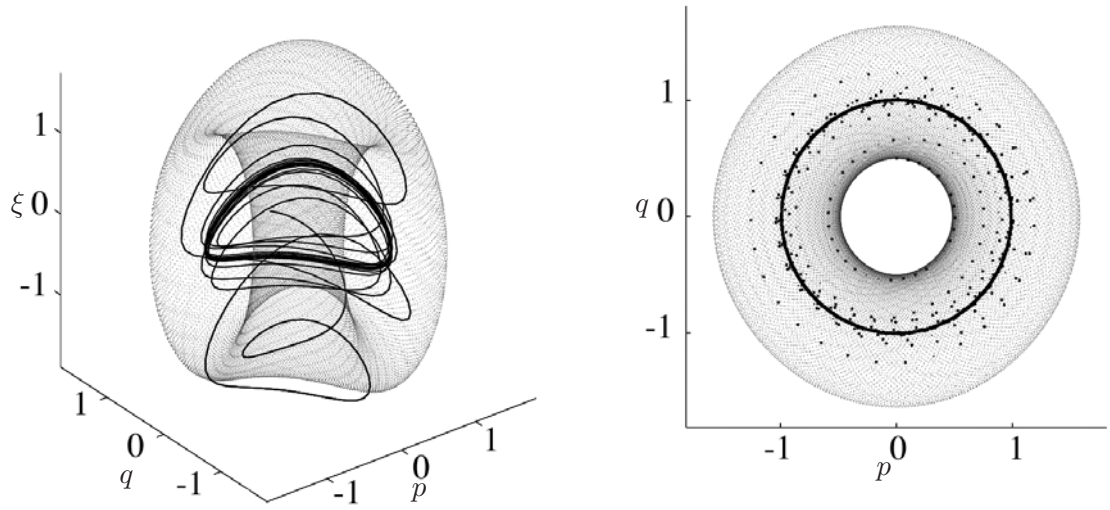

Figure 6.2: Collapse of TRMD dynamics trajectory (dark) to a lower-dimensional submanifold for a harmonic oscillator (q,p,ξ) space (left), with projection onto *qp*-plane (right). The corresponding NHD trajectory is shown in light grey.

neighbourhood of a constant energy trajectory, in this case a circle, having the desired average kinetic energy.

6.3 Equilibration of a Nonadiabatic Perturbation

As a test of TRMD for this type of thermostatting, we use again a Lennard-Jones model simulated with the following nonadiabatic perturbation: a rapid increase in the Lennard-Jones radius. In our simulation, we start with the previously described 108 atom model, with the system initially relaxed at temperature $\beta^{-1} = 1.31$; between time $t = 20$ and $t = 21$, the parameter σ is increased from $\sigma = 1.0$ to $\sigma = 1.05$ by successive rescaling at each timestep. When microcanonical dynamics is used, the result is as shown in Figure 6.3. When the perturbation is applied, there is a rapid drift in temperature, demonstrating that thermostatting is needed here to restore the system during and after the onset of the kick.

We expect the thermostatted scheme to maintain the system at the desired target temperature during the kick. As we see in the upper panel of Figure 6.4, Nosé-Hoover (here used with a target temperature of $\beta^{-1} = 1.31$ and thermostat parameter $\mu = 1$) is able to achieve this. In fact there is no evidence in the temperature profile that any disturbance was introduced. This also means that in those situations where kinetic fluctuation is the driver for a nonequilibrium process, Nosé-Hoover may unfavourably

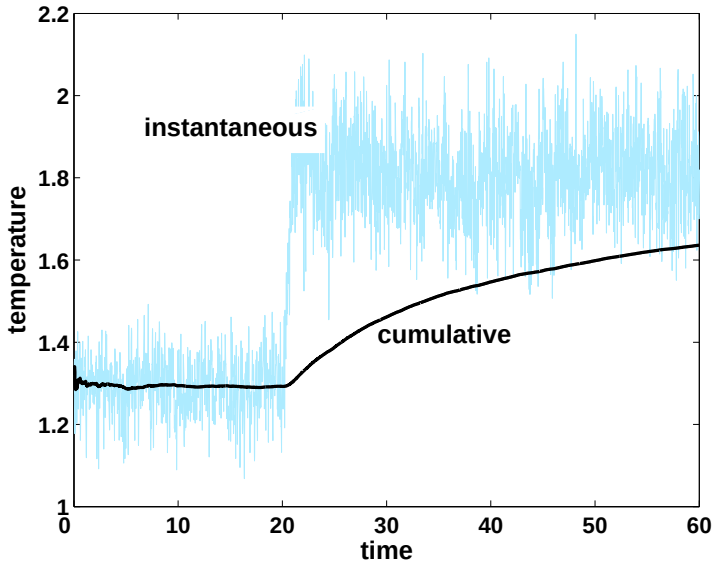

Figure 6.3: Recorded temperature through nonadiabatic perturbation for a microcanonical simulation. Cumulative temperature is shown in bold.

restrict the extent of those fluctuations.

The TRMD scheme also performs the thermalisation task, although in a different way (Figure 6.4, lower panel). At the onset of the kick, the system is allowed to exhibit a momentary initial rise in temperature. After this initial rise, the system relaxes back to thermal equilibrium at the target temperature. Figure 6.5 compares the energetic evolution with the three methods. TRMD and NHD get the correct energy following the change, while the microcanonical system, due to the lack of temperature control, gives incorrect results. We also observe on Figure 6.5 that the energy fluctuations are smaller with TRMD than with NHD. This signifies that the TRMD method keeps the energy closer to the microcanonical energy while properly controlling the temperature. Finally Figure 6.6 shows the comparative evolution of ξ for each of TRMD and NHD, demonstrating that the temperature control is always strongly active in NHD whereas TRMD represents a much smaller perturbation and only shows a slight rise to cope with the nonadiabatic change between $t = 20$ and $t = 21$. These qualitative observations were similar for many choices of the TRMD parameter ($0.001 < \tau < 10$), although the choice of τ does lead to differences in the sensitivity to change in the solution and/or the observed energetic fluctuations.

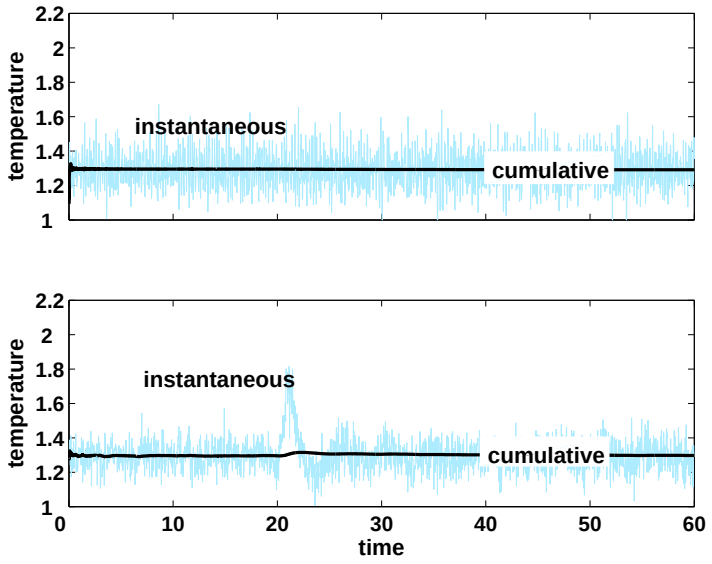

Figure 6.4: Recorded temperature through nonadiabatic perturbation for Nosé-Hoover simulation (upper panel) and TRMD (lower panel). Cumulative temperatures are shown in bold.

6.3.1 Vibrational Diffusion

We next study the vibrational diffusion observed in a model consisting of a bonded atom pair in a liquid bath. In the previously described system of atoms of unit mass interacting pairwise with a Lennard-Jones potential, we incorporate a stiff harmonic spring with rest length equal to the LJ equilibrium separation. Stiffness was chosen so that the frequency of the resulting vibration was about 5× the fastest mode of the equilibrium LJ lattice. The entire system was equilibrated at $kT = 1$ and then the velocity autocorrelation function associated to the stretch was computed using different thermostatting methods. The purpose of the model is to provide a simple illustration of the thermal exchange process between solute and solvent in models with bonded atoms.

The appearance of the autocorrelation functions in Figure 6.8 reflects the strong harmonic component in the model which exhibits a weakly damped periodic profile. When a thermostat is applied to a system like this, it introduces artificial perturbations to the dynamics of the model. We compared Langevin dynamics using the well established Brunger-Brooks-Karplus algorithm [87], TRMD, and constant energy simulation. Atoms in the solvent naturally relax rapidly, so their autocorrelation functions tend rapidly to zero. In our experiments the solvent equilibrated rapidly in all sim-

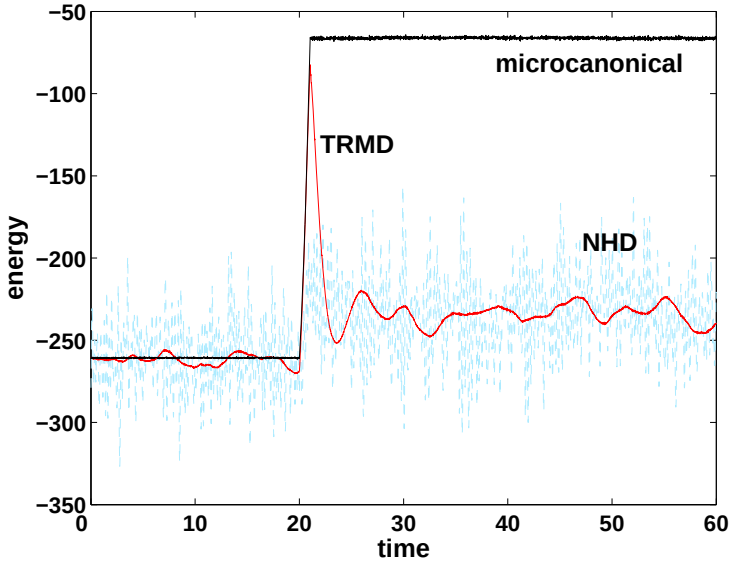

Figure 6.5: Comparison of energy fluctuation for NHD, TRMD and microcanonical simulations simulations.

ulations, see Figure 6.7. However, looking just at the bound pair, we observed very different behavior between, on the one hand, the two dynamics schemes, and, on the other hand, the Langevin method, depending on the choice of Langevin damping parameter. Obviously a damping coefficient $\gamma = 0$ would give a perfect autocorrelation function (since Langevin dynamics would reduce to Newtonian dynamics in that case). The choice of γ is model dependent and effects stability and strength of temperature control. Typical choices of the time constant γ used in practice range from 0.05 to 0.5, normalised with respect to the fastest period of the motion. Langevin dynamics is typically used in simulations involving water, with $\gamma = 5 - 50/\text{ps}$ [138], where the fast period is associated to the OH stretch, about 10fs. In our vibrational diffusion model a period of the vibrational motion is about 0.1 units of time, so the corresponding range of γ is $0.5 - 5.0$. In Figure 6.8, we show the autocorrelation function for the vibrational degree of freedom, using constant energy (the target), TRMD ($\mu = \tau = 1$), and Langevin dynamics with $\gamma = 1$. As we can see both thermostats introduce a defect, but it is more severe in the case of Langevin. The situation is improved for smaller γ. We also tried several values of τ in TRMD and found similar results in each case. The table below shows the root mean square of error in calculation of velocity autocorrelation function for vibrational degrees of freedom.

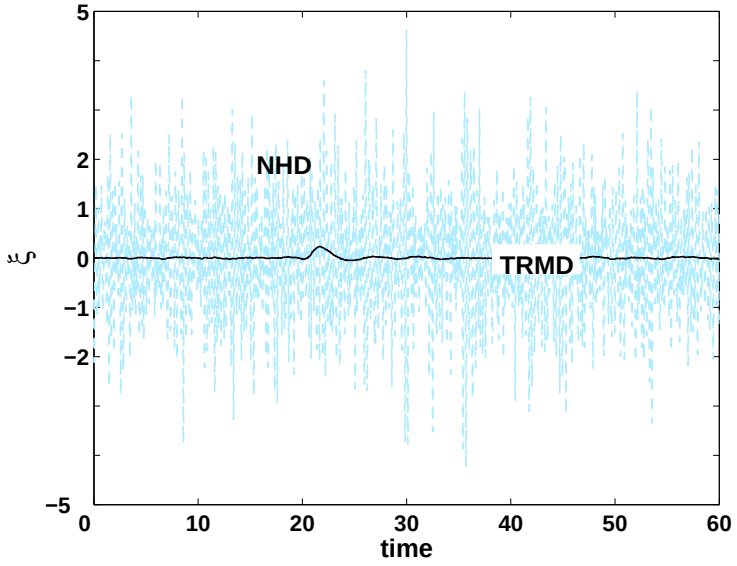

Figure 6.6: Variation of ξ using NHD (light) and TRMD (bold).

TRMD, $\tau = 0.5$	$\tau = 1.0$	$\tau = 5.0$	Langevin, $\gamma = 0.5$	$\gamma = 1.0$	$\gamma = 2.0$	Nose-Hoover
0.0079	0.0072	0.0082	0.0169	0.0227	0.0319	0.0105

6.4 Discussion and Conclusion

The new dynamics should be of interest for general MD simulation software, i.e., as a scheme for generating temperature-regulated trajectories for various situations which involve delicate thermalisation, such as for dislocation studies [134], in determination of nucleation rates [135], for glassy systems (where momenta relax rapidly but configurations much more slowly), and for evaluation of nonequilibrium statistical mechanics [139].

The extension of a history-based technique like that described here in combination with different types of alternative thermostats such as configurational thermostats [140] and DPD-style thermostats [141] is being explored.

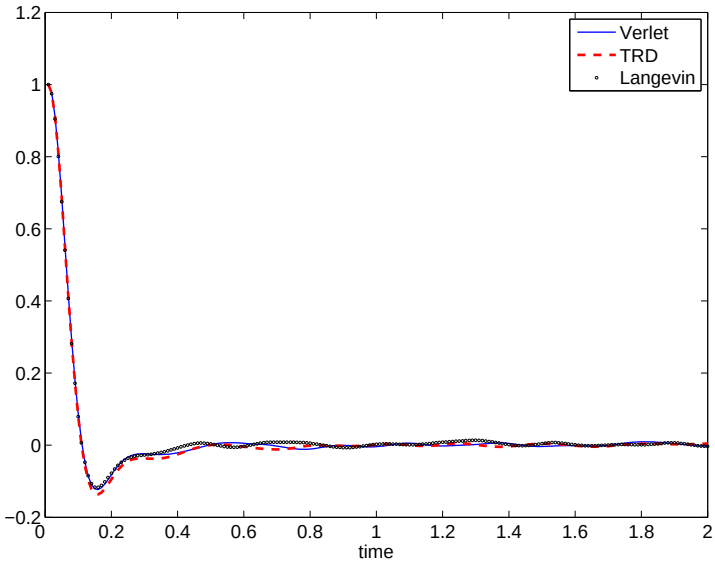

Figure 6.7: Velocity autocorrelation function for solvent degrees of freedom only, computed using TRMD and Langevin dynamics and compared to the Verlet (NVE) simulation.

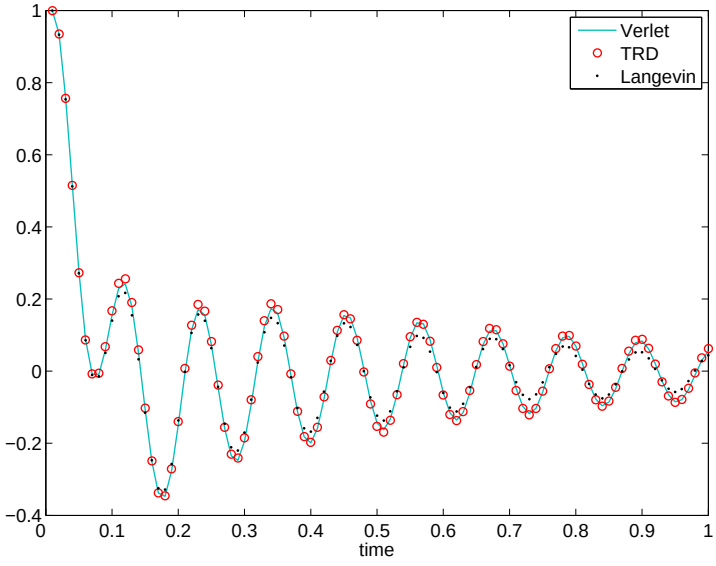

Figure 6.8: Velocity autocorrelation function for vibrational degrees of freedom only, computed using TRMD and Langevin and compared to the Verlet (NVE) simulation.

Chapter 7

Free Energy Calculations

So far we have learned how to sample from the Boltzmann-Gibbs measure, and studied different methods and their properties for computations of averages and autocorrelation functions. We mentioned that the convergence rate is dependent on the temperature, the potential function and its associated *metastabilities*. In this chapter we study the techniques that enable sampling of infrequent events by overcoming the metastabilities of the potential function.

In complex systems arising in physics, chemistry, biology, etc., there are regions of phase space where trajectories spend most of their time. We call these regions *meta-stable* sets. They are associated with the minima of the potential of the system. For example, different configurations of a protein correspond to different meta-stable sets. The meta-stable sets are separated by high barriers, hence the transition between them is very rare. In such systems, we need to be able to identify the meta-stable sets, calculate the transition rates, and also understand the transition mechanism, that is, the most likely path for the transition (see Figure 7.1).

To clarify this, let $x = (q, p)$ be the process solving the Langevin equation

$$\mathrm{d}x = \mathbb{J}\nabla H(x)\,\mathrm{d}t - \Gamma x\,\mathrm{d}t + \Sigma\,\mathrm{d}W, \tag{7.1}$$

where

$$\Gamma = \begin{pmatrix} 0_n & 0_n \\ 0_n & I_n \end{pmatrix}, \quad \Sigma\Sigma^T = \begin{pmatrix} 0_n & 0_n \\ 0_n & \frac{2}{\beta}M \end{pmatrix}.$$

Next, consider the Hamiltonian with a potential function $V : \mathcal{M} \subseteq \mathbb{R}^n \to \mathbb{R}$ that has two local minima at $q = a$, $q = b$, and a local maximum between them at $q = d$. Now consider the problem of the escape of the particles from the left local minimum a. The

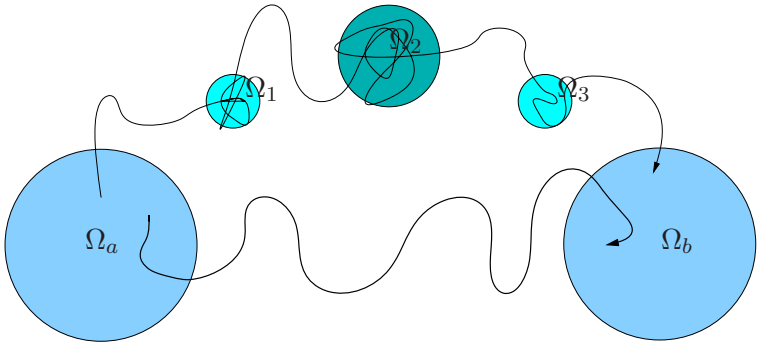

Figure 7.1: Schematic representation of the possible meta-stable sets of a bio-molecular system. The dominant sets are Ω_a and Ω_b with the highest barrier ΔE_{ab} between them; the intermediate sets are Ω_1, Ω_2 and Ω_3. As it is shown in the picture there is a short path that goes directly from Ω_a to Ω_b and a longer path which visits other sets before reaching Ω_b. Indeed, the preferred path is dependent on temperature and the method we use for sampling. Thus finding the intermediate sets is a delicate task. We conjecture that the sampling methods that are small perturbations of the dynamics are more likely to find the intermediate sets.

height of the barrier that particles have to overcome is

$$\Delta E = V(d) - V(a).$$

If the temperature is low

$$\frac{1}{\beta} \ll \Delta E, \tag{7.2}$$

then particles are most likely to be found either in Ω_a (the neighbourhood of a) or in Ω_b (the neighbourhood of b). This is an example of a rare event. Starting from $x \in \Omega_a \times \mathbb{R}^n$ we define the first exit time of $x(t)$ from $\Omega_a \times \mathbb{R}^n$, $\tau_a(x)$, as

$$\tau_a(x) = \inf\left\{t > 0; x(t) \notin \Omega_a \times \mathbb{R}^n\right\}.$$

The average of the random variable $\tau_a(x)$ with respect to the density of x is called *mean first passage time* or *exit time*:

$$\tau := \mathbf{E}\tau_a(x).$$

It can be shown that τ solves an appropriate boundary value problem:

$$\begin{cases} -\mathcal{L}\tau = 1, \quad x \in \Omega_a \times \mathbb{R}^n, \\ \tau = 0, \quad x \in \partial\Omega_a \times \mathbb{R}^n, \end{cases} \tag{7.3}$$

where $\mathcal{L}$ is the generator of the Langevin equation (7.1) (see [83, 142, 21] for details and derivation). The solution τ is of the form

$$\tau = \frac{1}{\nu} e^{\beta \Delta E},$$

where ν is the unknown *rate coefficient*. The rate at which particles escape Ω_a (*reaction rate*) is of order $\frac{1}{\tau}$:

$$\kappa = \nu e^{-\beta \Delta E}. \tag{7.4}$$

Equation (7.4) is known as Arrhenius formula, it describes the rate of chemical reaction and has been observed experimentally. Except for some special cases, like the one dimensional double well, it is not possible to solve the Dirichlet problem (7.3) exactly nor numerically using discretization, such as finite difference or finite element methods, due to the high dimensionality of $\Omega_a \times \mathbb{R}^n$. Thus the first step is to reduce the dimension of the problem.

Finding the meta-stable sets is like looking for a needle in a haystack: it is hopeless unless we find a systematic way to sort through all the hay. One way to deal with the high dimensionality of the problem is to find a minimal set of functions of positions $\xi = (\xi_1, \cdots, \xi_m)$, where $m \ll n$, termed *collective variables* or *reaction coordinates*, that can capture all the metastabilities. The collective variables must also be rich enough to describe the transition mechanism adequately. The challenge is to find a projected dynamics onto the collective variables, more precisely to find an effective potential of ξ. The effective potential is called the *free energy* and is a function of ξ.

Definition 11. *A reaction coordinate (commitor function) is a smooth map $\xi : \mathcal{M} \subseteq \mathbb{R}^n \to \mathbb{R}^m$, of constant rank m (i.e. $\operatorname{rank}(\nabla_q \xi) = m$, $\forall q \in \mathbb{R}^n$). Then for every point $z \in \mathbb{R}^m$,*

$$\Sigma_z := \xi^{-1}(z) = \{q \in \mathcal{M} \,|\, \xi(q) = z\}$$

is a $(n-m)$-dimensional smooth submanifold of $\mathcal{M}$. Furthermore we have

$$\mathcal{M} = \bigcup_{z \in \mathbb{R}^m} \Sigma_z, \text{ for disjoint } \Sigma_z.$$

Note that in practice ξ is not an arbitrary map, since it is chosen to control different macroscopic states of the physical system, for instance different conformations of a protein. In the simplest case ξ is just a parameter. Then, if H_a and H_b are energies for macroscopic states Ω_a and Ω_b, using

$$H(q,p;\xi) = \frac{p^T M^{-1} p}{2} + V(q,\xi), \quad \xi \in [0,1],$$

where $H(q,p;0) = H_a$ and $H(q,p;1) = H_b$, enables us to shift the system from one state to another.

Now we are ready to define the free energy along ξ.

Definition 12. *The free energy as a function of the reaction coordinates is given by*

$$A(\xi) = -\beta^{-1} \log Z(\xi), \tag{7.5}$$

where $Z(\xi)$ is given by

$$Z(\xi) = \int_{\mathcal{M} \times \mathbb{R}^n} e^{-\beta H(q,p)} \delta(\xi(q) - \xi) \, \mathrm{d}q \, \mathrm{d}p, \tag{7.6}$$

where $\xi(q)$ is the reaction coordinates and $\xi \in \mathbb{R}^m$ is the value of $\xi(q)$.

Note that it is possible to write $Z(\xi)$ as an integral over Σ_ξ:

$$Z(\xi) = \int_{\Sigma_\xi \times \mathbb{R}^n} e^{-\beta H(q,p)} \frac{\mathrm{d}\Sigma_\xi \, \mathrm{d}p}{\sqrt{\det(\nabla_q \xi(q))^T (\nabla_q \xi(q))}}.$$

The calculation of the free energy surface (free energy landscape) of a complex system such as a protein cannot be achieved by using conventional dynamical methods, due to the long time scale which is apparent in the dynamics. Given $\xi_1, \xi_2 \in \mathbb{R}^m$, the equation (7.5) concludes that for $\Delta A = A(\xi_2) - A(\xi_1) > \frac{1}{\beta}$, the probability $Z(\xi_2)$ is reduced considerably. This agrees with (7.2) and the results in [143], which says that the reaction events are rare if the free energy barrier separating reactants from products is higher that the average thermal energy. In other words, the conformations with large free energy have low probabilities and therefore are sampled poorly in the simulation.

The problems that we want to solve are:

- Calculation of the free energy surface;
- Identifying the meta-stable sets: that is enhancing the sampling so that the different basin of the energy surface can be visited in a computationally accessible time scale;
- Given two meta-stable sets what is the transition rate at which a trajectory switches from one state to another?
- Understanding the mechanism of transition: what is the most likely path for the transition?

In this chapter we are mainly concerned with the first two of the above.

7.1 Review of Some Methods

Many algorithms have been developed to overcome the sampling issue. They can be categorised as follows:

Thermodynamic Integration

This was first proposed by Kirkwood in [144]. Intuitively we could argue that if the dynamics were constrained on the submanifold Σ_ξ, then the sampling issue could be overcome, since the delta function in (7.6) is always one on Σ_ξ. One method that implements this idea by using reaction coordinates as constraints is the blue-moon ensemble method, [145, 146, 147, 148]. This method achieves a very good sampling even in transition states. We will study this method and constrained simulation in detail in Section 7.1.2.

Umbrella Sampling and Biasing The Potential

In the umbrella sampling [149, 150] we split the computational interval along the reaction coordinates ξ into subintervals. Hence the free energy barrier is reduced within each interval and a better sampling is achieved. In addition, in each interval a biasing potential can be used to further improve the sampling. In general the biasing potential

needs to be guessed beforehand or can be gradually improved using an iterative refinement process. Figure 7.2 illustrates the idea of sampling intervals and biasing potential for free energy along one reaction coordinate.

One drawback of a biasing potential is that it is usually difficult in complex systems to make a good initial guess for it. Moreover, there might be intermediate states from Ω_1 to Ω_2, and a biasing potential can lead to an incorrect calculation of the free energy.

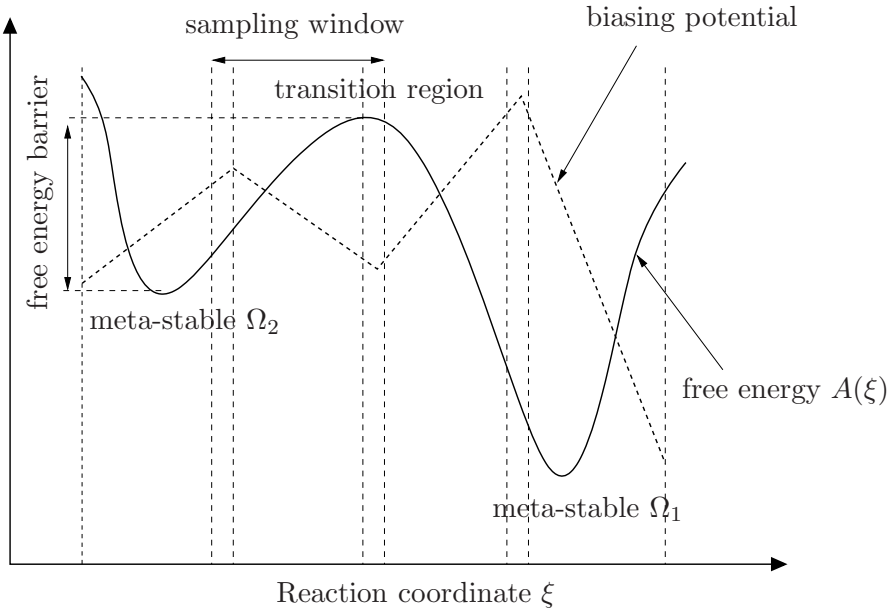

Figure 7.2: The free energy profile as a function of ξ. The umbrella sampling method bins the computational interval of interst in ξ and uses a biasing potential to overcome the barrier.

Accelerated Dynamics

The Idea is to accelerate the dynamics by some means (usually higher temperature for the ξ direction or biasing the potential) so that the trajectories could sample regions with low probabilities in a computationally accessible time scale. Such methods are the Hyper dynamics method [151] and the temperature accelerated methods introduced by Sorensen and Voter in [152] and by Maragliano and Vanden-Eijnden in [153]

Another approach is the adiabatic free energy dynamics (AFED) method [154, 155]. AFED works by associating a large mass and a high temperature to the reaction coordinate. It was shown that in the adiabatic limit (i.e. $t\frac{\mathrm{d}\xi}{\mathrm{d}t} \ll \xi$, t is the time period of the computation) the free energy can be recovered from the probability density function. The large mass ensures that the reaction coordinate moves slowly and the

high temperature ensures a good uniform sampling for the interval of interest in ξ. However, AFED requires an explicit definition of the generalised coordinates as well as careful analysis to determine the appropriate mass and the temperature to be used for the reaction coordinate. There is also a computational limit on the adiabatic condition, since a too large mass will slow the process and can severely reduce the computational efficiency of the method.

Nonequilibrium Dynamics

The representatives of this category are methods proposed by Jarzynski [156, 157, 158] and Crooks [159, 160, 161, 162]. In these methods the switching steps between Ω_1 and Ω_2 do not need to be infinitely slow and can be finite. The Jarzynski method is based on a new equality that links the work W done on the system during the switching process to the free energy difference on the system:

$$\langle e^{-\beta W} \rangle = e^{-\beta \Delta A}. \tag{7.7}$$

This result is independent of the path from Ω_1 to Ω_2 and the rate at which the system moves along the path. It signifies that ΔA is proportional to the average of the exponential work done on the system during each switching. Since the switching is finite, the Jarzynski method is referred to as a nonequilibrium free energy method. However if $\frac{\mathrm{d}\xi}{\mathrm{d}t}$ is large, significant nonequilibrium effects are going to be present, which in general lead to a heating of the system and an increase in its energy. It has been observed in [163] and several others that even though the equality (7.7) is correct, a fast switching process leads to large statistical errors that require very long simulation time to diminish.

Adaptive Dynamics

The idea of adaptive dynamics is to include a biasing term in the dynamics that forces the system to leave regions where enough samples are collected. Examples are the adaptive biasing force (ABF) method of Darve and Pohorille [164, 165], and the metadynamics method of Laio and Parrinello [166]. We describe the ABF method in more detail in Section 7.1.4.

7.1.1 A Direct Calculation: Free Energy Perturbation

In situations where there is a small change in the energy of the system which can be neglected to a first order approximation, one can directly calculate free energy using perturbation theory.

Let us write the energy as

$$H(q,p) = H_0(q,p) + \nu(q,p), \tag{7.8}$$

where ν is a small term. To calculate the free energy we substitute (7.8) in the definition of free energy (A.7) (see the appendix):

$$A = -\frac{1}{\beta}\log\left(\int \exp\left(-\beta H_0(q,p) - \beta\nu(q,p)\right)\,\mathrm{d}q\,\mathrm{d}p\right).$$

After expansion in powers of ν and omitting terms above second order, we obtain

$$\begin{aligned}
A =& -\frac{1}{\beta}\log\left(\int \exp(-\beta H_0)\left(1-\beta\nu+\frac{\beta^2\nu^2}{2}\right)\,\mathrm{d}q\,\mathrm{d}p\right)\\
=& -\frac{1}{\beta}\log\left(\int \exp(-\beta H_0)\,\mathrm{d}q\,\mathrm{d}p\left(1+\frac{\int(-\beta\nu+\frac{\beta^2\nu^2}{2})\exp(-\beta H_0)\,\mathrm{d}q\,\mathrm{d}p}{\int\exp(-\beta H_0)\,\mathrm{d}q\,\mathrm{d}p}\right)\right)\\
=& -\frac{1}{\beta}\log\left(\int \exp(-\beta H_0)\,\mathrm{d}q\,\mathrm{d}p\right) - \frac{1}{\beta}\log\left(1+\frac{\int(-\beta\nu+\frac{\beta^2\nu^2}{2})\exp(-\beta H_0)\,\mathrm{d}q\,\mathrm{d}p}{\int\exp(-\beta H_0)\,\mathrm{d}q\,\mathrm{d}p}\right).
\end{aligned}$$

Expansion of the second logarithm in series and again omitting terms higher than second order of ν, yields

$$\begin{aligned}
A =& A_0 + \left(\frac{\int(\nu-\frac{\beta\nu^2}{2})\exp(-\beta H_0)\,\mathrm{d}q\,\mathrm{d}p}{\int\exp(-\beta H_0)\,\mathrm{d}q\,\mathrm{d}p}\right) + \frac{\beta}{2}\left(\frac{\int\nu\exp(-\beta H_0)\,\mathrm{d}q\,\mathrm{d}p}{\int\exp(-\beta H_0)\,\mathrm{d}q\,\mathrm{d}p}\right)^2\\
=& A_0 + \langle\nu\rangle - \frac{\beta}{2}\langle\nu^2\rangle + \frac{\beta}{2}\langle\nu\rangle^2,
\end{aligned}$$

where $\langle\cdot\rangle$ represents averaging with respect to Boltzmann-Gibbs distribution. Since

$$\left\langle(\nu-\langle\nu\rangle)^2\right\rangle = \langle\nu^2\rangle - \langle\nu\rangle^2,$$

we have

$$A = A_0 + \langle\nu\rangle - \frac{\beta}{2}\left\langle(\nu-\langle\nu\rangle)^2\right\rangle. \tag{7.9}$$

Thus the first order correction to the free energy is just the mean value of the energy

perturbation ν. The second order correction is always negative and is the fluctuation of ν. If $\langle\nu\rangle$ is zero then the perturbation reduces the free energy. Both $\langle\nu\rangle$ and $\left\langle(\nu - \langle\nu\rangle)^2\right\rangle$ are roughly proportional to the number of particles of the system. Hence we can conclude that perturbation method is applicable if the perturbation energy per particle is small in comparison with $\frac{1}{\beta}$, so this method would not work well in situations where there is a high free energy barrier.

7.1.2 Thermodynamic Integration and Constrained Dynamics

The free energy difference between two thermodynamics states Ω_1 and Ω_2 is the reversible work required to move the system between these two states along a reaction coordinate ξ (it is independent of the choice of ξ). The free energy difference is written as

$$\Delta A(\xi) := A(\xi_2) - A(\xi_1) = -\frac{1}{\beta}\log\left(\frac{Z(\xi_2)}{Z(\xi_1)}\right).$$

The above formula cannot be computed in the molecular dynamics simulation, since it is not a time average of some function of phase space variables. Hence, special techniques are needed to determine free energy. A nice review of numerical methods and their applicability is given in [167, 8, 168, 169]. One approach to calculate free energy in molecular dynamics is the thermodynamic integration method.

Thermodynamic integration method utilises the fact that the derivative of the free energy is the mean force which is needed to move the system from Ω_1 to Ω_2 along the reaction coordinate. Thus, integration of the mean force gives the desired free energy difference:

$$A(\xi_2) - A(\xi_1) = \int_{\xi_1}^{\xi_2} \nabla_\xi A(\xi)\,\mathrm{d}\xi = \int_{\xi_1}^{\xi_2} \langle f_\xi\rangle_\xi\,\mathrm{d}\xi. \tag{7.10}$$

The aim is to calculate the mean force $\langle f_\xi\rangle_\xi$, where the subscript means that the average is taken with respect to a fixed value of ξ, hence, $\langle f_\xi\rangle_\xi$ is a function of ξ. Taking the derivative of (7.5) with respect to ξ, we obtain

$$\nabla_\xi A(\xi) = -\beta^{-1}\frac{\nabla_\xi Z(\xi)}{Z}. \tag{7.11}$$

Now consider a coordinate transformation:

$$u = (\xi, \hat{q}_1, ..., \hat{q}_{n-m}), \text{ such that } u = u(q) \text{ and } q = q(u).$$

Let

$$v = (p_\xi, \hat{p}_1, \ldots, \hat{p}_{n-m})$$

be the conjugate momenta of u. The Hamiltonian of the system in (u, v) coordinates is

$$\hat{H}(u, v) = \frac{1}{2} v^T \mathbf{\Lambda}^{-1} v + V(u), \tag{7.12}$$

where $\mathbf{\Lambda} = J^T M J$ is the mass-metric matrix which is obtained by transforming the kinetic energy of the old coordinates to the kinetic energy of the new coordinates. J is the Jacobian of the transformation, defined as $J_{ij} = \frac{\partial q_i}{\partial u_j}$. The matrix $\mathbf{\Lambda}$ is given by

$$\mathbf{\Lambda}_{cd} = \sum_{i=1}^{n} m_i \frac{\partial q_i}{\partial u_c} \frac{\partial q_i}{\partial u_d}, \quad 1 \leqq c, d \leqq n.$$

In general, for m reaction coordinates $\xi = (\xi_1, ..., \xi_m)$, we can write $\mathbf{\Lambda}$ in a block form

$$\mathbf{\Lambda} = \begin{pmatrix} \Lambda_\xi & \Lambda_{\xi q} \\ \Lambda_{q\xi} & \Lambda_q \end{pmatrix},$$

where Λ_ξ is an $(m \times m)$ matrix, $\Lambda_{\xi q}$ is an $(m \times n-m)$ matrix and Λ_q is an $(n-m \times n-m)$ matrix. Moreover, $\Lambda_{q\xi} = \Lambda_{\xi q}^T$, $\mathbf{\Lambda} = \mathbf{\Lambda}^T$ and $\mathbf{\Lambda}^{-1} = \left(\mathbf{\Lambda}^T\right)^{-1} = \left(\mathbf{\Lambda}^{-1}\right)^T$. The $\mathbf{\Lambda}^{-1}$ is given by

$$\mathbf{\Lambda}^{-1}_{cd} = \sum_{i=1}^{n} \frac{1}{m_i} \frac{\partial u_c}{\partial q_i} \frac{\partial u_d}{\partial q_i}$$

and can also be written in a block form

$$\mathbf{\Lambda}^{-1} = \begin{pmatrix} Z_\xi & Z_{\xi q} \\ Z_{q\xi} & Z_q \end{pmatrix}.$$

Expansion of the identity $\mathbf{\Lambda}^{-1}\mathbf{\Lambda} = I_n$ yields useful relations between the submatrices in $\mathbf{\Lambda}^{-1}$ and $\mathbf{\Lambda}$. An instance of these relations is $|\Lambda_q| = |\mathbf{\Lambda}||Z_\xi|$.

Using the new Hamiltonian (7.12), we can write $Z(\xi)$ as

$$Z(\xi) = \int e^{-\beta \hat{H}(u,v)} \, \mathrm{d}\hat{q}_1 \cdots \mathrm{d}\hat{q}_{n-m} \, \mathrm{d}v. \tag{7.13}$$

Substituting (7.13) in (7.11) we obtain the following expression

$$\nabla_\xi A(\xi) = \frac{\int \nabla_\xi \hat{H} e^{-\beta \hat{H}} \, \mathrm{d}\hat{q}_1 \cdots \mathrm{d}\hat{q}_{n-m} \, \mathrm{d}v}{\int e^{-\beta \hat{H}} \, \mathrm{d}\hat{q}_1 \cdots \mathrm{d}\hat{q}_{n-m} \, \mathrm{d}v} = \left\langle \nabla_\xi \hat{H} \right\rangle_\xi . \tag{7.14}$$

The subscript represents an average over the equilibrium ensemble which corresponds to a fixed value of ξ. Now that we have defined the mean force $\langle f_\xi \rangle_\xi := \left\langle \nabla_\xi \hat{H} \right\rangle_\xi$ we can rewrite (7.10) as

$$A(\xi_2) - A(\xi_1) = \int_{\xi_1}^{\xi_2} \nabla_\xi A(\xi) \, \mathrm{d}\xi = \int_{\xi_1}^{\xi_2} \left\langle \nabla_\xi \hat{H} \right\rangle_\xi \mathrm{d}\xi. \tag{7.15}$$

The expression for the mean force in (7.15) depends on both positions and momenta. Next we derive an expression which is independent of the momenta. Integration over momenta in (7.6) yields

$$Z(\xi) = Z_M \int_{\mathcal{M}} e^{-\beta H(q,p)} \delta(\xi(q) - \xi) \, \mathrm{d}q,$$

where

$$Z_M = \int_{\mathbb{R}^n} e^{-\beta \frac{p^T M^{-1} p}{2}} \, \mathrm{d}p.$$

Using the change of variable $q \to u$, we get

$$Z(\xi) = Z_M \int_{\mathcal{M}} e^{-\beta V} |J| \, \mathrm{d}\hat{q}_1 \cdots \mathrm{d}\hat{q}_{n-m}.$$

Thus we have

$$\nabla_\xi A(\xi) = \frac{\int_{\mathcal{M}} \left(\nabla_\xi V |J| - \beta^{-1} \nabla_\xi |J| \right) e^{-\beta V} \, \mathrm{d}\hat{q}_1 \cdots \mathrm{d}\hat{q}_{n-m}}{\int_{\mathcal{M}} e^{-\beta V} |J| \, \mathrm{d}\hat{q}_1 \cdots \mathrm{d}\hat{q}_{n-m}}.$$

Now changing the variables back to q, we get

$$\begin{aligned} \nabla_\xi A(\xi) =& \frac{\int \left(\nabla_\xi V - \beta^{-1} \frac{\nabla_\xi |J|}{|J|} \right) e^{-\beta V} \delta(\xi(q) - \xi) \, \mathrm{d}q}{\int e^{-\beta V} \delta(\xi(q) - \xi) \, \mathrm{d}q} \\ =& \frac{\int \left(\nabla_\xi V - \beta^{-1} \nabla_\xi \log |J| \right) e^{-\beta V} \delta(\xi(q) - \xi) \, \mathrm{d}q}{\int e^{-\beta V} \delta(\xi(q) - \xi) \, \mathrm{d}q} \\ =& \left\langle \nabla_\xi V - \beta^{-1} \nabla_\xi \log |J| \right\rangle_\xi . \end{aligned} \tag{7.16}$$

This is the fundamental result of [145, 164, 170, 171, 172, 146]: it shows that the derivative of the free energy consists of two terms, a mean mechanical force acting

along ξ and the mean changes of the volume element of phase space. The average is with respect to the equilibrium measure that corresponds to fixed ξ.

The derivative with respect to ξ requires the definition of generalised coordinate which is not convenient for the numerical computation, especially when the system has many degrees of freedom. An alternative that does not require the calculation of $|J|$ is

$$\nabla_\xi A = \left\langle \nabla_q V . \frac{\omega}{\omega . \nabla_q \xi} + \beta^{-1} \nabla_q . \frac{\omega}{\omega . \nabla_q \xi} \right\rangle_\xi , \tag{7.17}$$

where ω is an arbitrary vector field such that $\omega . \nabla \xi \neq 0$. Equation (7.17) was derived by Darve [164], Otter [172] and also in [147]. One choice for ω is $\omega = \nabla_q \xi$, which gives

$$\nabla_\xi A = \left\langle \frac{1}{\|\nabla_q \xi\|^2} \left(\nabla_q V \cdot \nabla_q \xi - \frac{1}{\beta} \left(\Delta_q \xi - 2 \frac{(\nabla_q \xi)^T (\nabla_q \nabla_q \xi) \nabla_q \xi}{\|\nabla_q \xi\|^2} \right) \right) \right\rangle_\xi . \tag{7.18}$$

Constrained Dynamics

So far we have found expressions to compute the free energy, but we still need to sample the equilibrium measure that corresponds to the fixed value of ξ. One way to do this is to use constrained dynamics, an example is the blue-moon ensemble method [145, 146, 147]. The idea behind the blue-moon ensemble method is to control the microscopic state of the system by using the reaction coordinates as holonomic constraints. Let us assume for simplicity that there is one reaction coordinate, but our result is also true for multiple reaction coordinates. In a constrained simulation, at each step a force λ in the direction of the normal to the constraint surface is applied, which ensures that ξ remains constant throughout the simulation. Since $\frac{\partial A}{\partial \xi}$ is seen as a mean force acting on ξ, we expect that in the constrained simulation $\frac{\partial A}{\partial \xi} \approx \langle \lambda \rangle$. However, in a constrained simulation the distribution of momenta is not independent of positions, hence we need to find the correction term that relates the averages in constrained simulation to the averages with respect to a fixed value of ξ.

Consider the unconstrained Hamiltonian in (u, v) coordinates:

$$\begin{aligned} \hat{H}(u,v) =& \frac{1}{2} v^T \mathbf{\Lambda}^{-1} v + V(u) \\ =& \frac{1}{2} \left(p_\xi^T Z_\xi p_\xi + 2 p_\xi Z_{\xi q} \hat{p} + \hat{p}^T Z_q \hat{p} \right) + V(\xi, \hat{q}). \end{aligned} \tag{7.19}$$

Using (7.19) the free energy is

$$A(\xi) = -\frac{1}{\beta} \log \left(\int e^{-\beta \hat{H}} \, \mathrm{d}\hat{q} \, \mathrm{d}p_\xi \, \mathrm{d}\hat{p} \right).$$

The integration with respect to p_ξ can be done exactly

$$\int \exp\left(-\frac{\beta}{2} \left(p_\xi^T Z_\xi p_\xi + 2 p_\xi Z_{\xi q} \hat{p} \right) \right) \mathrm{d}p_\xi = \sqrt{\frac{\pi}{2\beta}} (Z_\xi)^{-1/2} \exp\left(\frac{1}{2} \hat{p}^T Z_{q\xi} Z_\xi^{-1} Z_{\xi q} \hat{p} \right). \tag{7.20}$$

Now we may write

$$A(\xi) = -\frac{1}{\beta} \log \int e^{-\beta H_\xi^F(\hat{q},\hat{p})} \, \mathrm{d}\hat{q} \, \mathrm{d}\hat{p} - \frac{1}{\beta} \log \sqrt{\frac{\pi}{2\beta}}, \tag{7.21}$$

where

$$H_\xi^F(\hat{q},\hat{p}) = H_\xi(\hat{q},\hat{p}) + \frac{1}{2\beta} \log Z_\xi(\hat{q}).$$

The first term is the constrained Hamiltonian (obtained from (7.19) by fixing ξ and using the fact that $\mathrm{d}\xi/\mathrm{d}t = 0$):

$$H_\xi = \frac{1}{2} \hat{p}^T Z_q \hat{p} + V(\hat{q}),$$

and the second term is called the Fixman potential. From (7.20) we see that the contribution of p_ξ to the averages is proportional to $Z_\xi^{-1/2}$, thus, calculations of averages in the constrained simulation need to be weighted by the factor $Z_\xi^{-1/2}$. The weighted averages can be written in term of the modified Hamiltonian H_ξ^F:

$$Z_\xi^{-1/2} e^{-\beta H_\xi} = e^{-\beta \left(H_\xi + \frac{1}{2\beta} \log Z_\xi \right)}.$$

Thus for an arbitrary function of position $O(q)$ we have

$$\langle O \rangle_\xi = \langle O \rangle_{\xi\dot{\xi}}^F,$$

where $\langle \cdot \rangle_\xi$ means average with respect to the equilibrium measure which corresponds to fixed value of ξ, and $\langle \cdot \rangle_{\xi\dot{\xi}}^F$ means average with respect to the equilibrium measure of the constrained dynamics (i.e. ξ is fixed and $\dot{\xi} = 0$) such that its density is proportional to $e^{-\beta H_\xi^F}$.

Now using (7.21) we have

$$\frac{\partial A}{\partial \xi} = \left\langle \frac{\partial H_\xi^F}{\partial \xi} \right\rangle_{\xi,\dot{\xi}}^F.$$

The derivative $\frac{\partial H_\xi^F}{\partial \xi}$ can be interpreted as a force acting on ξ: infact for constrained dynamics of the form

$$H^F(q,p) = H(q,p) + \frac{1}{2\beta}\log Z_\xi + \lambda^F(\xi - \xi(q)), \tag{7.22}$$

it was shown in [167] that

$$\frac{\partial A}{\partial \xi} = \left\langle \lambda^F \right\rangle_{\xi,\dot{\xi}}^F,$$

where λ^F is a Lagrange multiplier. If we don't add the Fixman potential in (7.22) and use the constrained Hamiltonian

$$\tilde{H}(q,p) = H(q,p) + \lambda(\xi - \xi(q)), \tag{7.23}$$

then we need to add the contribution of the Fixman potential to the mean force and reweight the average by $Z_\xi^{-1/2}$:

$$\frac{\partial A}{\partial \xi} = \frac{\left\langle Z_\xi^{-1/2}\left(\lambda + \frac{1}{2\beta Z_\xi}\sum_i \frac{1}{m_i}\frac{\partial \xi}{\partial q_i}\frac{\partial \log Z_\xi}{\partial q_i}\right)\right\rangle_{\xi,\dot{\xi}}}{\left\langle Z_\xi^{-1/2}\right\rangle_{\xi,\dot{\xi}}}.$$

7.1.3 The Temperature Accelerated Method

Another way of enhancing sampling and crossing the free energy barrier is to use hotter temperature for collective variables. The idea of the temperature accelerated method [153] is to augment the original system by m new variables, then constrain them to the collective variables using harmonic springs. Finally we contact the extended variables to a different heat bath at higher temperature. The following is a new formulation of the temperature accelerated method [153].

The extended Hamiltonian is given by

$$\tilde{H}(q,p,z,p_z) = \frac{p^T M^{-1} p}{2} + \frac{p_z^T p_z}{2\mu} + V(q) + \frac{1}{2}k\left\|\xi(q) - z\right\|^2,$$

where p_z are the conjugate momenta of z. Let $\xi = (\xi_1(q), \cdots, \xi_m(q))$ be the reac-

tion coordinates or collective variables, and define the orthogonal projection onto the tangent space $T_q\Sigma_{\xi(q)}$ to $\Sigma_{\xi(q)}$ by

$$R(q) := \left(I_n - \left(\frac{\nabla_q\xi_1 \otimes \nabla_q\xi_1}{\|\nabla_q\xi_1\|^2}\right)\cdots\left(\frac{\nabla_q\xi_m \otimes \nabla_q\xi_m}{\|\nabla_q\xi_m\|^2}\right)\right) q,$$

and the orthogonal projection onto the normal space $N_q\Sigma_{\xi(q)}$ to $\Sigma_{\xi(q)}$ by

$$\hat{R}(q) := \left(\left(\frac{\nabla_q\xi_1 \otimes \nabla_q\xi_1}{\|\nabla_q\xi_1\|^2}\right)\cdots\left(\frac{\nabla_q\xi_m \otimes \nabla_q\xi_m}{\|\nabla_q\xi_m\|^2}\right)\right) q,$$

where for $x, y \in \mathbb{R}^n$ their tensor product $x \otimes y$ is a $n \times n$ matrix with entries $\{x \otimes y\}_{i,j} = x_i y_j$.

Now consider the following set of stochastic differential equations:

$$\frac{\mathrm{d}q}{\mathrm{d}t} = M^{-1}p, \tag{7.24}$$

$$\mathrm{d}p = -\nabla_q V(q)\,\mathrm{d}t + k(z - \xi(q))\nabla_q\xi(q)\,\mathrm{d}t - \gamma R(q)M^{-1}p\,\mathrm{d}t + \sqrt{\frac{2\gamma}{\beta}}R(q)\,\mathrm{d}W^q, \tag{7.25}$$

$$\frac{\mathrm{d}z}{\mathrm{d}t} = p_z, \tag{7.26}$$

$$\mathrm{d}p_z = -\mu k(z - \xi(q))\,\mathrm{d}t - \frac{\vartheta}{\mu}p_z\,\mathrm{d}t + \sqrt{\frac{2\vartheta}{\theta}}\,\mathrm{d}W^z, \tag{7.27}$$

where W^q and W^z are n and m dimensional standard Brownian motions, and $\gamma, \vartheta \in \mathbb{R}^+$. To improve the sampling we use $\theta^{-1} > \beta^{-1}$. In the case $\theta = \beta$ we can show (using a similar calculation to that of Chapter 3 and 4) that the process solving (7.25)-(7.27) is ergodic with respect to the stationary density which is proportional to $e^{-\beta\tilde{H}}$. In the general case $\theta \neq \beta$ it is not clear if the corresponding Fokker-Planck equation of (7.25)-(7.27) is well-posed. However based on the work by Eckmann et. al. [22, 173], it may be possible to find conditions on k, ϑ and θ such that there exists a unique density for process solving (7.25-7.27).

Suppose we have $\mu \gg 1$, then the variables z evolve at a much longer time-scale than q. Hence, in the limit of large μ, the dynamics of q can be assumed to evolve according to a fixed value of z, and the distribution of q converges approximately to the conditional distribution which corresponds to the fixed z:

$$f_k(q|z) = \frac{1}{Z_k(z)}\exp\left(-\beta\left(V(q) + \frac{1}{2}k\left\|\xi(q) - z\right\|^2\right)\right), \tag{7.28}$$

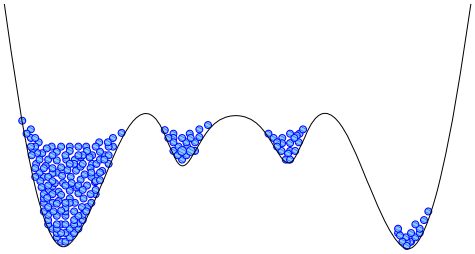

Figure 7.3: By updating the biasing force λ, ABF gradually fills the basin to overcome the barrier.

where

$$Z_k(z) = \int \exp\left(-\beta\left(V(q) + \frac{1}{2}k\left\|\xi(q) - z\right\|^2\right)\right) \mathrm{d}q.$$

If (7.28) holds, then it can be shown (see [153]) that in the limits $\mu \gg 1$ and $\beta k \gg 1$, we have

$$-\int k(z - \xi(q)) f_k(q|z)\, \mathrm{d}q = \nabla_\xi A(z) + \epsilon(\sigma, k),$$

where $A(z)$ is the free energy along ξ and $\epsilon(\mu, k)$ is an error term that depends on μ and k. Thus, in these limits, z will evolve according to an effective potential which is the free energy of the system.

7.1.4 The Adaptive Biasing Force Method

A more recent approach to improve the sampling in free energy calculation is the Adaptive Biasing Force (ABF) method [164, 165]. The idea behind ABF is similar to umbrella sampling (US) which adds a biasing potential to the system to smooth the free energy barriers, and hence improve the sampling. ABF also adds a potential to the system but rather than guessing or predicting the biasing potential, it does this in a more systematic way. This method computes the mean force $\frac{\partial A(\xi)}{\partial \xi}$ on the reaction coordinate ξ and adds it as the biasing force to the dynamics. Therefore ABF effectively adds "$-A(\xi)$" to the potential which leads to a uniform sampling in the reaction coordinates ξ. In the following we present a new formulation of the ABF method which is easy to implement.

Assuming that the dynamics is ergodic, ABF can be expressed as:

$$\frac{\mathrm{d}q}{\mathrm{d}t} = M^{-1}p, \tag{7.29}$$

$$\frac{\mathrm{d}p}{\mathrm{d}t} = -\nabla_q V(q) - \lambda(\xi(q), t)\nabla_q \xi, \tag{7.30}$$

$$\lambda(\xi, t) = \frac{\int_0^t f_\xi \delta(\xi(q) - \xi)\,\mathrm{d}t}{\int_0^t \delta(\xi(q) - \xi)\,\mathrm{d}t}. \tag{7.31}$$

Here, as usual, ξ is the reaction coordinate and f_ξ is an instantaneous force on ξ (see equation (7.16)). The biasing force λ is refined as more samples are collected and in the limit, $t \to \infty$ we have $\lambda \to \nabla_\xi A(\xi)$. In this sense it is an adaptive method. Figure 7.3 shows how ABF gradually fills the basins to overcome the barrier.

The above equations are delay differential equations and they are not convenient to use from a numerical point of view. However, it is possible to derive a closed system of differential equations. Taking the derivative of $\lambda(\xi, t)$ with respect to time yields:

$$\frac{\mathrm{d}\lambda}{\mathrm{d}t} = \left(\frac{\delta(\xi(q) - \xi)}{\int_0^t \delta(\xi(q) - \xi)\,\mathrm{d}t}\right)(f_\xi - \lambda).$$

Let $\nu = \int_0^t \delta(\xi(q) - \xi)\,\mathrm{d}t$ and approximate the δ function by a Gaussian function of the form

$$\mathcal{G}(x, \epsilon) = \frac{1}{\epsilon\sqrt{\pi}} e^{-\left(\frac{x}{\epsilon}\right)^2}.$$

Then we obtain a set of smooth differential equations:

$$\frac{\mathrm{d}q}{\mathrm{d}t} = M^{-1}p, \tag{7.32}$$

$$\frac{\mathrm{d}p}{\mathrm{d}t} = -\nabla_q V(q) - \lambda(\xi(q), t)\nabla_q \xi(q), \tag{7.33}$$

$$\frac{\mathrm{d}\lambda}{\mathrm{d}t} = \left(\frac{\mathcal{G}(\xi(q) - \xi)}{\nu}\right)(f_\xi - \lambda), \tag{7.34}$$

$$\frac{\mathrm{d}\nu}{\mathrm{d}t} = \mathcal{G}(\xi(q) - \xi). \tag{7.35}$$

In the limit we have:

$$\lim_{t\to\infty} \lambda(\xi, t) = \nabla_\xi A(\xi).$$

Considering the constrained Hamiltonian

$$\tilde{H} = \frac{p^T M^{-1} p}{2} + V(q) + \lambda(\xi(q) - \xi)$$

the relation between the constrained simulation technique and ABF becomes clear. Both methods try to sample the submanifold Σ_ξ of the phase space. The constrained simulation method achieves this by exerting a force λ on the reaction coordinate to make sure that the dynamics stays on Σ_ξ, hence sampling ξ. However, rather than constraining the system, ABF shifts the system to the region of phase space where $q \in \Sigma_\xi$.

7.2 An Adaptive Method for Exploring the Free Energy Surface

The main challenge in approximating $A(\xi)$ is the sampling of $\xi = (\xi_1, \ldots, \xi_m)$ which becomes exponentially hard as the dimension of ξ increases (i.e., $m > 2$). The sampling issue is the manifestation of high barriers between meta-stable sets along ξ. However, if there are no patterns on the energy surface along ξ, then the sampling is effectively reduced to a random walk that can take a long time when the dimension of ξ is large, for example when $m > 2$.

This suggests that we should develop a sampling method that smooths the barriers but retains the important features of the dynamics. In this way the crossing of the barriers is overcome, and moreover the sampling is guided by the dynamics. Thus, the sampling is concentrated in the regions of phase space that are more relevent to the desired macroscopic states, such as conformations of a protein.

We approach this problem in the spirit of the Adaptive Biasing Force (ABF) [164, 165, 174, 175, 176]. The philosophy of ABF is to construct a biasing force that is the derivative of free energy on the fly and add it to the force acting on the system, so that the system would evolve in a potential surface that is locally flat. However ABF is not efficient when $m > 2$ because it effectively reduces the sampling to a random walk which can be slow in high dimension. Our primary aim is to improve the computation of averages of observables that are functions of ξ. In particular we are interested in the case where $m > 2$. We will enhance the sampling by lowering the free energy barrier: this is done by extending the idea of ABF so that the biasing force is localised both in time and space. In this way, we do not fill the basins completely, and hence we avoid sampling of regions that have already been sampled and the dynamics will guide us to explore other meta-stable sets.

The method is given by the following set of stochastic differential equations:

$$\frac{\mathrm{d}q}{\mathrm{d}t} = M^{-1}p, \tag{7.36}$$

$$\mathrm{d}p = -\nabla_q V(q)\,\mathrm{d}t + \lambda(\xi(q),t)\nabla_q\xi\,\mathrm{d}t - \gamma p\,\mathrm{d}t + \sigma\,\mathrm{d}W, \tag{7.37}$$

$$\frac{\mathrm{d}\gamma}{\mathrm{d}t} = \frac{1}{\mu}\left(p^T M^{-1}p - \frac{n}{\beta}\right), \tag{7.38}$$

$$F_k = \frac{\int_0^t \psi(t-s) f_\xi(\xi)\chi_{I_k}(\xi)\,\mathrm{d}s}{\int_0^t \psi(t-s)\chi_{I_k}(\xi)\,\mathrm{d}s}, \quad I_k = \{z \in \mathbb{R}^m : \|z-\xi_k\| \le h\}, \quad k = 1,\cdots,N, \tag{7.39}$$

$$\begin{cases} \text{Find } \lambda(t,\xi) = \sum_{i=1}^{\hat{N}} c_i\varphi_i(\xi) \text{ such that for every } \varphi_j,\ j = 1,\cdots,\hat{N} \\ \int \varphi_j(\xi)\sum_{i=1}^{\hat{N}} c_i\varphi_i(\xi) = \int \varphi_j(\xi)\sum_{k=1}^{N} F_k\chi_{I_k}(\xi). \end{cases} \tag{7.40}$$

In the above system, ξ_k, $k = 1,\ldots,N$ are N values of $\xi(q)$, h is the mesh-size, μ is the control parameter for kinetic energy, $\sigma \in \mathbb{R}$ is the diffusion coefficient , W is n-dimensional Brownian motion, $\beta = \frac{1}{k_B T}$ is the inverse temperature, $\psi(t)$ is the prescribed weight function, χ_{I_k} is the normalised characteristic function of I_k defined by

$$\begin{cases} \chi_{I_k}(\xi) & = 1, \quad \text{if } \xi \in I_k, \\ & = 0, \quad \text{if } \xi \notin I_k, \end{cases}, \quad \text{and } \|\chi_{I_k}(\xi)\|_{L^2}^2 = 1,$$

f_ξ is the instantaneous force on ξ (see equation (7.16)) and

$$\{\varphi_i : \|\varphi_i(\xi)\|_{L^2}^2 = 1,\ i = 1,\cdots,M\}$$

is an appropriate set of radial basis (test) functions which will be defined later.

The equations (7.36)-(7.39) are delay-differential equations, however it is possible to formulate them as ordinary differential equations for the purpose of efficient numerical treatment. Let us define

$$\psi(t) = e^{-t/\tau}$$

and introduce new variables

$$\mathcal{N}_k = \int_0^t \psi(t-s)\, f_\xi(\xi)\, \chi_{I_k}(\xi)\, \mathrm{d}s,$$
$$\mathcal{M}_k = \int_0^t \psi(t-s)\, \chi_{I_k}(\xi)\, \mathrm{d}s.$$

Now we have

$$\frac{\mathrm{d}\mathcal{N}_k}{\mathrm{d}t} = \psi(0) f_\xi(\xi)\chi_{I_k}(\xi) + \int_0^t \frac{\mathrm{d}\psi}{\mathrm{d}t}(t-s)\, f_\xi(\xi)\, \chi_{I_k}(\xi)\ \mathrm{d}s = f_\xi(\xi)\chi_{I_k}(\xi) - \frac{1}{\tau}\mathcal{N}_k,$$
$$\frac{\mathrm{d}\mathcal{M}_k}{\mathrm{d}t} = \psi(0)\chi_{I_k}(\xi) + \int_0^t \frac{\mathrm{d}\psi}{\mathrm{d}t}(t-s)\, \chi_{I_k}(\xi)\ \mathrm{d}s = \chi_{I_k}(\xi) - \frac{1}{\tau}\mathcal{M}_k,$$

and $F_k = \frac{\mathcal{N}_k}{\mathcal{M}_k}$. Hence (7.39) can be replaced by

$$\frac{\mathrm{d}\mathcal{N}_k}{\mathrm{d}t} = f_\xi(\xi)\chi_{I_k}(\xi) - \frac{1}{\tau}\mathcal{N}_k, \qquad k = 1, \cdots, N, \tag{7.41}$$
$$\frac{\mathrm{d}\mathcal{M}_k}{\mathrm{d}t} = \chi_{I_k}(\xi) - \frac{1}{\tau}\mathcal{M}_k, \qquad k = 1, \cdots, N, \tag{7.42}$$
$$F_k = \frac{\mathcal{N}_k}{\mathcal{M}_k}, \qquad k = 1, \cdots, N. \tag{7.43}$$

Remark

In some applications it is desirable to have a more gentle and smoother stochastic dynamics. Hence, as an alternative to equations (7.36)-(7.38) we introduce a highly degenerate diffusion version, where only one Brownian motion interacts with the second derivative of the momenta.

$$\frac{\mathrm{d}q}{\mathrm{d}t} = M^{-1}p, \tag{7.44}$$
$$\frac{\mathrm{d}p}{\mathrm{d}t} = -\nabla_q V(q) + \lambda(\xi(q), t)\nabla_q \xi - \gamma p, \tag{7.45}$$
$$\mathrm{d}\gamma = \frac{1}{\mu}\left(p^T M^{-1} p - \frac{n}{\beta}\right)\mathrm{d}t - \gamma\, \mathrm{d}t + \sigma\, \mathrm{d}W_\gamma, \tag{7.46}$$

where $\gamma > 0$ and $\sigma^2 = \frac{2}{\beta\mu}\gamma$, and W_γ is one-dimensional Brownian motion.

Remark

The equations (7.36)-(7.38) are effectively nonequilibrium dynamics, since we use the weight function ψ (i.e. λ does not converge to a limit). It is possible to correct this dynamics by a Metropolis algorithm, so that the hybrid method would have the Boltzmann-Gibbs measure as its invariant measure and enhanced convergence rate. We leave this extension for future work.

7.2.1 Gaussian Radial Basis Functions

One choice for functions in

$$\{\varphi_i : \|\varphi_i(\xi)\|_{L^2}^2 = 1,\ i = 1, \cdots, M\}$$

is a Gaussian function of the form

$$\varphi_i(\xi) = \frac{1}{\mathcal{Z}} \exp\left(-a\left(\frac{\xi - \xi_i}{\delta}\right)^2\right), \tag{7.47}$$

where $\mathcal{Z}$ is the normalization constant and is given by

$$\mathcal{Z} = \|\varphi_i\|_{L^2}^2 = \int_{\mathbb{R}^m} \varphi_i^2(\xi)\, \mathrm{d}\xi,$$

a is a shape parameter and $\xi_i,\ i = 1, \cdots, M$ are discrete values along ξ. With this choice of basis functions equation (7.40) amounts to solving the following linear system

$$\Lambda c = b,$$

where $\Lambda \in \mathbb{R}^{\hat{N} \times \hat{N}}$, its entries given by

$$\Lambda_{i,j} = \int_{\mathbb{R}^m} \varphi_i(\xi)\varphi_j(\xi)\, \mathrm{d}\xi,$$

$c \in \mathbb{R}^{\hat{N}}$ is a vector of unknown coefficients $(c_1, \cdots, c_M)^T$ and $b \in \mathbb{R}^{\hat{N}}$ such that

$$b_j = \sum_{k=1}^{N} F_k \int_{\mathbb{R}^m} \varphi_j(\xi)\chi_{I_k}(\xi)\, \mathrm{d}\xi.$$

It worth noting that there is an optimal choice of Gaussian basis function that should be found for best approximation of λ.

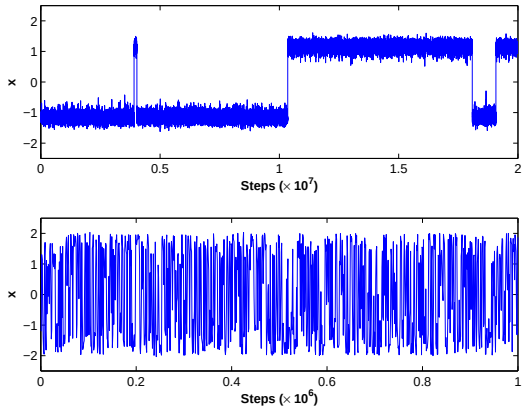

Figure 7.4: The top graph shows the evolution of x for a Langevin simulation during 10 million time steps of size $\Delta t = 0.01$. It rarely switches from the meta-stable set at -1 to the other set at 1. The lower graph shows evolution of x for the adaptive method (7.36)-(7.38), (7.41) and (7.42) during one million time steps of size $\Delta t = 0.01$. It clearly overcomes the barrier and achieves good sampling even in the transition region

7.2.2 Numerical Results

We used the following numerical discretization for equations (7.36)-(7.38), (7.41) and (7.42):

$$
\begin{aligned}
p^{l+\frac{1}{2}} =& p^l - \frac{\Delta t}{2}\nabla V(q^l) + \frac{\Delta t}{2}\lambda(\xi(q^l), l\Delta t)\nabla\xi(q^l) - \frac{\Delta t}{2}p^{l+\frac{1}{2}} + \frac{\sqrt{\Delta t}}{2}\sigma\eta^l,\\
q^{l+1} =& q^l + \Delta t(M^{-1}p^{l+\frac{1}{2}}),\\
\gamma^{l+1} =& \gamma^l + \frac{\Delta t}{\mu}\left(\sum_{i=1}^{n}\frac{1}{m_i}\left(p_i^{l+\frac{1}{2}}\right)^2 - \frac{n}{\beta}\right),\\
\mathcal{N}_k^{l+1} =& \mathcal{N}_k^l + \Delta t f_\xi(\xi(q^{l+1})\chi_{I_k}(\xi(q^{l+1})) - \frac{\Delta t}{\tau}\mathcal{N}_k^{l+1}\chi_{I_k}(\xi(q^{l+1})),\ k = 1, \cdots, N,\\
\mathcal{M}_k^{l+1} =& \mathcal{M}_k^l + \Delta t\chi_{I_k}(\xi(q^{l+1})) - \frac{\Delta t}{\tau}\mathcal{M}_k^{l+1}\chi_{I_k}(\xi(q^{l+1})),\ k = 1, \cdots, N,\\
F_k^{l+1} =& \frac{\mathcal{N}_k^{l+1}}{\mathcal{M}_k^{l+1}},\ k = 1, \cdots, N,\\
p^{l+1} =& p^{l+\frac{1}{2}} - \frac{\Delta t}{2}\nabla V(q^{l+1}) + \frac{\Delta t}{2}\lambda(\xi(q^{l+1}), l\Delta t + \Delta t)\nabla\xi(q^{l+1}) - \frac{\Delta t}{2}p^{l+1} + \frac{\sqrt{\Delta t}}{2}\sigma\eta^l,
\end{aligned}
$$

where, as usual $\{\eta^l\}$ are independent normal random variables with mean zero and variance 1.

A Simple Example: One Dimensional Reaction Coordinate

Here we consider a one dimensional reaction coordinate example which was studied in [177]. The Hamiltonian is given by

$$H(q,p) = \frac{1}{2}p^T M^{-1} p + V(q), \tag{7.48}$$

where $q = (x, y)$ is the position vector and $p = (p_x, p_y)$ is its conjugate momentum. The potential $V(q)$ is defined by

$$V(q) = c_1(x^2 - a^2)^2 + \frac{1}{2}c_2 y^2 + c_3 xy.$$

The potential $V(q)$ has a quartic function of x, hence there are two minimums in the direction of x. Therefore it is natural to consider x as our reaction coordinate (i.e., $\xi(q) := x$). For this example it is possible to calculate $A(x)$ analytically:

$$A(x) = -\beta^{-1} \log Z(x),$$

where

$$\begin{aligned} Z(x) =& \int_{\mathbb{R}^2} \exp\left(-\tfrac{\beta}{2} p \cdot M^{-1} p\right) \mathrm{d}p \int_{\mathbb{R}^2} \exp\left(-\beta V(q)\right) \delta(\xi(q) - x) \, \mathrm{d}q \\ =& \sqrt{\det(M^{-1})} \left(\frac{2\pi}{\beta}\right) \exp\left(-\beta c_1 (x^2 - a^2)^2\right) \int_{\mathbb{R}} \exp\left(-\beta \left(\frac{1}{2}c_2 y^2 + c_3 xy\right)\right) \mathrm{d}y \\ =& \sqrt{\frac{\det(M^{-1})}{c_2}} \left(\frac{2\pi}{\beta}\right) \exp\left(-\beta c_1 (x^2 - a^2)^2 + \beta \frac{c_3^2}{2c_2} x^2\right) \\ & \qquad \int_{\mathbb{R}} \exp\left(-\frac{\beta}{2}\left(\sqrt{c_2} y + \frac{c_3}{\sqrt{c_2}} x\right)^2\right) \sqrt{c_2} \, \mathrm{d}y. \end{aligned}$$

Using a change of variable of $u = \sqrt{c_2} y + \frac{c_3}{\sqrt{c_2}} x$, we obtain

$$Z(x) = \sqrt{\frac{\det(M^{-1})}{c_2}} \left(\frac{2\pi}{\beta}\right)^{\frac{3}{2}} \exp\left(-\beta c_1 (x^2 - a^2)^2 + \beta \frac{c_3^2}{2c_2} x^2\right),$$

which implies that

$$A(x) = c_1(x^2 - a^2)^2 - \frac{c_3^2}{2c_2} x^2 + C, \tag{7.49}$$

where C is constant.

It is worth noting that this numerical test is merely to show that the method works.

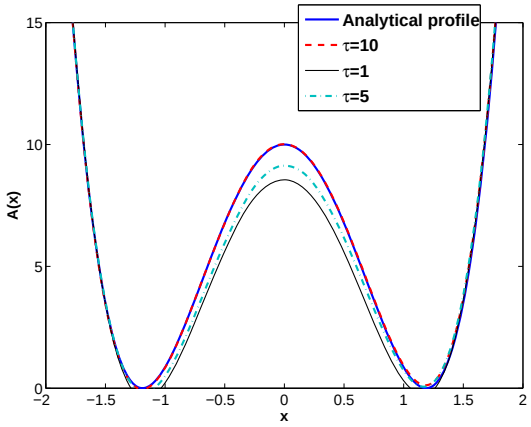

Figure 7.5: The approximation of the free energy profile (7.49) for different τ. The thick solid line is the exact solution. In the limit $\tau \to \infty$ the method converges to ABF method.

It is only a toy model and it is not compatible with our main goal, that is the case of multiple reaction coordinates. The case $m > 2$ for a complex system, such as the computation of the free energy function of a Tripeptide (a peptide consisting of three amino acids joined by peptide bonds) in water, is left for future work.

Chapter 8

Summary

In this thesis, we began by presenting background materials and introducing the problem of sampling the canonical ensemble corresponding to the Boltzmann-Gibbs probability measure. Next, we briefly surveyed sampling methods for molecular simulations. In particular, we described stochastic methods, hybrid methods and dynamical methods. We also suggested some numerical integrators for Langevin dynamics.

In Chapter 3, we studied the approach to equilibrium. We described the logarithmic Sobolev inequality and introduced the concept of hypoellipticity. We followed with the proof of Theorem 6 which effectively says that if the corresponding Fokker-Planck operator of a stochastic process is hypoelliptic, then the process is ergodic. Next we illustrated techniques for obtaining the rate of convergence to equilibrium by obtaining an explicit rate of convergence for gradient flow dynamics. Finally we investigated the rate of convergence to equilibrium for the homogeneous heat bath and Langevin dynamics.

In Chapter 4, we presented a new thermostat (a highly degenerate diffusion) for generating the canonical distribution in molecular dynamics simulations. This thermostat is derived by combining Nosé-Hoover and Langevin dynamics together with the aim to achieve a provable correct distribution, while at the same time minimising the effect on the dynamics. Using the concept of hypoellipticity we proved that the solution of the new thermostat is geometrically ergodic for systems with quadratic potentials. We validated our theoretical results using numerical experiments. In particular we found that the new thermostat is more efficient than Langevin dynamics for calculation of dynamical averages such as autocorrelation functions.

In Chapter 5, we introduced a measure of efficiency for stochastic molecular dynamics by finding a quantity which is the ratio of the rate of convergence to equilibrium to a

measure of the growth of perturbations that are added to the dynamics. We found that the highly degenerate thermostat introduced in Chapter 4 is more efficient, especially for systems with many degrees of freedom.

In Chapter 6, we presented an adaptive method for controlling the kinetic energy in molecular dynamics. We illustrated, using numerical experiments, that the new method is useful for nonequilibirum simulations.

In Chapter 7, we studied the problem of sampling of rare events in molecular systems. We briefly reviewed the techniques for overcoming metastabilities and rare events. In particular we described the blue moon ensemble method, the temperature accelerated method and the adaptive biasing force method for calculating the free energy difference. We finished the chapter by presenting an adaptive method for calculating averages of observables that are functions of reaction coordinates. The new method is based on the adaptive biasing force method, with the difference that the biasing force is localised both in time and space. We tested the method using a simple toy model, further investigations using more complex example are left for future works. The biasing force is localised in time and does not converges to a fixed value, hence the method has a nonequilibirum dynamics. The nonequilibrium effects can be corrected by using the Metropolis algorithm. This extension of combining our adaptive method with Metropolis scheme is left for future works.

8.1 Primary Contributions of This Thesis

- We presented the homogeneous heat bath for molecular dynamics as

$$\mathrm{d}x = \mathbb{J}\nabla H(x) - \Gamma(x)\nabla H(x)\,\mathrm{d}t + \Sigma(x)\,\mathrm{d}W, \tag{8.1}$$

  where H is the Hamiltonian of the system, W is $2n$ family of independent Brownian motion, $\Gamma(x) \in \mathbb{R}^{2n\times 2n}$, $\Sigma(x) \in \mathbb{R}^{2n\times 2n}$ and

$$\mathbb{J} = \begin{pmatrix} 0 & I_n \\ -I_n & 0 \end{pmatrix}.$$

Using the logarithmic Sobolev inequality we were able to obtain the following convergence result:

$$\|f - f_\beta\|_{L^1} \leq \sqrt{2H(f_0|f_\beta)}e^{-r\beta^{-1}t},$$

where f is the time dependent solution of the corresponding Fokker-Planck equation and f_β is the density of the Boltzmann-Gibbs probability measure.

- We presented the highly degenerate thermostat which is a combination of the Nosé-Hoover thermostat and Langevin dynamics. We were able to prove that the corresponding Fokker-Planck operator of the highly degenerate thermostat is hypoelliptic for systems with quadratic potential. Next, using the techniques developed in [84], we were able to prove that the highly degenerate thermostat is geometrically ergodic.

- Assuming the the system is not far from equilibrium (see Assumption 1 in Chapter 5) we were able to obtain the rate of equilibration for the highly degenerate thermostat introduced in Chapter 4. We also calculated the rate for the growth of the perturbations. Finally we calculated the efficiency of the highly degenerate thermostat as the ratio of the equilibration rate to the rate of growth of perturbations.

- We developed an adaptive method for controlling temperature in molecular dynamics simulations. We ran a simulation of 108 Lennard-Jones atoms in a periodic box. The system was initially relaxed at temperature $\beta^{-1} = 1.31$; we then perturbed it during a fixed interval of time. We found that the new method captures the effect of the perturbations correctly, i.e. similarly to the microcanonical dynamics, with the advantage of correcting the kinetic energy and thermalising the system.

- We developed an adaptive method for calculating averages of observables that are functions of reaction coordinates. The new method is based on the adaptive biasing force method, with the difference that the biasing force is localised both in time and space.

Published Papers

[P1] Leimkuhler B. and Noorizadeh E. and Theil F.:A gentle stochastic thermostat for molecular mynamics. J. Stat. Phys. **135**, 261-277 (2009)

[P2] Leimkuhler B., Legoll F. and Noorizadeh E.: A temperature control technique for nonequilibrium molecular simulation. J. Chem. Phys., **128**, 074105 (2008)

Appendix A

Free Energy

The first law of thermodynamics is concerned with the conservation of energy:

$$\frac{\mathrm{d}E}{\mathrm{d}t} = \frac{\mathrm{d}Q}{\mathrm{d}t} + \frac{\mathrm{d}W}{\mathrm{d}t},$$

where W is the work done on the system and Q is the heat flow into the system. This equation demonstrates that W and Q are just ways of transferring energy. Using the first law, the work done on the body during an infinitesimal isothermal reversible change of state (i.e. at constant temperature T) can be written as a differential

$$\mathrm{d}W = \mathrm{d}E - \mathrm{d}Q = \mathrm{d}E - T\,\mathrm{d}S = \mathrm{d}A, \tag{A.1}$$

where S is the entropy and $A = E - TS$ is another function of the state of the system, called the Helmholtz free energy. In other words, the work done on the body in a reversible isothermal process is equal to the change in its free energy. The work W can be divided into two parts:

$$W = W_r + W_d,$$

that is, a reversible and a dissipative part. Hence we have

$$\mathrm{d}W \geqq \mathrm{d}A, \tag{A.2}$$

where the equality is realised only for a reversible isothermal process. This inequality was used in [156] to derive a relation between the exponential of average work and the free energy.

The differential of the free energy can be written as

$$\mathrm{d}A = -S\,\mathrm{d}T - P\,\mathrm{d}V, \tag{A.3}$$

where P is pressure and V is volume. Another equation of state with respect to the variables P, T can be derived by using $P\,\mathrm{d}V = \mathrm{d}(PV) - V\,\mathrm{d}P$ in (A.3):

$$\mathrm{d}G = -S\,\mathrm{d}T + V\,\mathrm{d}P,$$

with a new quantity

$$\begin{aligned} G =& E - TS + PV \\ =& A + PV \\ =& R - TS, \end{aligned} \tag{A.4}$$

where $R = E + PV$ is a heat function. The quantity G is called the Gibbs free energy.

A.1 Free Energy in The Gibbs Distribution

The entropy of a body can be calculated as the mean logarithm of the density f of its distribution function ρ:

$$S = -k_B \langle \log f \rangle . \tag{A.5}$$

Here $\langle \cdot \rangle$ means averaging with respect to f, k_B is the Boltzmann's constant which enables us to convert temperature measured in degrees into energy units in numerical calculations.

Using the Boltzmann-Gibbs density

$$f_\beta(q,p) = \frac{1}{Z} e^{-\beta H(q,p)}, \tag{A.6}$$

where

$$Z = \int f_\beta(q,p)\,\mathrm{d}q\,\mathrm{d}p$$

is the normalisation constant, $\beta = \frac{1}{k_B T}$ and H is the Hamiltonian of the system, in

(A.5) gives

$$S = -k_B \log\left(\frac{1}{Z}\right) + \frac{\langle H\rangle}{T},$$
$$\log\left(\frac{1}{Z}\right) = \frac{\langle H\rangle - TS}{k_B T}.$$

The mean Hamiltonian $\langle H\rangle$ is just what is meant by the term energy E in thermodynamics, hence we obtain

$$A = -\beta \log Z. \tag{A.7}$$

This signifies the fact that the normalization constant of the distribution is directly related to the free energy of the body. Thus, f_β may be written in the form

$$f_\beta(q,p) = e^{-\beta(H(q,p)-A)}. \tag{A.8}$$

Bibliography

[1] Le Bris, C.: Computational chemistry from the perespective of numerical analysis. Acta Numer. **14**, 363–444 (2005)

[2] Marx, D.: An introduction to ab initio molecular dynamics dimulations. Computational Nanoscience: Do It Yourself! **31**, 195–244 (2006)

[3] Arnold, V.: Mathematical methods of classical mechanics. Springer (1989)

[4] Marsden, J.E., Ratiu, T.S.: Introduction to mechanics and symmetry. Springer-Verlag (1994)

[5] Leimkuhler, B.J., Reich, S.: Simulating Hamiltonian dynamics, vol. 14. Cambridge University Press (2005)

[6] Landau, L.D., Lifshitz, E.M.: Course of Theoretical Physics : Mechanics. Butterworth-Heinemann, 3rd edition (1982)

[7] Allen, M.P., Tildesley, D.J.: Computer simulation of liquids. Oxford University Press (1989)

[8] Frenkel, D., Smit, B.: Understanding molecular simulation. Acadamic Press (2002)

[9] Neumaier, A.: Molecular modeling of proteins and mathematical prediction of protein structure. SIAM Rev. **39**, 407–460 (1997)

[10] Hairer, E., Lubich, C., Wanner, G.: Geometric numerical integration, vol. 31. Springer (2002)

[11] Hairer, E.: Backward analysis of numerical integrators and symplectic methods. Ann. Numer. Math. **1**, 107 (1994)

[12] Hairer, E., Lubich, C.: The life-span of backward error analysis for numerical integrators. Numer. Math. **76**(4), 441–462 (1997)

[13] Reich, S.: Backward error analysis for numerical integrators. Siam J. Numer. Anal. **36**(5), 1549–1570 (1999)

[14] McLachlan, R.I., Atela, P.: The accuracy of symplectic integrators. Nonlinearity **4**, 541–562 (1992)

[15] Skeel, R.D., Hardy, D.J.: Practical construction of modified Hamiltonians. SIAM J. Sci. Comput. **23**(4), 11721188 (2001)

[16] Skeel, R.D., Zhang, G., Schlick, T.: A family of symplectic integrators: stability, accuracy, and molecular dynamics applications. SIAM J. Sci. Comput. **18**(1), 203–222 (1997)

[17] Reich, S.: Symplectic integration of constrained Hamiltonian systems by composition methods. SIAM J. Numer. Anal. **33**(2), 475–491 (1996)

[18] Verlet, L.: Computer experiments on classical fluids. I. Thermodynamical properties on Lennard-Jones molecules. Phys. Rev. **159**, 98–103 (1967)

[19] Ford, G.W., Kac, M., Mazur, P.: Statistical mechanics of assemblies of coupled oscillators. J. Mathematical. Phys. **6**, 504–515 (1965)

[20] Ford, G.W., Kac, M.: On the quantum Langevin equation. J. Statist. Phys. **46**(5-6), 803–810 (1987)

[21] Zwanzig, R.: Problems in nonlinear transport theory, in systems far from equilibrium. Springer p. 198225 (1980)

[22] Eckmann, J.P., Pillet, C.A., Rey-Bellet, L.: Non-equilibrium statistical mechanics of anharmonic chains coupled to two heat baths at different temperatures. Comm. Math. Phys. **201**(3), 657–697 (1999)

[23] Meyn, S.P., Tweedie, R.: Markov chains and stochastic stability. Springer-Verlag, London, (1993)

[24] Roberts, G., Rosenthal, J.: Quantitative bounds for convergence rates of continuous time Markov processes. Electronic Journal of Probability, **1**, 1–21 (1996)

[25] Roberts, G., Tweedie, R.: Exponential convergence of Langevin distributions and their discrete approximations. Bernoulli **2**, 341363 (1996)

[26] Down, D., Meyn, S.P., Tweedie, R.L.: Exponential and uniform ergodicity of markov processes. Ann. Probab. **23**(4), 1671–1691 (1995)

[27] Kontoyiannis, I., Meyn, S.P.: Spectral theory and limit theorems for geometrically ergodic markov processes. Ann. Appl. Probab. **13**(1), 304–362 (2003)

[28] Robert, C.P., Casella, G.: Monte Carlo statistical methods. Springer (1999)

[29] Metropolis, N., Rosenbluth, A., Rosenbluth, M., Teller, A., Teller, E.: Equations of state calculations by fast computing machines. J. Chem. Phys. **21**(6), 1087–1091 (1953)

[30] Hastings, W.: Monte Carlo sampling methods using Markov chains and their applications. Biometrika **57**, 97–109 (1970)

[31] Rosenthal, J.S., Roberts, G.O.: Coupling and ergodicity of adaptive Markov chain Monte Carlo algorithms. J. Appl. Probab. **44**(2), 458–475 (2007)

[32] Roberts, G.O., Rosenthal, J.S.: Geometric ergodicity and hybrid Markov chains. Elect. Comm. in Probab. **2**, 13–25 (1997)

[33] Roberts, G.O., Rosenthal, J.S.: Optimal scaling of various Metropolis-Hastings algorithms. Statistical Science **16** (2001)

[34] Roberts, G.O., Gelman, A., Gilks, W.R.: Weak convergence and optimal scaling of random walk Metropolis algorithms. Ann. Appl. Prob. **7**, 110120 (1997)

[35] Duane, S., Kennedy, A., Pendleton, B., Roweth, D.: Hybrid Monte Carlo. Phys. Lett. B **195**, 216–222 (1987)

[36] Schütte, C.: Habilitation thesis, freie Universität Berlin (1999)

[37] Izaguirre, J.A., Hampton, S.S.: Shadow hybrid Monte Carlo: an efficient propagator in phase space of macromolecules. J. Comput. Phys. **200**(2), 581–604 (2004)

[38] Akhmatskaya, E., Reich, S.: GSHMC: an efficient method for molecular simulation. J. Comput. Phys. **227**(10), 4934–4954 (2008)

[39] Akhmatskaya, E., Bou-Rabee, N., Reich, S.: A comparison of generalized hybrid Monte Carlo methods with and without momentum flip. J. Comput. Phys. **228**(6), 2256–2265 (2009)

[40] Sweet, C.R., Hampton, S.S., Izaguirre, J.A.: Tech. rep. tr-2006-09, University of Notre Dame

[41] Sweet, C.R., Hampton, S.S., Skeel, R.D., Izaguirre, J.A.: A separable shadow hybrid Monte Carlo method. J. Chem. Phys. (2009)

[42] Anderson, H.C.: Molecular dynamics at constant pressure and/or temperature. J. Chem. Phys. **72**, 23842393 (1980)

[43] E, W., Li, D.: The Andersen thermostat in molecular dynamics. Comm. Pure. Appl. Math. **61**(1), 96–136 (2007)

[44] Li, D.: On the rate of convergence to equilibirum of the Anderson thermostat in molecular dynamics. J. Stat. Phys. **129**, 265–287 (2007)

[45] Hoogerbrugge, P.J., Koelman, J.M.V.A.: Simulating microscopic hydrodynamic phenomena with dissipative particle dynamics. Europhys. Lett. **19**, 155–160 (1992)

[46] Lowe, C.P.: An alternative approach to dissipative particle dynamics. Europhys. Lett. **47**, 145–151 (1999)

[47] Koopman, E.A., Lowe, C.P.: Advantages of a Lowe-Andersen thermostat in molecular dynamics simulations. J. Chem. Phys. **124**, 204,103–5 (2006)

[48] Peters, E.A.J.F.: Elimination of time step effects in DPD. Europhys. Lett. **66**, 311–317 (2004)

[49] Pastewka, L., Kauzlari, D., Greiner, A., Korvink, J.G.: Thermostat with a local heat-bath coupling for exact energy conservation in dissipative particle dynamics. Phys. Rev. E **73**, 037,701–5 (2006)

[50] Nordholm, S., Zwanzig, R.: A systematic derivation of exact generalized Brownian motion theory. J. Statist. Phys. **13**(4), 347–371 (1975)

[51] Stuart, A.M., Warren, J.O.: Analysis and experiments for a computational model of a heat bath. J. Statist. Phys. **97**, 687–723 (1999)

[52] Kramers, H.A.: Brownian motion in a field of force and the diffusion model of chemical reactions. Physics. **7**(4), 284304 (1940)

[53] Hörmander, L.: The analysis of linear partial differential operators. Springer Verlag (1985)

[54] Helffer, B., Nier, F.: Hypoelliptic estimates and spectral theory for Fokker-Planck operators and Witten Laplacians. Springer Verlag (2005)

[55] Hairer, M.: Introduction to Hypoelliptic Schrödinger type operators (2007)

[56] Nosé, S.: A unified formulation of the constant temperature molecular dynamics method. J. Chem. Phys. **81**, 511–519 (1984)

[57] Nosé, S.: A molecular dynamics method for simulations in the canonical ensemble. Mol. Phys. **52**, 255–268 (1984)

[58] Hoover, W.: Canonical dynamics: equilibrium phase space distributions. Phys. Rev. A. **31**, 1695–1697 (1985)

[59] Evans, D., Holian, B.: The Nosé-Hoover thermostat. J. Chem. Phys. **83**, 4069–4074 (1985)

[60] Legoll, F., Luskin, M., Moeckel, R.: Non-ergodicity of Nosé-Hoover dynamics. Nonlinearity **22**, 1673–1694 (2009)

[61] Legoll, F., Luskin, M., Moeckel, R.: Non-ergodicity of the Nosé-Hoover thermostatted harmonic oscillator. Arch. Rational. Mech. Anal. **184**, 449–463 (2007)

[62] Martyna, G.J., Klein, M.L., Tuckerman, M.: Nosé-Hoover chains: the canonical ensemble via continuous dynamics. J. Chem. Phys. **97**(4), 2635–2643 (1992)

[63] Cancs1, E., Legoll, F., Stoltz, G.: Theoretical and numerical comparison of some sampling methods for molecular dynamics. M2AN **41**(2), 351–389 (2007)

[64] Nosé, S.: Constant temperature molecular dynamics methods. Prog. Theor. Phys. Suppl. **103**, 1–46 (1991)

[65] Bulgac, A., Kusnezov, D.: Canonical ensemble averages from pseudomicrocanonical dynamics. Phys. Rev. A. **42**, 5045–5048 (1990)

[66] Melchionna, S., Ciccotti, G., Holian, B.L.: Hoover NPT dynamics for systems varying in size and shape. Mol. Phys. **78**(3), 533–544 (1993)

[67] Martyna, G.J., Tobias, D.J., Klein, M.L.: Constant pressure molecular dynamics algorithms. J. Chem. Phys. **101**(5), 4177–4189 (1994)

[68] Jia, Z., Leimkuhler, B.: Molecular simulation in the canonical ensemble and beyond. M2AN **41**(2), 333–350 (2007)

[69] Jang, S., Voth, G.A.: Simple reversible molecular dynamics algorithms for Nosé-Hoover chain dynamics. J. Chem. Phys. **22**(107), 9514–9526 (1997)

[70] Martyna, G.J., Tuckerman, M., Tobias, D.J., Klein, M.L.: Explicit reversible integrators for extended systems dynamics. Mol. Phys. **87**(5), 1117–1157 (1996)

[71] Bond, S.B., Leimkuhler, B.J., Laird, B.B.: The Nosé-Poincaré method for constant temperature molecular dynamics. J. Comput. Phys. **151**(1), 114–134 (1999)

[72] Sun, G.: Symplectic partitioned Runge-Kutta methods. J. Comput. Math. **11**, 365 (1993)

[73] Leimkuhler, B.J., Sweet, C.R.: A Hamiltonian formulation for recursive multiple thermostats in a common timescale. SIAM J. Appl. Dyn. Syst. **4**(1), 187–216 (2005)

[74] Sweet, C.R.: Phd Thesis. University of Leicester (2004)

[75] Barth, E., Leimkuhler, B., Sweet, C.: Approach to thermal equilibrium in biomolecular simulation. Lecture Notes in Computational Science and Engineering. **49**, 125–140 (2005)

[76] Milstein, G.N., Repin, Y.M., Tretyakov, M.V.: Symplectic integration of Hamiltonian systems with additive noise. SIAM J. Numer. Anal. **39**(6), 2066–2088 (2002)

[77] Milstein, G.N., Tretyakov, M.V.: Quasi-symplectic methods for Langevin-type equations. IMA J. Numer. Anal. **23**, 593–626 (2003)

[78] Melchionna, S.: Design of quasisymplectic propagators for Langevin dynamics. J. Chem. Phys. **127**, 044,108 (2007)

[79] Yoshida, H.: Construction of higher order symplectic integrators. Phys. Lett. A **150**, 262 – 268 (1990)

[80] Bussi, G., Parrinello, M.: Accurate sampling using Langevin dynamics. Phys. Rev. E. **75**(5) (2007)

[81] Bou-Rabee, N., Owhadi, H.: Boltzmann-Gibbs preserving stochastic variational integrator. http://arxiv.org/abs/0712.4123 (2007)

[82] Kloeden, P.E., Platen, E.: Numerical solutions of stochastic differential equations. Springer (1992)

[83] Gardiner, C.W.: Handbook on stochastic methods (third ed). Springer-Verlag (2004)

[84] Mattingly, J.C., Stuart, A.M., Higham, D.J.: Ergodicity for SDEs and approximations: locally Lipschitz vector fields and degenerate noise. Stochastic Process. Appl. **101**(2), 185–232 (2002)

[85] Bou-Rabee, N., Owhadi, H.: Geometric Langevin algorithm (2009). URL http://arxiv.org/abs/0712.4123

[86] Davidchack, R.L., Handel, R., Tretyakov, M.V.: Langevin thermostat for rigid body dynamics. J. Chem. Phys. **130**(23), 234,101 (2009)

[87] Brünger, A., Brooks, C.B., Karplus, M.: Stochastic boundary conditions for molecular dynamics simulations of st2 water. J. Chem. Phys. Lett. **105**(5), 495–500 (1984)

[88] Schlick, T.: Molecular modeling and simulation. Springer (2002)

[89] Mishra, B., Schlick, T.: The notion of error in Langevin dynamics. J. Chem. Phys. **105**(1), 299–318 (1996)

[90] Skeel, R.D., Izaguirre, J.A.: An impulse integrator for langevin dynamics. Mol. Phys. **100**, 3885 (2002)

[91] Skeel, R.D.: The graduate student's guide to numerical analysis, edited by M. Ainsworth, L. Levesley and M. Marletta. Springer Series in Computational Mathematics (1999)

[92] Vanden-Eijnden, E., Ciccotti, G.: Second-order integrators for Langevin equations with holonomic constraints. Chem. Phys. Lett. **429**, 310–316 (2006)

[93] Wang, W., Skeel, R.D.: Analysis of a few numerical integration methods for the Langevin equation. Mol. Phys. **101**(14), 2149–2156 (2003)

[94] Shardlow, T.: Splitting for dissipative particle dynamics. SIAM J. Sci. Comp. **24**(4), 1267–1282 (2003)

[95] Villani, C.: Topics in optimal transportation. American Mathematical Society **58** (2003)

[96] Csiszar, I.: Information-type measures of difference of probability distributions and indirect observations. Stud. Sci. Math. Hung. **2**, 299–318 (1967)

[97] Kullback, S.: A lower bound for discrimination information in terms of variation. IEEE Trans. Info. Theo. **4**, 126–127 (1967)

[98] Pinsker, M.: Information and information stability of random variables and processes. Holden-Day, San Francisco (1964)

[99] Marton, K.: A measure concentration inequality for contracting Markov chains. Geom. Funct. Anal. **6**, 556–571 (1996)

[100] Talagrand, M.: Transportation cost for Gaussian and other product measures. Geom. Funct. Anal. **6**(3), 587–600 (1996)

[101] Robinson, J.C.: Infinite dimensional dynamical systems. Cambridge University Press (2001)

[102] Stam, A.: Some inequalities satisfied by the quantities of information of Fisher and Shannon. Inform. Control. **2**, 101–112 (1959)

[103] Gross, L.: Logarithmic Sobolev inequalities. Amer. J. Math. **13**(1), 1061–1083 (1975)

[104] Toscani, G.: Entropy production and the rate of convergence to equilibrium for the Fokker-Planck equation. Quart. Appl. Math. **57**(3), 521–541 (1999)

[105] Beckner, W., Pearson, M.: On sharp Sobolev embedding and the logarithmic Sobolev inequality. Bull. London Math. Soc. **30**(1), 80–84 (1998)

[106] Rothaus, O.: Diffusion on compact Riemannian manifolds and logarithmic Sobolev inequalities. J. Funct. Anal. **42**, 102–109 (1981)

[107] Bakry, D., Emery, M.: Diffusions hypercontractives. Sem. Proba. XIX, Lect. Notes in math. **1123**, 177–206 (1985)

[108] Holley, R., Stroock, D.: logarithmic Sobolev inequalities and stochastic Ising models. J. Stat. Phys. **46**(5-6), 1159–1194 (1987)

[109] Otto, F., Villani, C.: Genezation of an inequality by Talagrand and links with the logarithmic Sobolev inequality. J. Funct. Anal. **173**, 361–400 (2007)

[110] Villani, C.: Entropy production and convergence to equilibrium. Lecture Notes in Mathematics (2001)

[111] Otto, F., Reznikoff, M.G.: A new criterion for the logarithmic Sobolev inequality and two applications. J. Funct. Anal. **243**, 121–57 (2007)

[112] Villani, C.: Hypocoercivity. To appear in Mem. Amer. Math. Soc. (2007). URL http://arxiv.org/abs/math/0609050

[113] Khinchin, A.I.: Mathematical foundations of statistical physics. Dover (1949)

[114] Bakry, D., Cattiaux, P., Guillin, A.: Rate of convergence for ergodic continuous Markov processes : Lyapunov versus Poincaré. J. Func. Anal. **254**, 727–759 (2008)

[115] Bakry, D., Barthe, F., Cattiaux, P., Guillin, A.: A simple proof of the Poincaré inequality for a large class of probability measures. Elect. Comm. in Probab. **13**, 6066 (2008)

[116] Friedman, A.: Partial Differential Equations. Dover Publications (2004)

[117] Qian, H., Qian, M., Tang, X.: Thermodynamic of the General Diffusion Process: Time-Reversibility and Entropy Production. J. Statist. Phys. **107**(5-6), 1129–1141 (2002)

[118] Jakśicć, V., Pillet, C.A.: Ergodic properties of the Langevin equation. Lett. Math. Phys. **41**, 49–57 (1997)

[119] Villani, C., Desvillettes, L.: On the trend to global equilibrium in spatially inhomogeneous systems. part I: the linear Fokker-Planck equation. J. Funct. Anal. **173**(2), 361–400 (2000)

[120] Hérau, F., Nier, F.: Isotropic hypoellipticity and trend to equilibrium for the Fokker-Planck equation with a high-degree potential. Arch. Ration. Mech. Anal. **171**(2), 151–218 (2004)

[121] Risken, H.: The Fokker-Planck equation. Springer-Verlag (1989)

[122] Pavliotis, G.A.: Applied stochastic processes. Lecture Notes, Pre-Print (2009)

[123] Berendsen, H.J.C., Postma, J.P.M., Van Gunsteren, W.F., DiNola, A., Haak, J.R.: Molecular dynamics with coupling to an external bath. J. Chem. Phys. **81**(8), 3684–90 (1984)

[124] Andersen, H.C.: Molecular dynamics at constant pressure and/or temperature. J. Chem. Phys. **72**, 2384–2393 (1980)

[125] Grest, G.S., Kremer, K.: Molecular-dynamics simulation for polymers in the presence of a heat bath. Phys. Rev. A **33**(5), 3628–3631 (1986)

[126] Soddemann, T., Dünweg, B., Kremer, K.: Dissipative particle dynamics: A useful thermostat for equilibrium and nonequilibrium molecular dynamics simulations. Phys. Rev. E **68**(4), 046,702 (2003)

[127] Samoletov, A., Chaplain, M.A.J., Dettmann, C.P.: Thermostats for "slow" configurational modes. J. Stat. Phys. **128**, 1321–1336 (2007)

[128] Bussi, G., Donadio, D., Parrinello, M.: Canonical sampling through velocity rescaling. J. Chem. Phys. **126**, 014,101 (2007)

[129] Quigley, D., Probert, M.: Langevin dynamics in constant pressure extended systems. J. Chem. Phys. **120**, 11,432 (2004)

[130] Mattingly, J.C., Stuart, A.M.: Geometric ergodicity of some hypo-elliptic diffusions for particle motions. Markov Process. Related Fields, **8**(2), 199–214 (2002)

[131] Shardlow, T., Yan, Y.: Geometric ergodicity for dissipative particle dynamics. Stochastics and Dynamics **6**(1), 123–154 (2006)

[132] Milstein, G.N., Tretyakov, M.V.: Stochastic numerics for mathematical physics. Springer (2004)

[133] Petravic, J., Delhommelle, J.: Conductivity of molten sodium chloride and its supercritical vapor in strong dc electric fields. J. Chem. Phys. **118**, 7477–7485 (2003)

[134] Weingarten, N., Selinger, R.: Size effects and dislocation patterning in two-dimensional bending. preprint submitted to Elsevier Science pp. http://arxiv.org/pdf/cond–mat/0606,789 (2006)

[135] Patriarca, M., A, K., Kaski, K.: Nucleation and dynamics of dislocations in mismatched heterostructures. Current Issues in Heteroepitaxial Growth– Stress Relaxation and Self Assembly **696** (2001)

[136] Sanz-Navarro, C., Kenny, S., R, S.: Nanotechnology **15**, 692–697 (2003)

[137] Ruelle, D.: Smooth dynamics and new theoretical ideas in nonequilibrium statistical mechanics. Journal of Statistical Physics **95**, 393–468 (1999)

[138] Widmalm, G., Pastor, R.W.: Comparison of Langevin and molecular dynamics simulations. Equilibrium and dynamics of ethylene glycol in water. J. Chem. Soc., Faraday Trans. **88**, 1747–1754 (1992)

[139] Teramoto, H., Sasa, S.: Microscopic description of the equality between violation of the fluctuation-dissipation relation and energy dissipation. Phys. Rev. E. **72**, 060,102 (2005)

[140] Braga, C., Travis, K.: A configurational temperature Nosé-Hoover thermostat. J. Chem. Phys. **123**, 134,101 (2005)

[141] Allen, M., Schmid, F.: A thermostat for molecular dynamics of complex fluids. Mol. Sim. **33**, 21–26 (2007)

[142] Hänggi, P., Talkner, P., Borkovec, M.: Reaction-rate theory: fifty years after Kramers. Rev. Modern. Phys. **62**(2), 251–342 (1990)

[143] Beveridge, D.L., DiCapua, F.M.: Free energy via molecular simulation: applications to chemical and biomolecular systems. Annu. Rev. Biophys. Biophys. Chem. **18**, 431–492 (1989)

[144] Kirkwood, J.G.: Statistical mechanics of fluid mixtures. J. Chem. Phys. **3**(5), 300–313 (1935)

[145] Carter, E.A., Ciccotti, G., Hanes, J.T., Kapral, R.: Constrained reaction coordinate dynamics for the simulation of rare events. J. Chem. Phys. Lett. **156**(5), 472–477 (1989)

[146] Sprik, M., Ciccotti, G.: Free energy from constrained molecular dynamics. J. Chem. Phys. **109**(18), 7737–7744 (1998)

[147] Ciccotti, G., Kapral, R., Vanden-Eijnden, E.: Blue moon sampling, vertical reaction coordinates and unbiased constrained dynamics. J. Chem. Phys. **6**, 1809–1814 (2005)

[148] Ryckaert, J.P., Ciccoti, G., Berendsen, H.J.C.: Numerical integration of the cartesian equations of motion of a system with constraints: molecular dynamics of n-alkanes. J. Comput. Phys. **23**, 327 (1977)

[149] Torrie, G.M., Valleau, J.P.: Nonphysical sampling distributions in Monte Carlo free-energy estimation: Umbrella sampling. J. Comput. Phys. **23**(2), 187–199 (1977)

[150] Kumar, S., Bouzida, D., Swenden, R., Kollman, P., Rosenberg, J.: The weighted histogram analysis method for free-energy calculations on biomolecules. J. Comput. Chem. **13**, 1011–1021 (1992)

[151] Votter, A.F.: A method for accelerating the molecular dynamics simulation of infrequent events. J. Chem. Phys. **106**(11), 4665–4677 (1997)

[152] Sorensen, M.R., Votter, A.F.: Temperature-accelerated dynamics for simulation of infrequent events. J. Chem. Phys. **112**(21), 9599–9606 (2000)

[153] Maragliano, L., Vanden-Eijnden, E.: A temperature accelerated method for sampling free energy and determining reaction pathways in rare events simulations. J. Chem. Phys. **426**, 168–175 (2006)

[154] Rosso, L., Minary, P., Zhu, Z.W., Tuckerman, M.E.: On the use of the adiabatic molecular dynamics techniques in the calculation of the free energy profiles. J. Chem. Phys. **116**(11), 4389–4402 (2002)

[155] Rosso, L., Abrams, J.B., Tuckerman, M.E.: Mapping the backbone dihedral free energy surfaces in small peptides in solution using adiabatic free energy dynamics. J. Phys. Chem. B **109**(9), 4162–4167 (2005)

[156] Jarzynski, C.: Nonequilibrium equality for free energy differences. Phys. Rev. Lett. **78**, 2690–2693 (1997)

[157] Jarzynski, C.: Equilibrium free-energy differences from nonequilibrium measurements: A master-equation approach. Phys. Rev. E **56**(5), 5018–5035 (1997)

[158] Jarzynski, C.: How does a system responds when driven away from thermal equilibrium. PANS **98**(7), 3636–3638 (2001)

[159] Crooks, G.E.: Path-ensemble averages in systems driven far from equilibrium. Phys. Rev. E **61**(3), 2361–2366 (2000)

[160] Crooks, G.E.: Entropy production fluctuation theorem and the nonequilibrium work relation for free energy differences. Phys. Rev. E **60**(3), 2721–2726 (1999)

[161] Hummer, G., Szabo, A.: Free energy reconstruction from nonequilibrium single-molecule pulling experiments. PANS **98**(7), 3658–3661 (2001)

[162] Schöll-Paschinger, E., Dellago, C.: A proof of jarzynski's nonequilibrium work theorem for dynamical systems that conserve the canonical distribution. J. Chem. Phys. **125**(9), 054,105 (2006)

[163] Rodriguez-Gomez, D., Darve, E., Pohorille, A.: Assessing the efficiency of free energy calculation methods. J. Chem. Phys. **120**(8), 3563–3578 (2004)

[164] Darve, E., Pohorille, A.: Calculating free energies using average force. J. Chem. Phys. **115**, 9169–9183 (2001)

[165] Darve, E., Wilson, M.A., Pohorille, A.: Calculating free energies using a scaled-force molecular dynamics algorithm. Mol. Sim. **28**, 113–144 (2002)

[166] Laio, A., Parrinello, M.: Escaping free-energy minima. Proc. Nat. Acad. USA **99**, 12,562 (2002)

[167] Chipot, C., Pohorille, A.E.: Free Energy Calculations. Springer (2007)

[168] Doltsinis, N.L.: Free Energy and Rare Events in Molecular Dynamics. Comput. Nano. NIC Series. **31**, 375–387 (2006)

[169] E, W., Ren, W., Vanden-Eijnden, E.: Energy landscapes and rare events. BEIJING **1**, 621 (2002). URL http://www.citebase.org/abstract?id=oai:arXiv.org:math/0212415

[170] Darve, E.: Numerical methods for calculating the potential of mean force. Lecture Notes in Computational Science and Engineering: New Algorithms for Macromolecular Simulation **49**, 213–249 (2006)

[171] den Otter, W.K., Briels, W.J.: The calculation of free-energy differences by constrained molecular-dynamics simulations. J. Chem. Phys. **109**(11), 4139–4146 (1998)

[172] den Otter, W.K.: Thermodynamic integration of the free energy along a reaction coordinate in Cartesian coordinates. J. Chem. Phys. **112**(17), 7283–7292 (2000)

[173] Eckmann, J.P., Pillet, C.A., Rey-Bellet, L.: Entropy production in nonlinear, thermally driven Hamiltonian systems. J. Statist. Phys. **95**(1-2), 305–331 (1999)

[174] LeLiévre, T., Rousset, M., Stoltz, G.: Long-time convergence of an adaptive biasing force method. Nonlinearity **21**, 1155–1181 (2008)

[175] LeLiévre, T., Rousset, M., Stoltz, G.: Computation of free energy profiles with adaptive parallel dynamics. J. Chem. Phys **126**, 134,111 (2007)

[176] LeLiévre, T., Rousset, M., Stoltz, G.: Computation of free energy differences through nonequilibrium stochastic dynamics: the reaction coorinate case. J. Comput. Phys **222**, 624–643 (2007)

[177] Rosso, L., Minary, P., Zhu, Z.W., Tuckerman, M.E.: On the use of the adiabatic molecular dynamics techniques in the calculation of the free energy profiles. J. Chem. Phys **116**(11), 4389–4402 (2002)